INAUGURAL-DISSERTATION

zur

Erlangung der Doktorwürde

der

Naturwissenschaftlich-Mathematischen Gesamtfakultät

der

Ruprecht-Karls-Universität

Heidelberg

Vorgelegt von

Diplom-Biochemiker Ralph Gareus

aus Forchheim

Tag der mündlichen Prüfung: _____

Thema

Profilin II - Novel functions in membrane-trafficking

Gutachter: Dr. habil. Jochen Wittbrodt
Dr. habil. Dietmar Manstein

Acknowledgements

I want to thank my supervisor Walter Witke for being an excellent teacher, his incredible patience with me during the whole time and occasional dog bites.

All the members of the Witke group made my time in the lab and in Italy most enjoyable: Hannse Stöffler, Alessia Di Nardo, Jim Sutherland, Christine Gurniak-Witke, Agnieszka Sadowska and Laura Spinardi. Special thanks to Ale, who helped me a lot settling down in Italy in the beginning and provided the profilin II mutant mice and other things. Thanks to Jim for friendship, ideas and plasmids. I thank Christine for POP-constructs. Thanks also to Chryssa Kanellopoulou who shared some good and bad times and also all the important gossip with me.

In addition I want to thank:
Elke Kurz who helped with experiments and the FACS.
Emerald Perlas who did the in-situs.
CNR- and EMMA people for their support, and especially Richard and Paolo for beer.
H.D. Söling, M. Way, P. DeCamilli, and F. Gertler who provided plasmids and antibodies.
Marco Sassoe'-Pogneto who took the electron microscopical pictures of profilin II at the synapse.

I want to thank the members of my thesis-committee, Carlos Dotti and Dirk Bohmann for helpful comments and suggestions.

My brother and my parents constantly supported me, and it always felt good to come home.

Most importantly, Silvia and Vale helped me remember that there is life not only in a test tube, but also outside the lab.

Profilin II - Novel functions in membrane-trafficking

Ralph Gareus - EMBL Mouse Biology Programme, Monterotondo, Italy

Profilin is an actin-binding protein expressed in all eukaryotic cells, regulating microfilament remodelling. Besides actin, it binds to poly-L-proline and phosphatidylinositol phoshates. Mice have three profilin genes, with profilin I being ubiquitously expressed, profilin II a brain specific isoform and profilin III expressed in kidney and testis. Via its poly-L-proline binding site profilin I and profilin II bind to ligands which had been shown to not only regulate the microfilament system, but also signal transduction and membrane traffic, suggesting novel, not yet investigated functions for the profilins.

One goal of this thesis was to analyze protein ligands for profilin I and profilin II in different mouse tissues, thus getting further insight on potential profilin functions.

Novel binding partners found for profilin I were the glycolytic enzyme GAPDH and the putative G-protein coupled receptor p40, further suggesting the idea of an involvement of profilin in signal transduction processes. The huntingtin-protein, mutations of which give rise to Huntington's disease and the phosphatidylinositol phosphatase synaptojanin were identified as new profilin II ligands, which are not found in the profilin I complex, linking this profilin isoform to lipid metabolism and disease.

The second goal of this thesis was to address the question of a possible role for profilin II in membrane trafficking, as suggested by a number of protein ligands found in the affinity complexes from mouse brain.

As shown in this work, profilin II acts as a negative regulator of membrane uptake. Overexpression of profilin II in cells inhibits membrane uptake and vice versa neurons from mice lacking this profilin isoform show an increase in membrane recycling. The effects are most likely mediated by direct interaction of profilin II with ligands such as POP-130, which is involved in late endocytic traffic. Furthermore, profilin II is a regulator of dynamin I in brain. It competes for the binding of effector molecules for dynamin, like src, Grb2, amphiphysin and endophilin, thus preventing the assembly of the endocytic machinery. Dissociation of profilin II from dynamin I is triggered by phosphatidylinositol-(4,5)-bisphosphate, permitting the incorporation of dynamin into functional complexes at the plasma membrane. Similarly, ATP-charged actin is set free from the profilactin complex and can be incorporated into actin filaments at sites of endocytosis. In this way profilin II can coordinate actin-polymerization and endocytosis at the membrane.

Supervisor: Dr. Walter Witke
First referee: PD Dr. Jochen Wittbrodt
Second referee: PD Dr. Dietmar Manstein

Table of contents

Abbreviations

μM	micromolar
6xHis	N-terminal tag consisting of six histidines
aa	amino acid
ATP	adenosine-5'-trisphosphate
BSA	bovine serum albumin
cDNA	complementary DNA
Ci	Curie
CNBr	cyanogen bromide
DMSO	dimethylsulfoxide
DNA	deoxyribonucleic acid
DTT	dithiothreitol
EDTA	ethylene diamine tetraacetae
EGFP	enhanced green fluorescent protein
EGTA	ethyleneglycol-bis[β-aminoethyl ether]-N, N, N', N'-tetraacetate
ELISA	enzyme-linked immunosorbent assay
F	Farad
FACS	fluorescence activated cell scanning
F-actin	filamentous actin
FCS	fetal calf serum
ft	flow-through
G-actin	globular actin
GFP	green fluorescent protein
GMP	guanosine-5'-monophosphate
GST	glutathione-S-transferase
GTP	guanosine-5'-trisphosphate
GTP-γ-S	guanosine-5'-O-(3-thiotrisphosphate)
HBSS	Hank's buffered salt solution
HEPES	N-2-Hydroxyethylpiperazine-N'-2-ethane sulfonic acid
HLB	Hepes-based lysis buffer
IP	immunoprecipitation

IPTG	isopropylthio-β-galactoside
kD	kilodalton
l	liter
LB	Luria-Bertani medium
m.o.i.	multiplicity of infection
MALDI-TOF	matrix assisted laser desorption-ionisation - time-of-flight
min.	minutes
mM	millimolar
mRNA	messenger RNA
Ni-NTA	nickel-nitriloacetic acid
nM	nanomolar
ON	overnight
PAGE	polyacrylamide-gel electrophoresis
PBS	phosphate-buffered saline
PCR	polymerase chain reaction
PFA	paraformaldehyde
PH	pleckstrin homology
PI	profilin I
PII	profilin II
PIP_2	phosphatidylinositol-(4,5)-bisphosphate
PLP	poly-L-proline
PRD	proline-arginine rich domain
RNA	ribonucleic acid
RT	room temperature
s	seconds
SDS	sodium dodecyl sulfate
SH3	src-homology 3
TLC	thin layer chromatography
Tris	tris-(hydroxymethyl) aminomethane
tRNA	transfer RNA
TX-100	Triton X-100
UTP	uridine-5'-trisphosphate
V	volts

x g	times gravity

1 INTRODUCTION

During its lifetime, a cell has to perform a plethora of motile activities: it has to divide, attach to its substratum, take up nutrients from the outside and secrete molecules, move, change its shape and adopt polarity. All of these processes depend on the interplay and integrity of various constituents of the cytoskeleton, and in particular the microfilament system or actin cytoskeleton (see Figure 1).

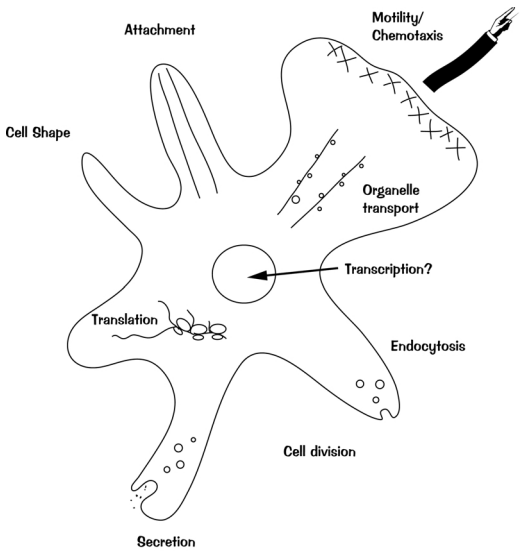

Figure 1: Actin-driven processes

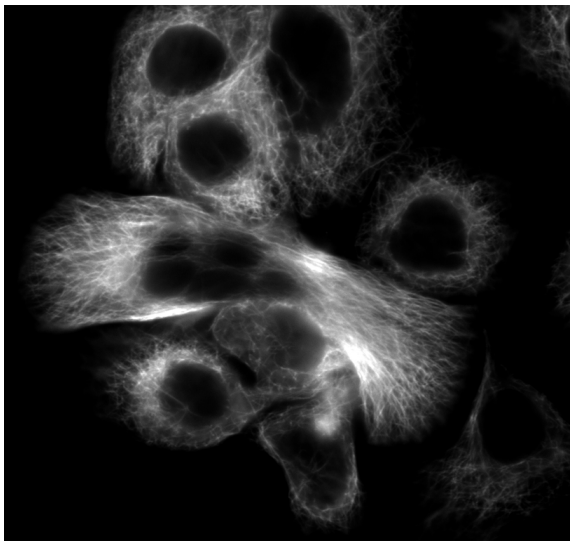

Figure 2: F-Actin in these cultured NBT-II cells was stained with phalloidin

Actin is a 45 kDa protein, which can exist in monomeric form (G-actin) or polymerize into filaments (F-actin). Together with myosin, actin filaments form the contractile

system of our muscles. In non-muscle cells, actin is arranged in a three-dimensional lattice, which gives cells shape and stability (see Figure 2).

All eukaryotic cells have actin; and in most organisms multiple genes for "conventional" actins have been found : alpha, beta and gamma isoforms, which are very similar (Herman 1993).

1.1 Actin polymerization

In a solution of appropriate salt content, actin tends to polymerize into filaments; the polymerization follows a kinetic like depicted in Figure 3.

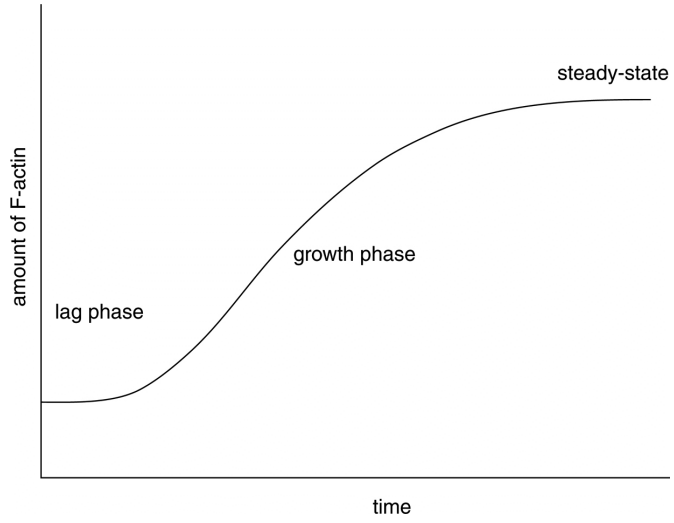

Figure 3: Kinetics of actin polymerization

The limiting step in actin polymerization is the formation of actin trimers, this nucleation step accounts for the lag-phase. From the trimer state, addition of actin monomers to the filament occurs readily during the growth-phase until the concentration of remaining free actin monomers reaches a point where addition of monomers equals monomer loss. This concentration is called the *critical concentration* at steady state.

Actin is an adenosine-nucleotide binding molecule with ATPase activity. *In vitro*, the assembly of actin into filaments is energy independent. However, ATP is consumed during the polymerization cycle. Actin-bound ATP hydrolyzes as the filament grows older. It has been shown that addition of ATP-bound actin to existing filaments occurs faster than addition of ADP-actin (Pollard 1986). This leads to the generation of

filaments which have polarity: one end has an "ATP-actin cap", the other end consists of ADP-actin. Since the affinity of ADP-actin for the filament is lower than that of ATP-actin, in steady state the filament loses actin-monomers from the ADP-end (also called slow-growing, pointed, or (-)-end), while new ATP-charged monomers add on to the ATP-end (also called fast-growing, barbed, or (+)-end). This leads to a process called *treadmilling*; a turnover of the filament without net change of filament length as depicted in Figure 4.

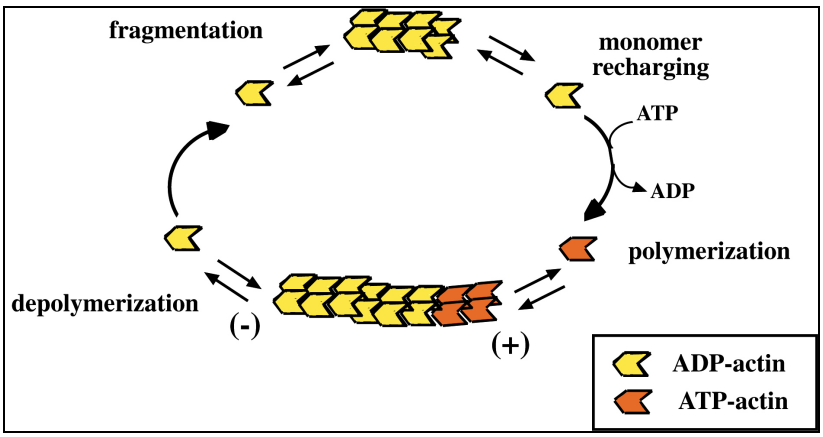

Figure 4: Treadmilling of actin filaments

The activation of neutrophils illustrates how fast this turnover can be in the cell: 10 seconds after stimulation, their F-actin level doubles, and returns to basal levels with a half-time of 3-10 seconds after removal of stimulant (Deaton et al. 1992).
Obviously, *in vivo* a very precise regulation of actin-polymerization in space and time is necessary for complex processes like activation of neutrophils, migration, shape-changes, or cell division. Actin alone, however, can only polymerize into filaments and depolymerize. Complexity and fine regulation are brought about by a vast number of cytosolic accessory proteins, called *actin-binding proteins* (ABPs).

1.2 Actin-binding proteins

Proteins which bind to actin can influence any of the three phases of actin polymerization (see Figure 3). They can control the length of filaments, cross-link and bundle individual filaments or connect actin to membranous structures or other cytoskeletal elements (Ayscough 1998). Most actin-binding proteins are thus

classified according to their *in vitro* functions: proteins which sever existing filaments (like gelsolin or actin depolymerizing factor), nucleate new filaments (Arp2/3 complex, Pollard et al. 2000), cross-linking proteins (like α-actinin or fimbrin), capping proteins (like capG, capZ) or proteins which keep actin in its monomeric form (thymosin β4, profilin). These proteins ultimately convey signals to the actin-cytoskeleton. One of the first actin-binding proteins to be identified was a molecule called profilin.

1.3 Profilin

1977 Carlsson and coworkers characterized a 15 kDa protein which co-purified in a 1:1 complex with monomeric actin from spleen and thymus and which kept it from forming filaments at concentrations where muscle actin normally is mostly in the F-state (Carlsson et al. 1977). They termed the protein profilin, because it kept actin in the "profilamentous" unpolymerized form.

Up to date, profilin has been found in all eukaryotes; and even the genome of Vaccinia virus encodes for a potential profilin gene (Blasco et al. 1991).

1.3.1 Profilin and actin

Initially it was thought that profilin's major role is to keep actin in the cell in a monomeric state. Some factor must be responsible for the fact that the concentration of unpolymerized actin in cells can be 50-200 μM, while the critical concentration (see chapter "Actin polymerization") for polymerization of purified actin is around 0.1 μM. Indeed, in *in vitro* polymerization assays, profilin is able to prevent actin from polymerizing, as illustrated in Figure 5.

Later, it was shown that other proteins like thymosin β4 are able to sequester actin efficiently (Safer et al. 1991) - and that cellular concentrations of profilin are unlikely to be sufficient to explain the amount of G-actin in cells (Southwick and Young 1990). Yet, profilin is unique in its ability to catalyze the exchange of adenosine-nucleotides on the actin molecule by as much as 1000-fold (Goldschmidt-Clermont et al. 1991b), thereby replacing ATP for ADP. Since ATP-actin was shown to polymerize faster and at lower critical concentrations than ADP-actin (Pollard 1986;

Pollard and Cooper 1986), profilin can speed up actin polymerization by delivering ATP-charged actin to uncapped barbed filament ends (Pring et al. 1992). The profilin-actin-complex can in fact be incorporated into barbed ends, although profilin dissociates soon from the filaments, due to its low affinity for F-actin (Gutsche-Perelroizen et al. 1999).

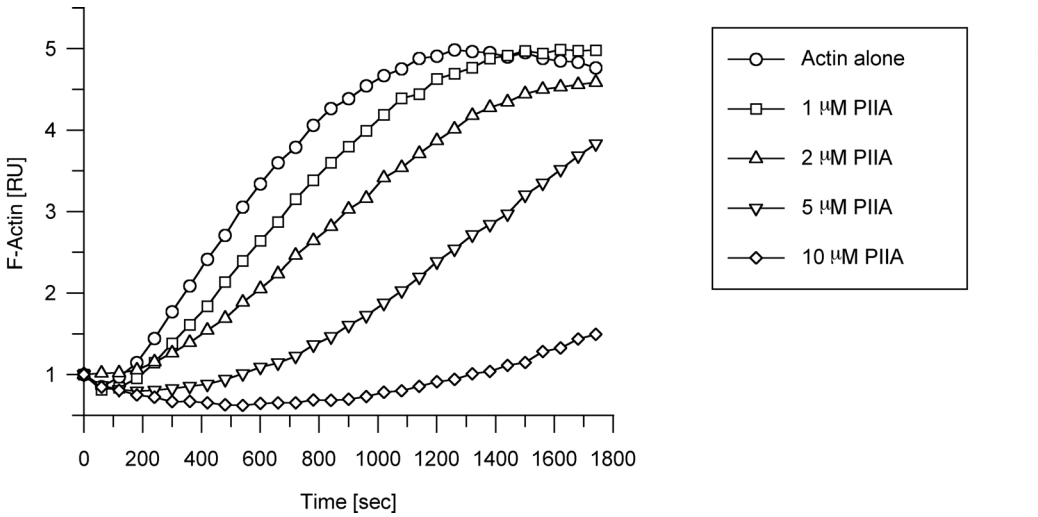

Figure 5: Pyrene-actin polymerization assay with 5 μM actin and increasing amounts of profilin IIA from mouse (PIIA)

The apparent paradox that profilin on one hand keeps actin from polymerizing, but on the other hand charges actin-monomers with ATP for incorporation into filaments, depends on the *in vitro* assay conditions. Profilin with actin alone behaves like a sequestering molecule in polymerization assays, while the profilactin complex can speed up actin polymerization when preexisting filaments are being uncapped by uncapping-proteins. In the cell, thymosin and profilin are thought to coordinate G-actin-pool maintenance and rapid actin polymerization in a concerted manner, with profilin acting as a sequestering protein when filament ends are capped but as a catalyst of polymerization on free barbed ends (Pantaloni and Carlier 1993) by capturing actin monomers from thymosin and shuffling them onto growing actin-filaments (Kang et al. 1999).

1.3.2 Profilin and membranes

Actin polymerization in cells always occurs in the vicinity of membranes. This implies that molecules regulating this process are located there. Indeed, several ABPs have been shown to interact with certain lipids, among them also profilin. One of the *Acanthamoeba*-profilin isoforms localizes strongly to the plasma-membrane (Bubb et al. 1998). Also in human leukocytes and platelets profilin has been found associated with regions of the cell membrane which are free of actin filaments (Hartwig et al. 1989).

Lassing and Lindberg showed that profilin can bind to anionic phospholipids, and especially well to phosphatidylinositol-4,5-bisphosphate (PIP_2) (Lassing and Lindberg 1985). Upon binding to PIP_2, profilin's CD-spectrum changes, implying a structural change (Raghunathan et al. 1992). The interaction was shown to be relatively strong, with a K_d in the micromolar range. In micelles, one profilin molecule binds seven molecules of PIP_2, and in lipid bilayers consisting mainly of other lipids, one profilin can bind 5 PIP_2 molecules. Due to this fact it has been proposed that profilin might act as a sequestering molecule for phosphoinositides (Goldschmidt-Clermont et al. 1990). The interaction of profilin with PIP_2 was shown to disrupt the profilactin complex, and it was argued that in this way ATP-charged actin monomers are set free, which in turn would then be readily available for incorporation into filaments.

These findings suggest a possible regulation of actin polymerization by membrane lipids. But not only regulates PIP_2 profilin function, profilin reciprocally protects PIP_2 from being hydrolyzed by phospholipase C-γ1 (PLC) if PLC is unphosphorylated (Goldschmidt-Clermont et al. 1990; Machesky et al. 1990). Phosphorylation of PLC by activated epidermal growth factor (EGF) receptor tyrosine kinase overcomes the inhibitory effect of profilin (Goldschmidt-Clermont et al. 1991a). This argues for an involvement of profilin in receptor tyrosine kinase signalling.

1.3.3 Profilin and poly-L-proline

More than ten years after characterizing profilin's interaction with actin, Tanaka and coworkers found that profilin and the profilactin complex can bind to immobilized synthetic poly-L-proline (Tanaka and Shibata 1985). They noticed that the affinity of profilin alone for poly-L-proline was higher than the affinity of

profilactin. This feature of profilin was exploited to purify the protein and the profilactin complex (Lindberg et al. 1988 Kaiser et al. 1989). All profilins identified so far except for the profilin of vaccinia virus (Machesky et al. 1994b) and the mouse profilin IIB splice form (Di Nardo et al. 2000) have been shown to be able to bind to poly-L-proline.

The functional importance of this feature remained a mystery for a long time. The first functional link of profilin with a ligand different from actin was made by Vojtek and coworkers in 1991, who found that overexpression of profilin could rescue *Saccharomyces cerevisiae* deficient for the proline-rich cyclase-associated protein (CAP) (Vojtek 1991).

In yeast, the ability of profilin to bind to polyproline was shown to be essential (Lu and Pollard 2001; Ostrander et al. 1999). Biochemically, the first ligand descibed to bind profilin via its poly-L-proline binding site was the focal-adhesion phosphoprotein VASP, which contains multiple proline-rich stretches (Reinhard et al. 1995). Meanwhile, a growing number of polyproline ligands has been identified: diaphanous (Watanabe et al. 1997) and other members of the formin-family of proteins (Manseau et al. 1996; Chang et al. 1997; Imamura et al. 1997), the Wiskott-Aldrich Syndrome protein (WASP) isoforms (Suetsugu et al. 1998), other members of the Ena/VASP-family, like mammalian Ena (Mena) and Evl (Ena-VASP-like) (Gertler et al. 1996), the brain proteins drebrin and gephyrin (Mammoto et al. 1998), which are important for clustering of neurotransmitter receptors (Reiss et al. 2001) and conferring synaptic plasticity, and a big (550 kDa) presynaptic scaffolding protein, azconin (Wang et al. 1999). WASP and the Ena/VASP-homologous (EVH)-proteins have been implicated in the control of actin dynamics at the leading edge of cells (Nakagawa et al. 2001) and growth-cone guidance in neurons (Korey and Van Vactor 2000), although the exact mechanisms still have to be unravelled. Additional polyproline-ligands have been identified by our lab (Witke et al. 1998) and are described in a following chapter (see "Profilin function in cells: actin binding vs. ligand binding").

1.3.4 Profilin structure

Three binding properties of profilin have been described: binding to actin, to polyproline and to acidic phospholipids. All of them map to different domains of the protein.

Profilin has been crystallized bound to actin (Schutt et al. 1993) and to a 10mer of poly-L-proline (Mahoney and Almo 1998; Mahoney et al. 1997; Mahoney et al. 1999).

As shown in Figure 6, the structure of profilin is formed by a central antiparallel β-pleated sheet which divides the molecule into two halves made up by sets of helices.

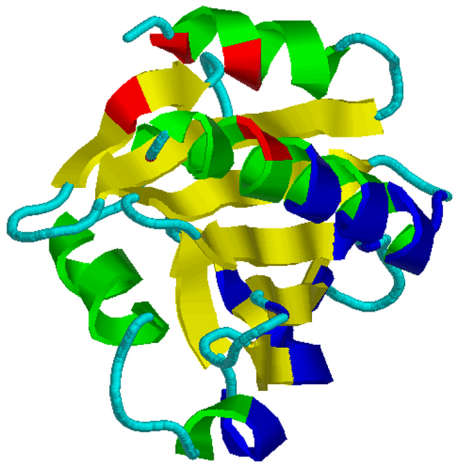

Figure 6: Crystal-structure of human profilin I (Metzler et al. 1995). α-helices are shown in green, β-sheets in yellow. Residues involved in actin binding are highlighted in blue, those involved in polyproline-binding in red.

The amino- and carboxy-termini form α-helices which come to lie in close proximity on one site of the sheet, forming a hydrophobic pocket with part of the underlying β-sheet. This domain forms a cleft which confers binding to polyproline (Mahoney et al. 1997; green in Figure 7).

The profilin-actin crystal structure revealed the position of residues responsible for binding to actin (Schutt et al. 1993; see Figure 8). Those lie mainly in loops connecting the central β-sheet with the helices and the sheet itself, but also residues on the carboxy-terminal helix of profilin (which is also involved in polyproline binding) participate in actin-binding (see blue colored parts of Figure 6).

Because the actin- and polyproline binding sites mostly lie on different parts of the molecule, actin- and polyproline binding can occur concomitantly. This explains why the profilactin complex can be purified on polyproline-beads.

Crystal structure has not yielded a location for a PIP_2-binding-site. Attempts to localize the binding site in the molecule using site-specific mutagenesis (Sohn et al. 1995) or cross-linking (Chaudhary et al. 1998) have mapped residues involved on different sites, once in the amino- and carboxy-terminal helices, once overlapping with the actin binding site.

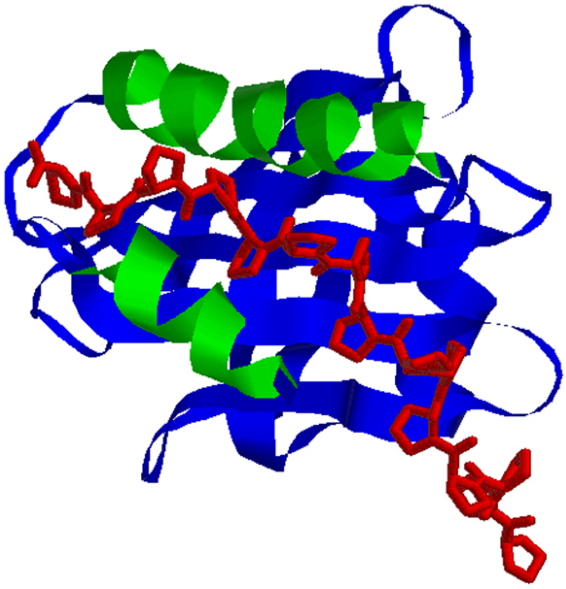

Figure 7: Crystal-structure of human platelet profilin and a decamer of poly-L-proline. The polyproline-helix is shown in red, profilin's N- and C-terminal helices in green.

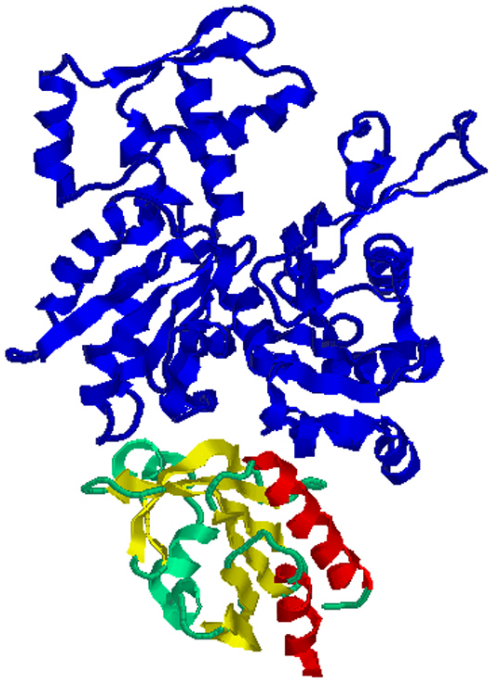

Figure 8: Crystal-structure of the bovine profilin I-β-actin-complex. Actin is shown in blue. In red, the two terminal helices of profilin, in yellow, the β-strands.

The overall structure of profilin is not homologous to other polyproline-binding domains like SH3- or WW-domains (Guruprasad et al. 1995; Mahoney et al. 1997), which indicates that profilin represents a novel binding module for proline-rich ligands. Instead, its structure shows similarity to the PAS-domain (for Per, ARNT and Sim (Ponting and Aravind 1997) of photoactive yellow protein (Borgstahl et al. 1995). PAS-proteins are a ubiquitous class of sensory transduction domains. The fold is also similar to the GAF-domain, a cGMP-binding domain (Ho et al. 2000), and, as only recently discovered, to Sec22b, a SNARE involved in ER/Golgi trafficking (Gonzalez et al. 2001). Figure 9 shows a comparison of these structures.

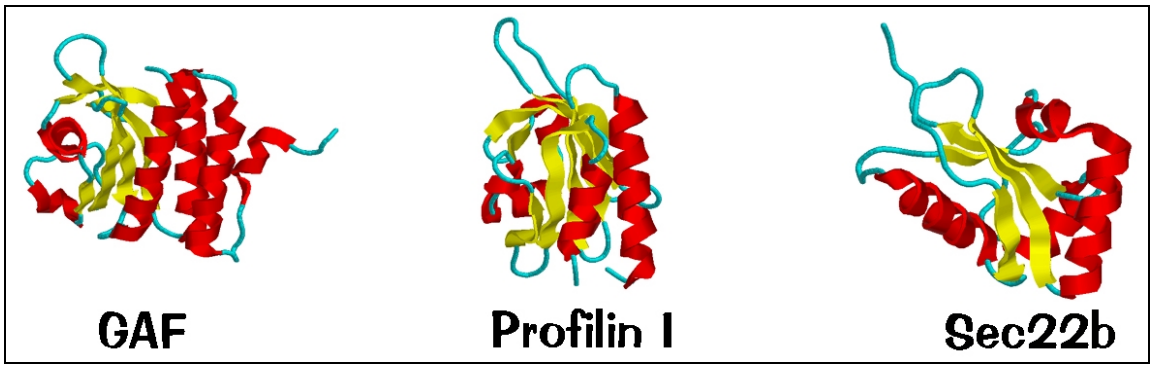

Figure 9: Structure comparison of the GAF-domain, profilin I and Sec22b. The recurring theme is two pairs of helices divided by a β-pleated sheet.

1.3.5 Profilin function in cells: actin binding vs. ligand binding

Profilin has been found in all eukaryotic organisms. Independent of evolutionary status, either one profilin (like in yeast and *Drosophila*) or more profilins are present. The slime molds *Physarum* and *Dictyostelium* Binette et al. 1990; Haugwitz et al. 1991) have two profilins. *Acanthamoeba* has three isoforms, profilin I being alternatively spliced (Kaiser et al. 1986). Kwiatkowski et al. proposed only one functional profilin gene in humans (Kwiatkowski et al. 1990; Kwiatkowski and Bruns 1988), but later on a second profilin was found (Honore et al. 1993) and very recently a third one (Hu et al. 2001).

Profilin structures from a variety of organisms have been solved, among them *S. cerevisiae* (Eads et al. 1998), cow (Cedergren-Zeppezauer et al. 1994; Schutt et al. 1993), humans (Metzler et al. 1993; Metzler et al. 1995), *Acanthamoeba* (Vinson et al. 1993) and plants (Fedorov et al. 1997; Thorn et al. 1997). Overall, profilins from different species, even with a considerable degree of sequence variation, share the same molecular architecture and global biochemical characteristics in terms of binding to actin, polyproline and phosphoinositides. However, binding affinities for these ligands differ among the isoforms, suggesting that different isoforms might have distinct cellular roles. For example, *Acanthamoeba* profilin isoforms I and II have similar affinities for both G-actin and polyproline, but profilin II binds 10-50 fold better to PIP_2 than *A. castellanii* profilin I (Kaiser et al. 1986, Machesky et al. 1990, Petrella et al. 1996).

The biochemical properties of human profilin I and profilin II are comparable to each other with respect to PIP_2- and poly-L-proline binding, but the affinity for actin is 4- to 5-fold higher for human profilin I compared with human profilin II (Gieselmann et al. 1995).

Like men, mice have three profilin genes, profilin I being ubiquitously expressed, while profilin II is a neuron-specific isoform (see Figure 10) and profilin III only expressed in kidney and testes (Hu et al. 2001, not shown).

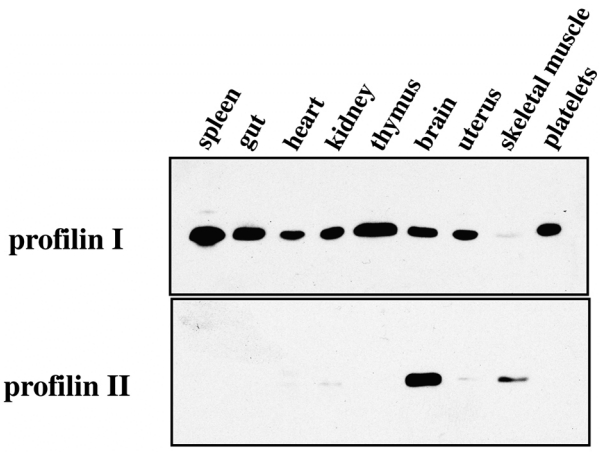

Figure 10: Tissue western blot for profilin I and profilin II expression in mouse. Profilin I is ubiquitously expressed with the exception skeletal muscle, while profilin II is mainly restricted to brain (taken from Witke et al. 1998)

Profilin II was shown to be alternatively spliced, producing a splice-form (profilin IIB) which has lost actin- and polyproline binding features (Di Nardo et al. 2000).

Various studies in lower eukaryotes have proved that profilin is important for the control of the actin-cytoskeleton and essential for life. Yeast lacking profilin also lack actin cables and are impeded in redistribution of actin to the contractile ring, which is necessary for cell division. *Cdc3*, the profilin homolog, is an essential gene in *S. pombe* (Balasubramanian et al. 1994). In *S. cerevisiae,* lack of profilin (*PFY1*) manifests in uncontrolled actin distribution and severe growth defects (Haarer et al. 1990) or lethality in some strains.

Dictyostelium cells only show defects when both profilin-isoforms are missing. They manifest in increased F-actin content and size as well as motility- and cytokinesis defects (Haugwitz et al. 1994).

Drosophila *chickadee*-mutants are severely defective in meiotic cytokinesis (Giansanti et al. 1998), their nurse-cells show uncontrolled shape-changes, unusual F-actin architecture and are impaired in transport of cytoplasm to the oocyte (Cooley et

al. 1992). Furthermore, *chickadee* has been shown to cooperate with a biochemically similar protein, *ciboulot*, in central brain metamorphosis (Boquet et al. 2000). Together with the *abl*-tyrosine kinase, it regulates motor axon outgrowth in Drosophila (Wills et al. 1999).

In vivo, profilin has been shown to be functionally involved in the formation of microspikes in cells after stimulation of the small GTPase Cdc42, by enhancing nucleation of new actin filaments through the Arp2/3 complex after activation of the Wiskott-Aldrich Syndrome Protein, WASP (Suetsugu et al. 1998; Yang et al. 2000). The Arp2/3 complex had first been identified by affinity-chromatography on profilin-sepharose from *Acanthamoeba* (Machesky et al. 1994a).

In mouse, ablation of the ubiquitously expressed profilin I gene is lethal. Mutant embryos seem to have cytokinesis defects and fail to implant in the uterus (Witke et al. 2001). On the contrary, mice lacking the neuron-specific profilin II gene are viable, but show behavioural defects (Di Nardo 2001). This supports the idea of profilin isoforms having different functions, with profilin I being the housekeeping gene while profilin II might have specialized tasks in the nervous system.

What may be the basis for functional differences between the profilin isoforms? The differences in actin binding of the two profilin isoforms in mouse are rather insignificant and unlikely to account for the diverse phenotypes of profilin mutant mice. One way of finding out about the *in vivo* function of a protein is to analyze the interaction with binding partners for this protein in the cell. Our lab has isolated the profilin ligands from mouse-brain for profilin I and II by affinity-chromatography on the immobilized recombinant proteins. Identification of some of the binding partners by mass spectrometry identified ligands which are involved in signal transduction and endocytosis (Witke et al. 1998, see Figure 11). Apart from actin, which is present in both complexes, the ligand pattern for the two profilin-isoforms is very different.

Proteins identified in the profilin I complex were clathrin, valosine containing protein (VCP), hsp 70 and tubulin. Clathrin forms a lattice around budding vesicles at the plasma membrane, while VCP is an ATP-binding protein with homology to the cdc48/sec18/NSF family (Frohlich et al. 1991) which forms a complex with clathrin and hsp 70 (Pleasure et al. 1993) involved in vesicle transport.

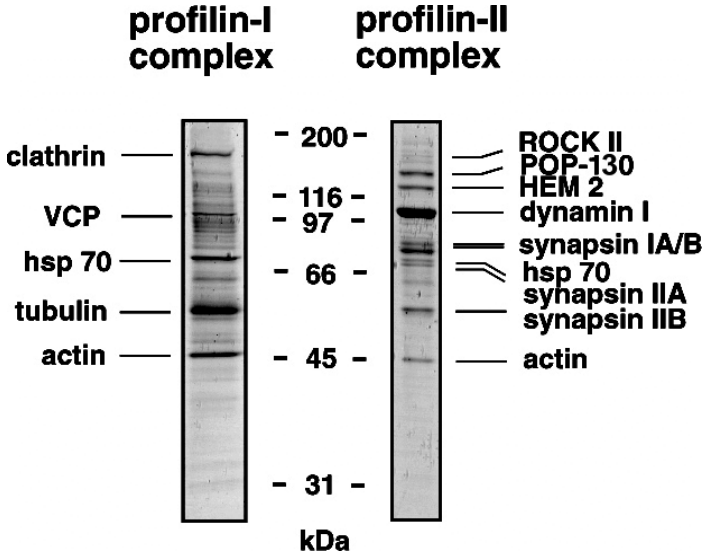

Figure 11: The profilin-complexes from mouse-brain. Ligands for the two profilin-isoforms were identified by mass spectrometry (from Witke et al. 1998)

Proteins found in the profilin IIA complex are involved both in membrane trafficking and signal transduction. Rho-associated coiled-coil kinase (ROCK) is a downstream-target of the small GTPase rho and cooperates with another known profilin-ligand, diaphanous, in actin-stress fiber formation (Watanabe et al. 1999). A novel protein of unknown function with a molecular weight of 130 kD named partner of profilin (POP-130) was found associated with profilin II. HEM 2 is a protein identical to the rat NAP1 (Kitamura et al. 1996), which was shown to bind to the small GTPase rac (Kitamura et al. 1997) and whose *Drosophila*-homolog is believed to be important for cytoskeletal regulation and axon guidance (Hummel et al. 2000). The synapsins are presynaptic phosphoproteins which are thought to be a link between the actin-cytoskeleton and synaptic vesicles (Doussau and Augustine 2000). A prominent band was identified as dynamin I, a neuron-specific member of the dynamin-family of large GTPases, who are key components of vesicular trafficking (McNiven et al. 2000a, see below" …and bigger ones").

Are ligands other than actin therefore important for profilin's function? *In vivo* evidence supports this view. So are the defects shown by yeast lacking profilin not only due to the actin-binding capabilities of profilin, since also profilin mutants deficient in polyproline binding cannot rescue lethality (Ostrander et al. 1999).
Also in mouse, apart from the mere control of actin dynamics, interaction with other ligands seems to be functionally important. So die mice which are heterozygous for

profilin I and deficient for the profilin ligand Mena *in utero* of exencephaly and show defects in neurulation (Lanier et al. 1999), while this is not the case in either of the separate genetic backgrounds.

If non-actin ligands are indeed important for the function of profilin, the presence of so many proteins involved in membrane trafficking processes in the profilin-complexes from mouse brain spurs the discussion of a possible involvement of profilin in events like exocytosis and endocytosis. *S. cerevisiae* profilin has already been genetically linked to Sec3p, a protein involved in vesicle maturation and exocytosis (Finger and Novick 1997). In *Dictyostelium*, profilin null cells were shown to have alterations in secretion and uptake of nutrients (Temesvari et al. 2000) and genetic interaction was seen with an integral membrane protein of the endosomal/lysosomal system, DdLIMP (Karakesisoglou et al. 1999). But since profilin is an actin-binding protein, the first step to address this question is to take a look at what actin is doing in processes like endocytosis, exocytosis, vesicle transport and recycling.

1.4 The actin cytoskeleton and membrane trafficking

1.4.1 Actin at the membrane: barrier or catalyst?

It has been suggested for a long time that actin is involved in membranedynamics, but relatively little is known about the underlying mechanisms, and results were often ambiguous.

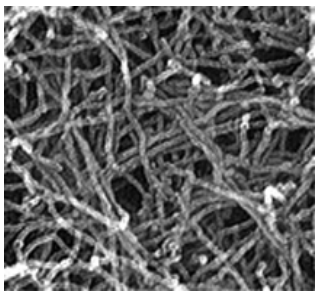

Figure 12: SEM-micrograph of *Xenopus* keratocyte actin-cytoskeleton in the cell cortex. Taken from Svitkina and Borisy 1999.

The cortical actin meshwork underneath the plasma membrane (see Figure 12) is believed to block access of exocytic vesicles to the membrane in neurosecretory cells (Trifaro et al. 2000). However, the role of actin in membrane trafficking cannot be completely inhibitory, since endocytosis can be inhibited in polarized epithelial cells upon actin depolymerization, while stabilization of actin filaments had no effect (Gottlieb et al. 1993). Actin sequestering agents like thymosin β4, DNAseI and latrunculin A have been shown to interfere with different early steps in the endocytic process (Lamaze et al. 1997). It is conceivable that actin forms a contractile structure around the necks of budding endocytic vesicles and thus helping in the pinching process, although evidence for this is not completely clear (Fujimoto et al. 2000). Furthermore, reports indicate that actin facilitates the uptake of receptor ligands and their shipping between endocytic compartments (Durrbach et al. 1996). On one hand, actin has been reported to be enriched at hot spots of endocytosis in nerve terminals (Gustafsson et al. 1998), on the other hand the immediate environment of coated pits has been shown to be almost completely devoid of actin (Fujimoto et al. 2000), suggesting that the dense actin meshwork underneath the membrane may have to be disassembled underneath coated pits. Perhaps sites of endocytosis are locally defined by actin serving as a diffusion barrier for membrane components involved in clathrin-coated pit formation (Gaidarov et al. 1999b; Roos and Kelly 1999), thereby indirectly favoring the kinetics of pit formation.

1.4.2 Hunting tiny vesicles

Some proteins interact directly with clathrin-coated vesicles and actin. The HIP1R (Huntingtin-interacting protein-related) protein, for example, was shown to be associated with clathrin-coated pits and and vesicles both at the plasma membrane and in the perinuclear region (Engqvist-Goldstein et al. 1999). Its C-terminal talin-like domain binds F-actin *in vitro* and localizes the protein to cortical actin *in vivo*, while the N-terminal half connects it to vesicles. This protein might therefore serve as a physical link between clathrin-coats and the actin-cytoskeleton.

Another family of proteins found in nerve terminals are the synapsins, which have been shown to bind to F-actin and synaptic vesicles in a phosphorylation-dependent

manner, and are thought to tether the reserve pool of synaptic vesicles to the F-actin-scaffold (Doussau and Augustine 2000).

1.4.3 Rocketing vesicles

After vesicles have pinched off their parental membrane, actin might help them to move around in the cytoplasm. Recently, vesicles have been described to propel through the cytoplasm on actin-rich "comet tails" (Merrifield et al. 1999; Rozelle et al. 2000; Taunton et al. 2000), a process, in which localized actin polymerization provides the driving force for propulsion. This is a mechanism known to be exploited by pathogens like *Listeria*, *Shigella* and *Vaccinia*-virus.

Long-range transport of vesicles in cells is usually carried out on microtubules by microtubule specific motor proteins. However, short-range transport or transport of exocytic vesicles in the vicinity of the plasma membrane as well as vesicle transport in nerve terminals can occur on actin cables (Evans and Bridgman 1995; Langford 1995). The microtubule- and the actin transport systems have been shown to interact directly (Huang et al. 1999), and it is thought that this interaction involves unconventional myosins (Huang et al. 1999; Tuxworth and Titus 2000).

1.4.4 Rafts and actin

Rafts are low-density, detergent-insoluble, cholesterol-enriched membrane microdomains. They accumulate glycosylphosphatidol(GPI)-anchored proteins and serve as signalling platforms in a variety of cells. Harder and Simons have shown that rafts can induce the formation of F-actin in a tyrosine-phosphorylation dependent manner (Harder and Simons 1999). Furthermore, rafts are thought to be important for synaptic vesicle formation (Martin 2000; Thiele et al. 2000) and trafficking from the trans-Golgi (Wang et al. 2000).

Almost fifty percent of cellular PIP_2 has been shown to localize to these domains (Liu et al. 1998; Pike and Casey 1996; Pike and Miller 1998). A major regulatory protein of actin nucleation and rearrangement downstream of the small GTPase Cdc42 and maybe tyrosine kinases, N-WASP, was shown to be activated by PIP_2 (Miki et al. 1996). This mechanism can lead to the propulsion of PIP_2-containing, raft-enriched

vesicles through the cytoplasm (Rozelle et al. 2000). Actin-regulatory proteins of the GMC-family (GAP43, myristoylated alanine-rich C kinase substrate (MARCKS), CAP23) were shown to modulate PIP_2 in these raft membrane patches, regulate actin dynamics and control neurite outgrowth *in vivo* (Frey et al. 2000; Laux et al. 2000).

1.4.5 Small G-proteins…

Small ras-related G-proteins of the rab family have been implicated in various steps of endocytic vesicle trafficking (Novick and Zerial 1997). Also GTPases of the rho family are being involved in coordinating peripheral membrane-dynamics and appropriate actin-rearrangements (Lamaze et al. 1996; Murphy et al. 1996). Upstream of those, another member of a yet different group of small G-proteins, the ADP-ribosylation factor member 6 (Arf6) seems to play a major role in vesicle recycling and cytoskeletal reorganization.

Arf6-expression overlaps with the transferrin receptor recycling compartment in cells (D'Souza-Schorey et al. 1998) and with the small GTPase rac1, which induces actin-rich lamellipodia and ruffles, on recycling endosomes and at the plasma membrane. Rac1-induced ruffling activity can be blocked by an Arf6 mutant (Radhakrishna et al. 1999). It has been speculated that Arf6 can control the shuffling of rac1 to the plasma membrane, where it excerts its actin-modulatory action.

A growing family of molecules catalyzing either GTP hydrolysis or nucleotide exchange on Arfs (ArfGAPs and -GEFs) is being identified, which localize to different cellular locations and are thought to regulate Arf6-activity in a spatially controlled manner (reviewed in de Curtis 2001). ArfGAPs of the ASAP1- and the GIT-family, for example, are thought to be responsible for the redistribution of adhesion and signalling molecules from focal complexes via the endosomal recycling compartment to the leading edge of migrating cells (de Curtis 2001; Randazzo et al. 2000).

1.4.6 …and bigger ones

One key-molecule in membrane-trafficking processes is the 100 kDa GTPase dynamin, which has also been found in complexes purified on affinity-columns of

profilin II from mouse brain (see Figure 11). Three dynamin isoforms have been described, with multiple splice forms. Dynamin II is ubiquitously expressed, dynamin I a neuron-specific isoform and dynamin III somewhat enriched in testis (Cao et al. 1998). It is believed that dynamin assembles in a ring-like structure around the necks of budding vesicles and helps in the pinching process. Whether it acts as a force-generating motor-enzyme or as a control molecule in the manner of small GTPases is still under discussion (Marks et al. 2001; McNiven 1998; Sever et al. 1999; Stowell et al. 1999; Yang and Cerione 1999). Nevertheless, it was shown to be an essential molecule for synaptic vesicle recycling, and various dynamin mutants have been described which inhibit endocytosis (Herskovits et al. 1993a). Recently, the dynamins, apart from pinching off vesicles at the plasma membrane, have been implied in a variety of other cellular processes, many of them are also known to involve actin function (Cao et al. 2000; Henley et al. 1999; McNiven et al. 2000a, see Figure 13) among them phagocytosis (Gold et al. 1999), trafficking of post-Golgi vesicles (Kreitzer et al. 2000) and also endosome-Golgi trafficking (Nicoziani et al. 2000).

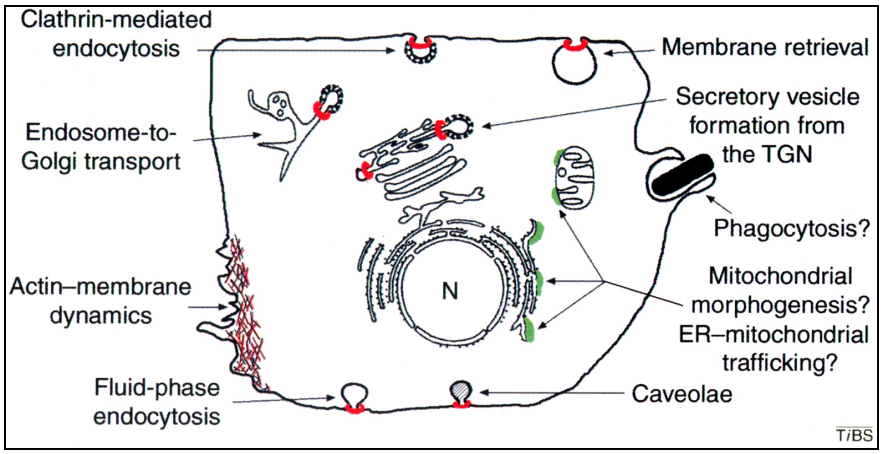

Figure 13: Dynamin functions in the cell. Figure taken from McNiven et al. 2000a.

Dynamin II has been found to co-localize with actin in ruffles and lamellipodia. The SH3-domain-containing actin-binding protein cortactin was shown to contribute to recruit dynamin to these structures (McNiven et al. 2000b). Dynamin was also found in adhesion-structures called podosomes (Ochoa et al. 2000), which are a columnar array of actin-filaments, often surrounding an invagination of plasmalemma roughly perpendicular to the substratum.

Besides a GTPase-domain, dynamin has a PH-domain which was shown to target it to the membrane and in turn stimulate its GTPase activity (Zheng et al. 1996). The C-terminus contains a basic proline-rich domain (PRD), which has been shown to be a docking site for many SH3-domain containing regulatory or adaptor molecules, some of which also stimulate dynamin's GTPase-activity (Gout et al. 1993). Among the molecules binding to the PRD are PLC-γ, Grb2 (Seedorf et al. 1994), endophilin (SH3P4) (Ringstad et al. 1997), amphiphysin (David et al. 1996), src-kinase (Foster-Barber and Bishop 1998; Herskovits et al. 1993b) and syndapin (Qualmann et al. 1999).

The amphiphysins interact with the AP2-adaptor complex and clathrin and are thought to link them to dynamin. Antisense oligonucleotides against amphiphysin lead to the collapse of growth cones and inhibited neurite-outgrowth in hippocampal neurons. In those cells, no changes in endocytosis were detected; suggesting that this phenotype is most probably not a secondary endocytosis-effect, yet rather has to do with the actin cytoskeleton. But on the other hand, no direct interaction of amphiphysin with F- or G-actin was found (Mundigl et al. 1998).

Endophilin (SH3P4) is a lysophosphatidic acid acyl transferase (Schmidt et al. 1999b) which interacts with dynamin (Ringstad et al. 1997) and the phosphatidylinositol-phosphatase synaptojanin (Micheva et al. 1997) via an SH3-domain that is very similar to Grb2 (Ringstad et al. 1997). It is thought to contribute to the pinching process of vesicles by introducing wedge-shaped phospholipids into the membrane and thereby promoting a shape-change of the lipid bilayer (Schmidt et al. 1999b).

Also the syndapins interact not only with dynamin, but also with synaptojanin, synapsin and N-WASP (Qualmann and Kelly 2000; Qualmann et al. 2000; Qualmann et al. 1999). They affect endocytosis as well as the actin cytoskeleton, maybe by triggering actin polymerization via N-WASP in the vicinity of sites of dynamin action.

Recently, the F-actin-binding protein Abp1 (SH3p7/HIP-55) was shown to bind to dynamin and has been implied in endocytosis. Overexpression of its SH3 domain blocked endocytosis, but when the actin-binding domain was added, endocytosis was restored (Kessels et al. 2001). This molecule may be a physical link between cortical actin and the endocytic machinery.

Apparently there are multiple physical links between membrane systems and the actin-cytoskeleton. This and the fact that actin polymerization occurs always in the vicinity of membranes *in vivo*, makes actin and membranes partners which reciprocically influence and depend on each other.

2 RESULTS

2.1 Antibodies as tools to analyze profilin-ligand interaction

2.1.1 Polyclonal antibodies

Rabbit antibodies were raised against profilin II, endophilin (SH3P4), VASP, Mena, POP-130 and dynamin I.

2.1.1.1 Profilin II

Recombinant profilin II (see Purification of recombinant profilin II) was partially digested with V8-protease, and the fragments used as an antigen in rabbits. The resulting antiserum ("2T") recognizes profilin II but not profilin I in tissue lysates (see Figure 14 A) and is able to immunoprecipitate the protein (shown in Figure 14 B).

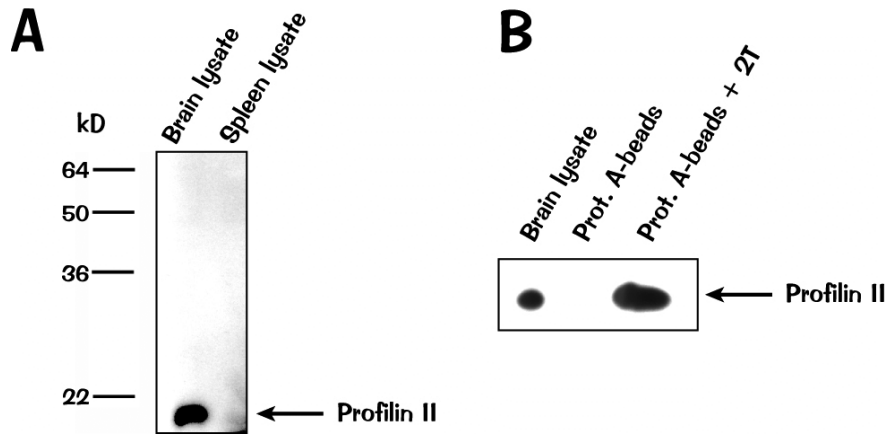

Figure 14: A: Western blot of tissue lysates probed with the anti-profilin II antiserum 2T. Spleen lysate was used as a control for cross-reactivity with profilin I. B: Immunoprecipitation experiment with the antiserum 2T. Protein A-beads were used as a control for unspecific binding.

2.1.1.2 POP-130

In order to generate a POP-specific polyclonal antibody, a 50 kD N-terminal truncated form of the protein was expressed with a 6xhistidine-tag. This fragment, as well as other parts of the protein expressed in E. coli, was insoluble. The fragment was purified from bacterial inclusion bodies and rabbits were immunized with it.

Figure 15 shows that the antiserum specifically recognized a protein of around 130 kD in brain lysate which was highly enriched in the profilin II-brain complex.

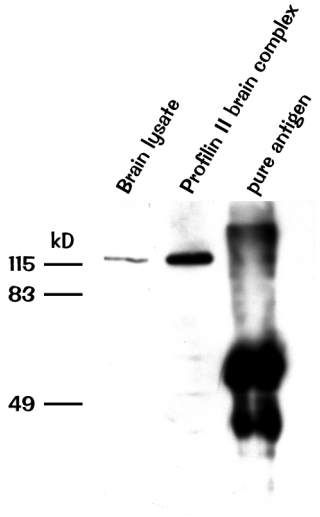

Figure 15: Western blot showing the reactivity of the anti-POP-130 antiserum on brain lysate, the profilin II complex from brain and on the antigen (50 kD) used for immunization.

2.1.1.3 Mena

Mena-protein was expressed in insect cells as an N-terminal 6x His-fusion. Baculovirus stocks were a gift from Frank Gertler. No full-length Mena could be obtained due to degradation of the protein already inside the cells. The resulting N-terminal truncates which bound to Ni-NTA resin were used as an antigen in rabbits.
The rabbit serum recognized two bands of 85 and 140 kD on western blots of brain lysates, which correspond to two different splice-forms of the Mena-protein. Both splice forms are highly enriched in the profilin II complex from mouse brain (see Figure 16 A). As Figure 16 B shows, the antiserum also works well in immunofluorescence, staining focal adhesion structures and actin stress fibers.

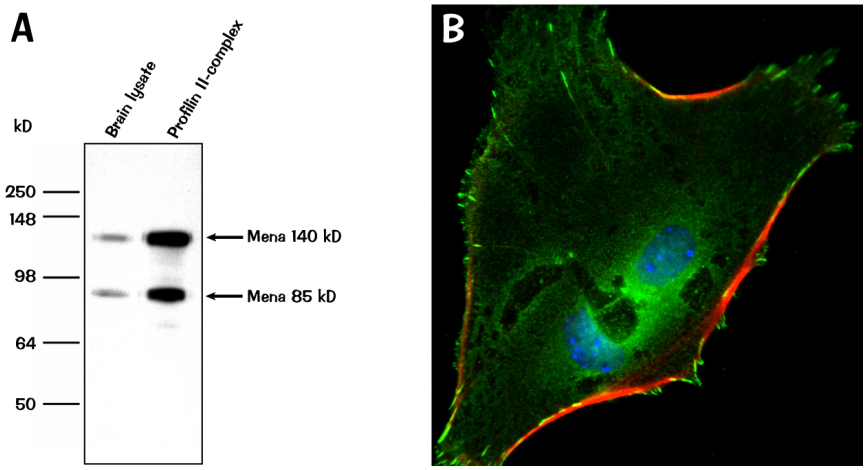

Figure 16: A: Western blot of brain lysate and the profilin II complex from mouse brain. The polyclonal Mena antibody shows two bands on the western blot: the lower band of around 85-90 kD resembles the ubiquitous splice form, the upper band of about 140 kD is a brain-specific splice form of Mena. Both forms are highly enriched in the profilin II complex. B: Immunofluorescence micrograph showing a fibroblast-like cell from a primary mouse brain culture. The green signal for Mena lights up in focal adhesions and along actin stress fibers. Actin is stained in red, nuclei in blue. Regions of overlap of the red and green signal are yellow.

2.1.1.4 Endophilin

Endophilin-cDNA was a gift from H.D. Söling. The antigen for endophilin was the full-length protein fused to GST expressed in *E.coli*. The antiserum shows reactivity with a single band of around 40 kD in size on western blots of brain lysate (see Figure 17

A). In immunostaining, a signal can be seen throughout cell body and neurites in neurons (see Figure 17 B).

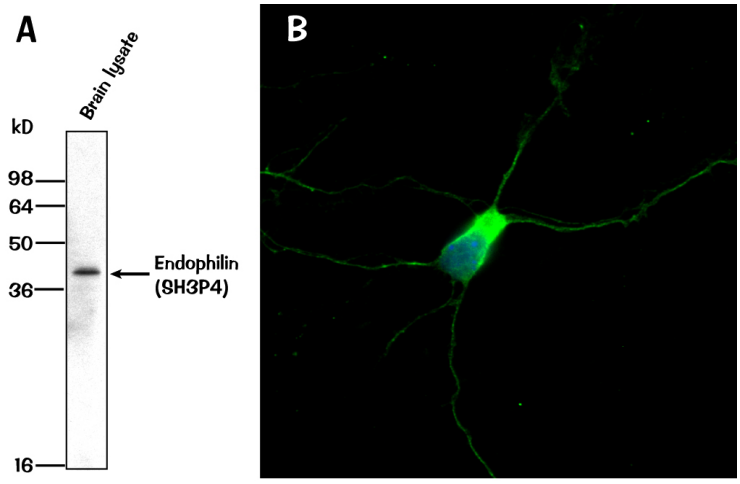

Figure 17: A: Western blot of brain lysate probed with the polyclonal endophilin antibody. A single band of about 40 kD is visible. B: Immunostaining of a primary cortical neuron with the same antibody. Reactivity (green) is seen throughout the cell body and the neurites.

2.1.1.5 Dynamin

The antigen for generation of a polyclonal antibody against dynamin was made by fusing the full-length dynamin Iaa cDNA to GST and expressing the construct in insect cells (see Expression and purification of full-length dynamin in insect cells). The whole GST-fusion protein served as antigen. The rabbit serum (KG-43) after immunization detected a single band of around 100 kD on western blot (see Figure 18A).

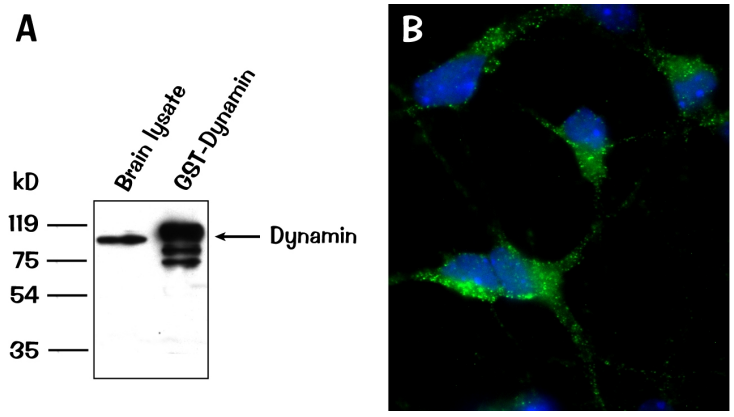

Figure 18:A: Western blot of brain lysate and the GST-fusion-protein used as an antigen probed with the polyclonal antibody KG-43 against dynamin. In brain lysate a single band of around 100 kD is visible. B:

Immunostaining with the same antibody on primary cortical neurons. The antiserum (green) shows a punctate pattern.

In immunofluorescence on mouse cortical neurons, the antiserum showed punctate staining as shown in Figure 18B. The serum worked in ELISA and also in immunoprecipitation (not shown).

2.1.1.6 VASP

A baculovirus strain encoding for His-tagged VASP, which was a gift from F. Gertler, served to express the full-length protein with an N-terminal addition of 6 histidines. This protein was used as an antigen to immunize rabbits.

The resulting rabbit serum showed a doublet on western blots of tissue lysates, which corresponds to the 46 and 50 kD forms of this phosphoprotein. The doublet was seen to be highly enriched in profilin complexes from tissues (see Figure 19 A).

In immunofluorescence, the antibody showed the typical staining pattern for adhesion sites (focal contacts), where VASP is known to localize to (see Figure 19 B).

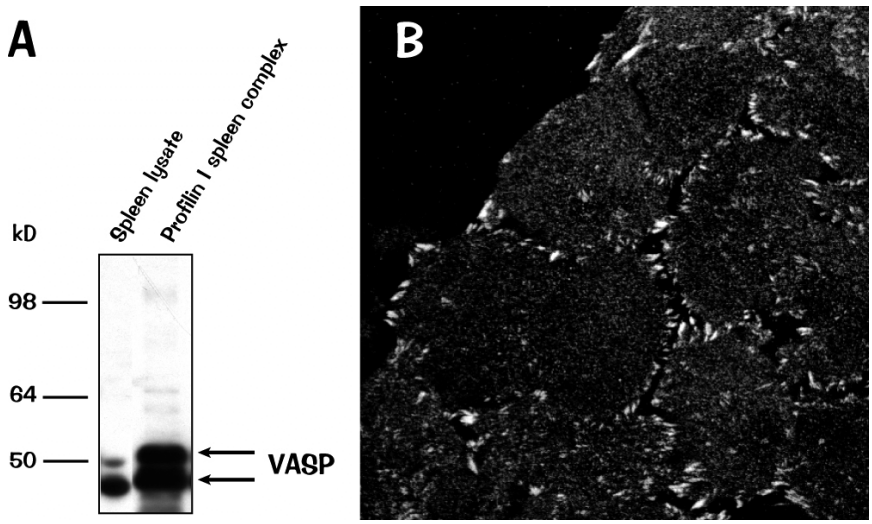

Figure 19: A: Western blot of spleen lysate and the profilin I complex from mouse spleen probed with the polyclonal antibody against VASP. VASP is known to be heavily phosphorylated and the antibody shows a double band on the tissue lysate, which have been described as 46 and 50 kD forms of VASP (Reinhard et al. 1992). The proteins is highly enriched in the profilin I complex. B: Confocal immunofluorescence micrograph showing staining for VASP in focal contacts of HeLa cells.

2.1.2 Monoclonal antibodies against profilin II

Mouse monoclonal antibodies were raised against profilin II. After immunizing mice with the full-length protein, bleeds were checked by western blot and ELISA. A serum positive mouse for profilin II was used for hybridoma fusion. Hybridomas were screened by ELISA and cloned by limiting dilution. The fusion yielded a number of positive clones which are listed in Table 1.

Clone		Subclass	Light chain	Specificity	ELISA	Western blot	IP
1A4	1A4D8	IgM	κ	PI+PII	+	-	nd
4C9	4C9G10	IgM	κ	PII	+	-	nd
5A7	5A7C11B8	IgG1	κ	PII	++	-	+
	5A7D6	IgG1	κ	PII	++	-	+
	5A7F11D5	IgG1	κ	PII	++	-	+
5D11	5D11C9G9	IgM	κ	PI+PII	+	-	nd
7D4	7D4G9D6	IgM	κ	PI+PII	+	-	nd
	7D4D8B5	IgM	κ	PI+PII	+	-	nd
8C8	8C8E8	IgM	κ	PI+PII	++	-	-

Table 1: Summary of the hybridoma-fusion for making monoclonal antibodies against profilin II. IP stands for immunoprecipitation.

All clones tested except for one produced antibodies of the IgM-subclass, and all antibodies had light chains of the κ-type. One clone, 5A7, produced profilin II-specific antibodies of the IgG1-subclass.

Despite the specificity of the mouse serum for profilin II before fusion, most of the hybridoma clones obtained produced antibodies which recognized profilin I and profilin II. Unfortunately, none of the hybridoma supernatants worked on western blot. However, antibodies produced by clone 5A7 (IgG1) worked nicely in ELISA and immunoprecipitation (see Figure 20).

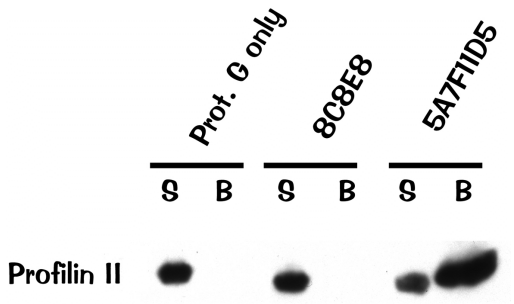

Figure 20: Immunoprecipitation from mouse brain lysate with two monoclonal antibodies. S: supernatant, B:bound.

2.2 Studies on the profilin complexes from mouse tissues

Previous work in our lab had identified a couple of different ligands for the profilin isoforms I and II from mouse brain (shown in Figure 21) by affinity-chromatography. Surprisingly, binding partners were mainly proteins involved in vesicle trafficking and signalling, which pointed at possible novel functions for the profilins. Furthermore, the two isoforms were binding to different sets of ligands, which may be the basis for isoform-specific functions.

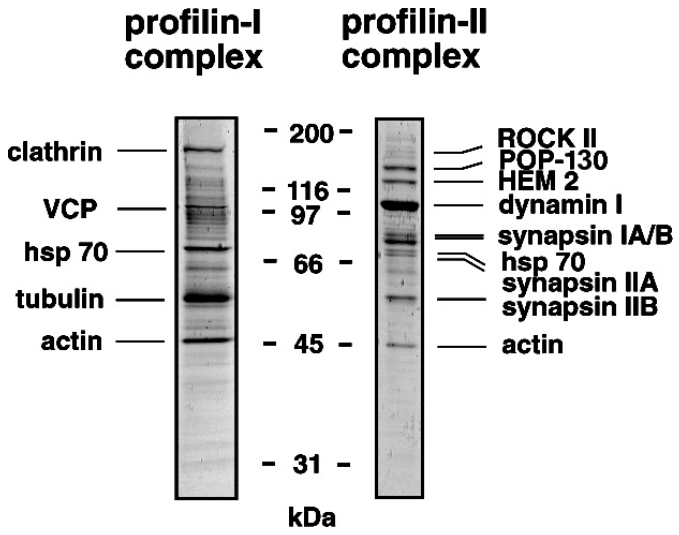

Figure 21: Silver-stained protein gel showing the profilin complexes from mouse brain. Ligands were identified by mass spectrometry. Figure from Witke et al. 1998.

In order to identify and characterize profilin ligands other than actin and to work out differences in ligand binding for profilin I and II, two strategies were followed: first, a careful study in brain was to reveal more non-actin ligands for both profilins, since this is the only organ, in which both profilin I and profilin II are expressed in abundance. Differences in ligand binding might then give hints at functional differences.

Second, a systematic study of non-actin ligands in other tissues was to answer the question whether the profilin-complexes are the same throughout the body, or whether there are tissue-specific differences, which might also help to clarify the function of profilin in those tissues.

As a prerequisite for affinity-chromatography, it was first necessary to purify functional recombinant profilin in good quantities. The pure protein could then be coupled to CNBr-activated resin to make affinity-beads.

2.2.1 Purification of recombinant profilin II

Recombinant profilin II (and analogously, profilin I) was expressed with a T7-based expression system in E. coli (see Material and Methods).

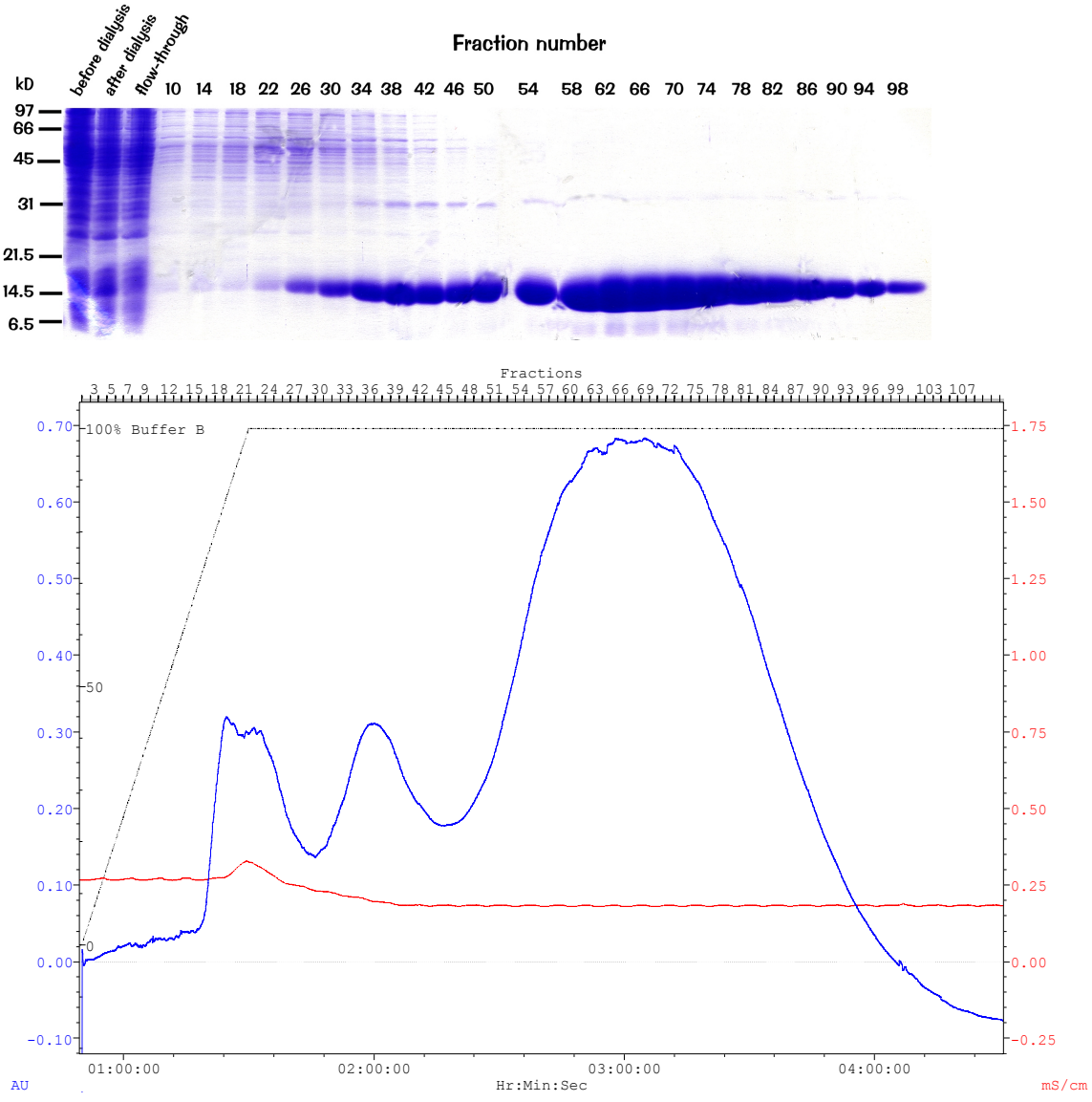

Figure 22: Purification of recombinant profilin II from bacteria. Below: Elution-profile of the poly-L-proline-column with a gradient of 2-8 M urea. Above: The corresponding Coomassie-gel with the fractions.

After denaturing lysis, the refolded protein was bound to a poly-L-proline-column and eluted with a urea-gradient, as shown in Figure 22.

The functionality of the recombinant profilin II in respect to its main binding characteristics, i.e. binding to actin, poly-L-proline and phospholipids was assessed. Since the protein was purified exploiting its ability to bind to poly-L-proline, functionality in this respect was taken for granted. Functionality in respect to actin binding was shown by solid-phase binding assays using G-actin-beads and in pyrene-actin-polymerization assays as described in Materials and Methods (see Figure 23).

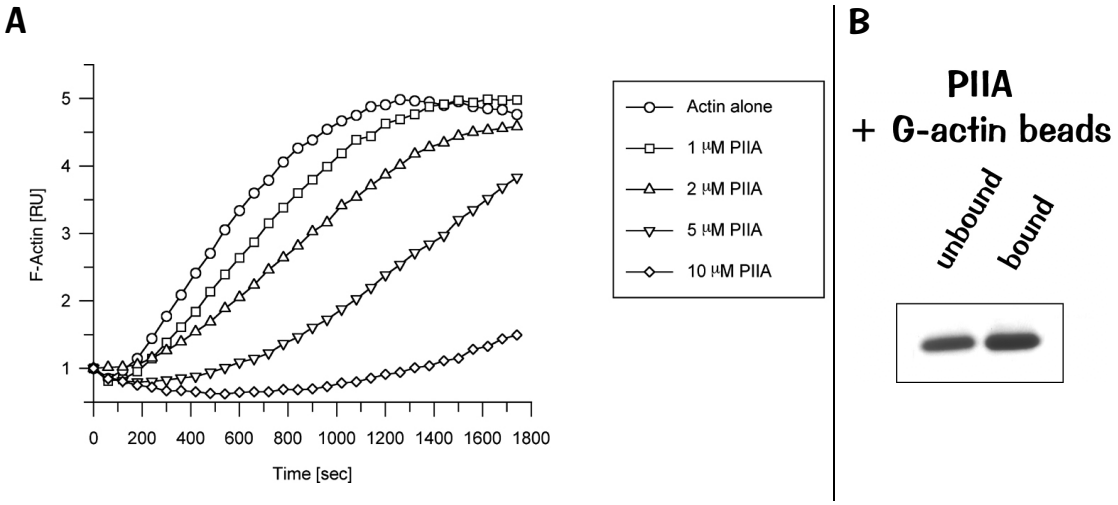

Figure 23: Actin-binding assays for recombinant profilin II. A: Pyrene-actin polymerization-assay with 5 μm actin and increasing amounts of recombinant profilin II. Increasing amounts of profilin II slow down the actin-polymerization kinetics by sequestering G-actin. B: Solid-phase binding assay on G-actin-beads. PIIA: profilin IIA, binds to actin-beads.

Binding to phosphatidylinositides was shown in a gel-filtration-based assay introduced by Lassing and Lindberg (Lassing and Lindberg 1985) (Figure 24). Profilin was allowed to bind to PIP_2-micelles and the mixture subjected to gel-filtration on a 15 cm Sephadex-200 column. Profilin bound to the PIP_2-micelles, which form structures of around 90 kD in aqueous solutions (Sugiura 1981) was detected as a shift in absorption at 280 nm. The lipid-micelles are not visible under these conditions, their presence was verified by precipitating PIP_2 as a calcium salt with $CaCl_2$.

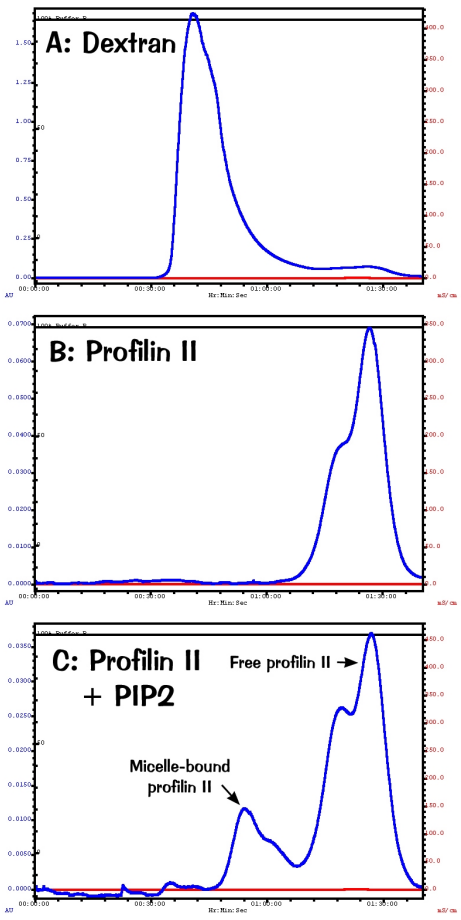

Figure 24: Assay for profilin binding to phosphatidyl-(4,5)-bisphosphate micelles by gel-filtration on a Sephadex-200 column. A: Blue dextran marks the void-volume of the column. B: Gel-filtration of profilin II alone. C: Gel-filtration of profilin II-PIP_2-micelle complexes.

2.2.2 The profilin complexes from mouse brain

After coupling of the recombinant profilins to CNBr-activated sepharose as described in Material and Methods, brain lysate was passed over the affinity beads, and after washing, the profilin complexes were eluted with SDS-sample buffer. Figure 25 shows a silver-stained protein gel with the profilin complexes from mouse brain. Glutathione-beads were used as a control for unspecific binding. This experiment reproduces published results and established the technique to prepare the complexes from other mouse tissues (see below).

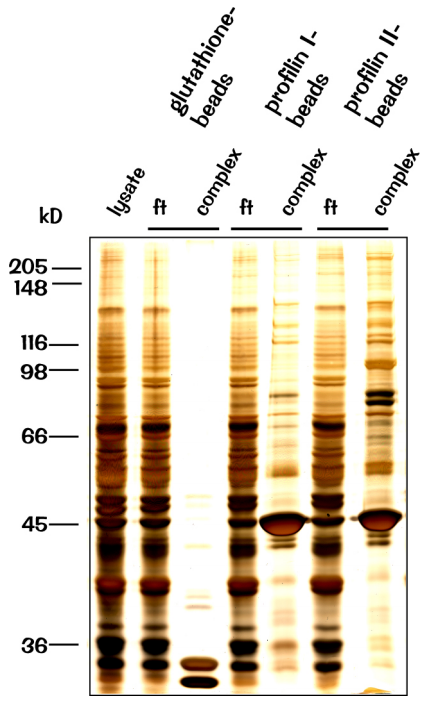

Figure 25: Silver-stained protein gel showing the profilin-complexes from mouse brain: complexes on glutathione-beads (control for non-specific binding), profilin I and profilin II. Ft: flow-through/unbound fraction.

To confirm that ligands isolated in the affinity-complexes can bind directly and *in vivo*, two examples of co-immunoprecipitation are shown in Figure 26. The adhesion-site protein Mena and the formin Diaphanous, both described as ligands for profilin, can be co-immunoprecipitated with an antibody against profilin II from brain lysate.

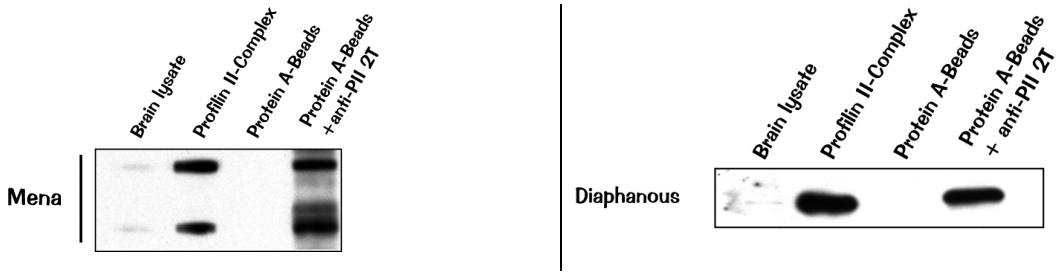

Figure 26: The profilin-ligands Mena and diaphanous found in the profilin II-complex can also be co-immunoprecipitated with the anti-profilin II antibody T2 from brain lysate. Western blot. The weak bands in the lysates result from the enrichment of those ligands in the complexes and loading of equal amounts of total protein.

By probing western blots of the brain complexes with protein-specific antibodies, two more novel profilin II-ligands were identified (see Figure 27): Profilin II binds the huntingtin-protein, mutations of which give rise to neurodegenerative disorders. Another profilin II-specific member of the brain complexes is the phosphatidylinositol phosphatase synaptojanin. Both proteins were not found in the profilin I-complexes.

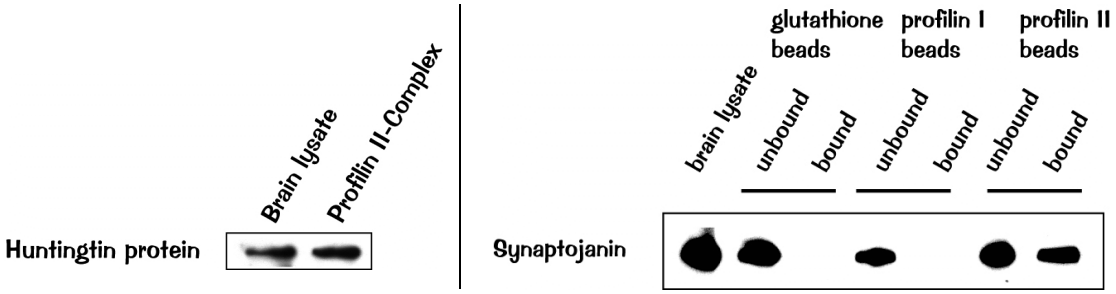

Figure 27: Novel ligands for profilin II in brain were identified by western blotting. Left, a western blot probed with a commercially available antibody against the Huntingtin protein (Chemicon, Temecula, USA). Right, brain complexes on profilin I and profilin II-beads probed with an antibody against synaptojanin (a gift from Dr Pietro DeCamilli).

2.2.3 The profilin complexes from other mouse tissues

To identify further ligands of the profilins, which might give a hint at profilin's function in the organism, the complexes from different organs of mice were isolated on affinity beads. The complexes on profilin I were purified from spleen, thymus, gut, heart and testis, while the profilin II-complexes were made from skeletal muscle and kidney, since the protein is expressed in these organs.

Figure 28 shows that both profilin-isoforms bind to a great number of ligands and that although there are common binding-partners the composition of the profilin-complexes differs in a tissue-specific manner.

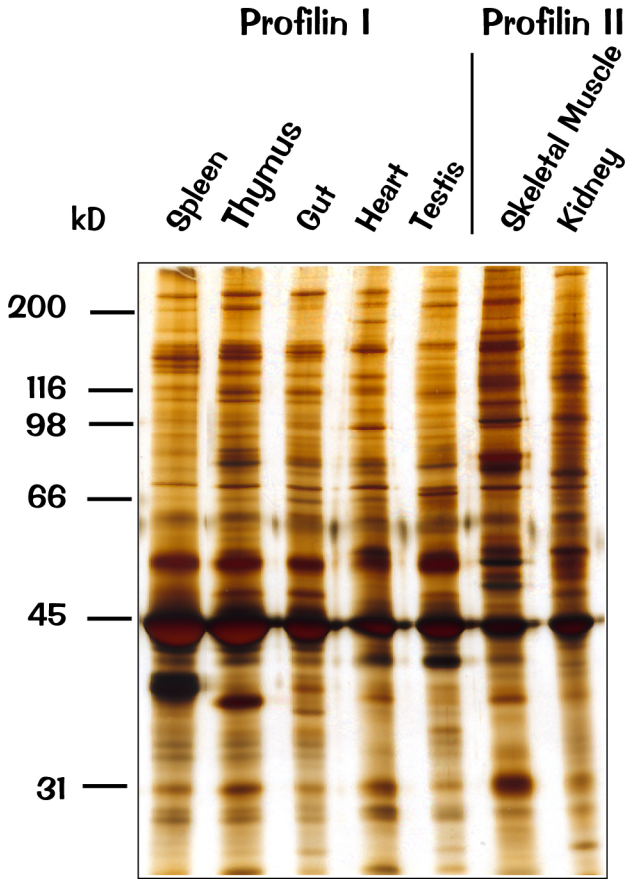

Figure 28: Silver-stained gel of profilin-complexes from various mouse-tissues

One way of identifying direct binding partners for the profilins is to do a blot-overlay. For this technique tissue lysates are blotted onto a membrane, the proteins allowed to renature and then overlaid with the recombinant profilins. Figure 29 shows this blot-overlay for the two profilin-isoforms. Also tissues in which profilin II is not normally expressed were included in the experiment to see if, like in brain, there are differences in the pattern of ligands binding to profilin I and profilin II from the same tissue extract.
Not all ligands are detected in this way, since not every protein renatures in a way that allows binding of the profilins (a good example is actin, which is not detectable on blot overlays). The ligand pattern shows that ligand-compositions for a given profilin-isoform is different from tissue to tissue. But the two isoforms also bind different sets of ligands in a given tissue (eg. compare the ligand pattern of uterus for profilin I and profilin II in Figure 29), like in brain.

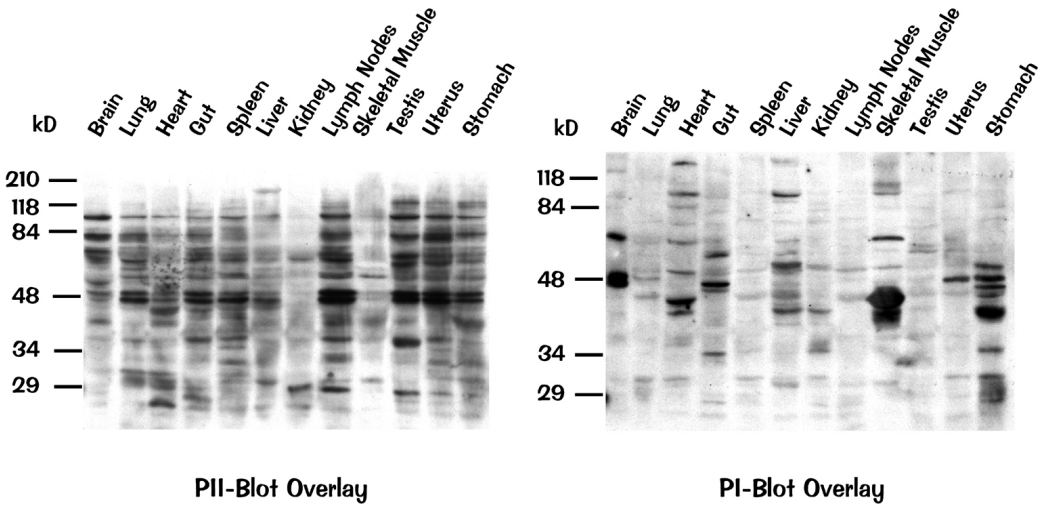

Figure 29: Blot-overlay with profilin I and profilin II on mouse organs

The tissue- and isoform-specific binding pattern for some profilin-complex members is also illustrated by western-blot: dynamin for example, is only found in profilin II-complexes, while tubulin is present preferentially in profilin I-complexes, like shown in Figure 30.

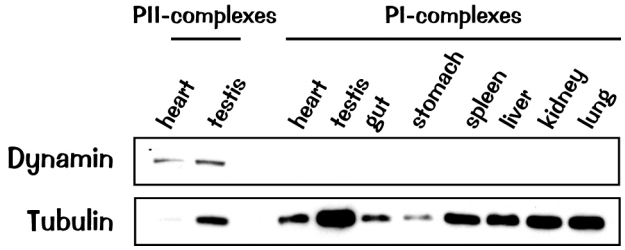

Figure 30: Western blot of some profilin-complexes probed with antibodies against dynamin (Hudy-1, Upstate biotechnology) and tubulin (Sigma).

Phosphatidylinositol-3-kinase, however, although speculated to interact with profilin (Bhargavi et al. 1998), has not been found in any of the complexes (see Figure 31). This also illustrates the specificity of the affinity-chromatography approach and might serve as an example for a ligand which is not found in the complexes.

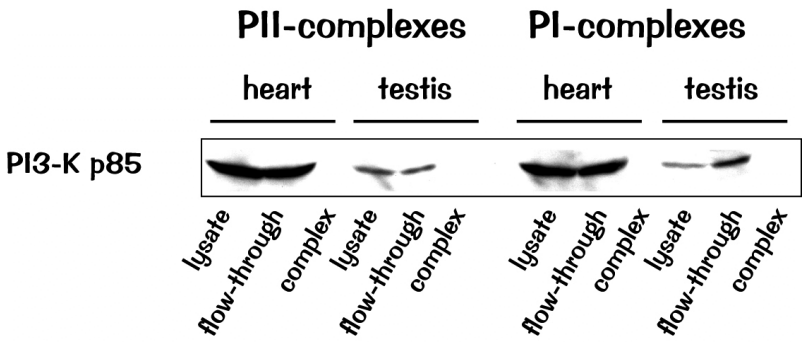

Figure 31: Western blot of the profilin-complexes from heart and testis probed with an antibody against the p85-subunit of PI3-kinase (Upstate Biotechnology, Lake Placid, USA)**.**

Besides testing the complexes for candidate proteins by western blot, a second approach was taken to characterize profilin ligands from different mouse tissues: analysis of excised bands from SDS-PAGE by mass spectrometry.

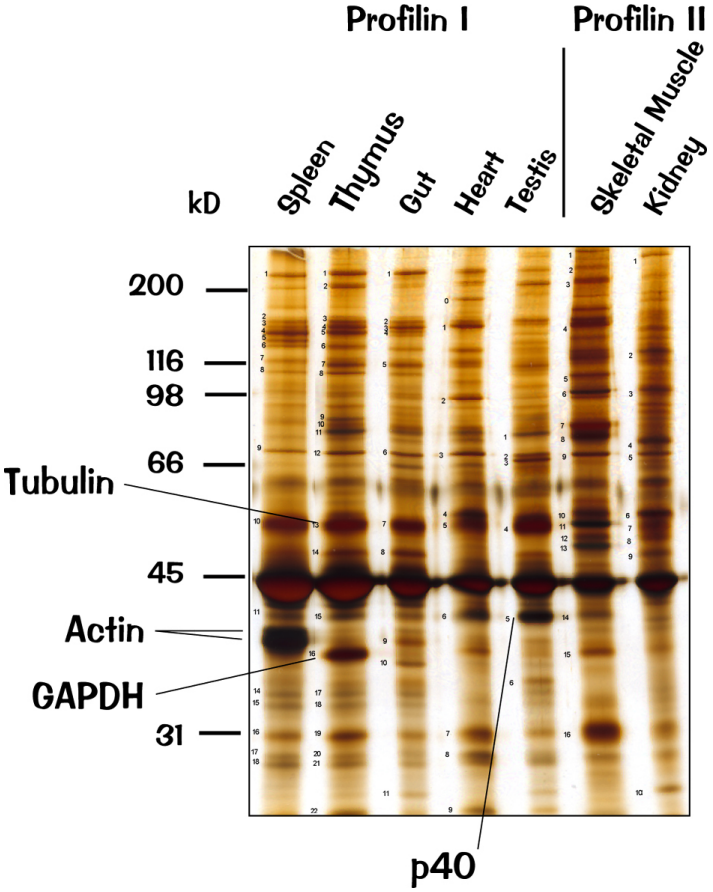

Figure 32: Silver-stained gel of profilin-complexes from mouse tissues. Numbered bands were excised. The identity of the labelled bands was determined by mass spectrometry in collaboration with M. Mann (University of Odense, Denmark).

Figure 32 shows a silver-stained gel of profilin-complexes from mouse. Numbered bands were excised and sent off for analysis by MALDI-TOF in collaboration with Matthias Mann's group (University of Odense, Denmark). Only a few bands gave unambiguos results, they are labelled in Figure 32.
The analysis identified already known ligands, like tubulin and actin, but also two novel ligands for profilin I were found. A major band in the profilin I-complex from thymus was identified as the glycolytic enzyme glycerol aldehyde phosphate dehydrogenase (GAPDH). Another strong protein band from the profilin I complex in testis proved to be p40. p40 has been reported to be a seven transmembrane putative G-protein coupled receptor, which is also expressed in neurons of brain and spinal cord and in thymocytes, megakaryocytes and macrophages (Mayer et al. 1998).

Obviously, the large number of ligands for the profilins makes it difficult to analyze all of them. Since a group of ligands especially for profilin II suggests that this protein might be involved in processes like exocytosis and endocytosis and synaptic vesicle recycling, we decided to address this question by focussing on the function of profilin II. Secondly, in order to find out about the role of profilin II ligands for its function, we looked in more detail at two of them: the GTPase dynamin and the novel 130 kD protein termed POP (Partner of profilin).

2.3 Functional characterization of profilin II in cells

To address the function of profilin II in cells, a heterologous system, which does not normally express this protein was used. In order to generate an easily accessible model system to study profilin II function and to learn more about its role in cells, HeLa cells were transfected with expression-constructs for profilin II. HeLa cells normally do not express profilin II. Due to difficulties of antibodies working faithfully in immunofluorescence, it was necessary to construct protein-expression vectors which were able to express either epitope-tagged versions of profilin or fusion-proteins of profilin with fluorescent proteins. Therefore, for localization-studies an C-terminal fusion of enhanced green fluorescent protein to profilin II, a profilin II with an N-terminal small epitope-tag from sendai-virus and an N-terminal fusion of profilin II with a red-fluorescent protein (Clontech) were used.

2.3.1 Functionality of red profilin II

Before performing functional assays, the biochemical features of the red profilin fusion protein were tested. Functionality of the profilin II-GFP-fusion proteins had been demonstrated previously (Di Nardo 2001, Wittenmayer et al. 2000).

Figure 33 shows a binding-experiment to address the functionality of red profilin in respect to binding to actin and poly-L-proline. A HeLa-cell line which was stably transfected with untagged profilin II was transiently transfected with red profilin II. HeLa cells usually do not express profilin II, but they have endogenous profilin I. After cell lysis, part of red profilin II, like profilin I is associated with the high-speed insoluble pellet which contains filamentous cytoskeletal components. The cell lysate was passed over affinity-beads either linked to poly-L-proline or G-actin. After extensive washing, the amounts of bound and free profilin were determined. Comparable amounts of red profilin II, untagged profilin II and profilin I bound to G-actin beads and to poly-L-proline beads. To test for regulation by phosphoinositides, the beads were also eluted with PIP_2-micelles. The interaction of red profilin II with poly-L-proline beads could be

completely disrupted by phosphoinositides, while untagged profilin II and profilin I show some residual binding after PIP_2-treatment, suggesting that the affinity of the red profilin under these conditions for poly-L-proline is higher than for the other profilins tested. More red profilin II eluted from G-actin-beads compared to untagged profilin II and profilin I, this suggesting that its interaction with actin can be more easily disrupted by phosphoinositides compared to the other profilins tested.

Altogether, these results show that the red fusion-protein is comparable to untagged cellular profilins in any of the characterized functions, but shows more sensitivity towards regulation by PIP_2.

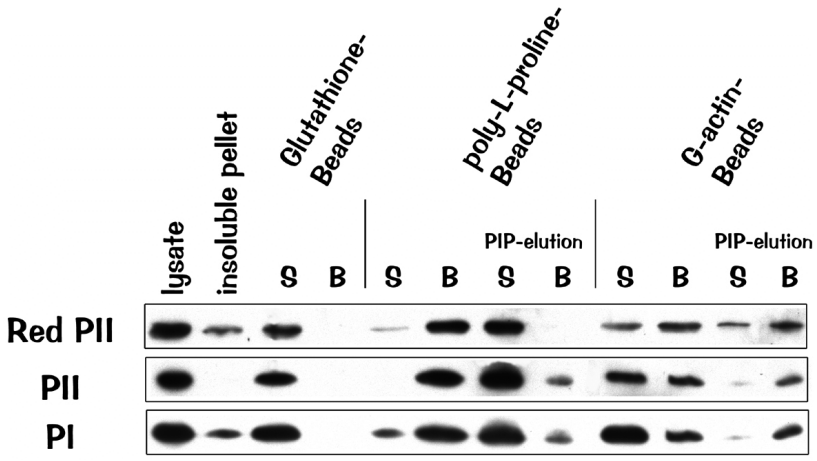

Figure 33: Western blot showing a binding experiment performed on affinity beads. The input was lysate of HeLa-cells expressing endogenous profilin I (PI) which were stably transfected with profilin II (PII) and transiently transfected with red profilin II (Red PII). PIP-elution was performed with 300 μM PIP_2 in micellar form. S: supernatant, B: bound.

2.3.2 Localization

The localization of profilin II might depend on the cell type it is being expressed in. Therefore, two different cell types were looked at: HeLa-cells, which normally do not have profilin II, and the neuron-like cell line PC12, which had been shown to express it.

When expressed in HeLa cells, sendai- and GFP-tagged profilins show an almost uniform distribution throughout the cytoplasm, with an enrichment at the membrane in zones with active actin-rearrangement. The red fusion protein, however, shows a striking localization to well-defined, elongated structures found mostly in the cell periphery resembling focal

contacts. Close examination shows the same structures also in cells expressing the other tagged forms of profilin (shown in Figure 34). In sendai-tagged and GFP-tagged profilin expressing cells, however, the cytosolic background is very high and obscures ready visualization of these structures.

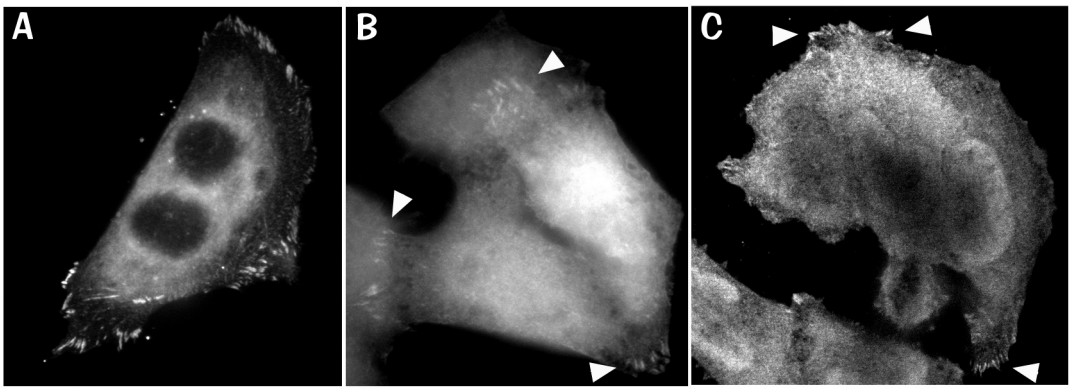

Figure 34: Microscopic images of HeLa-cells expressing different profilin II-constructs, but showing the same profilin-rich structures. A: Red profilin II; B: profilin II-GFP; C: profilin II tagged with the sendai-virus epitope-tag.

When counterstained with phalloidin, which binds to filamentous actin, these structures can be seen to localize to the ends of actin-stress-fibers, as shown in Figure 35.

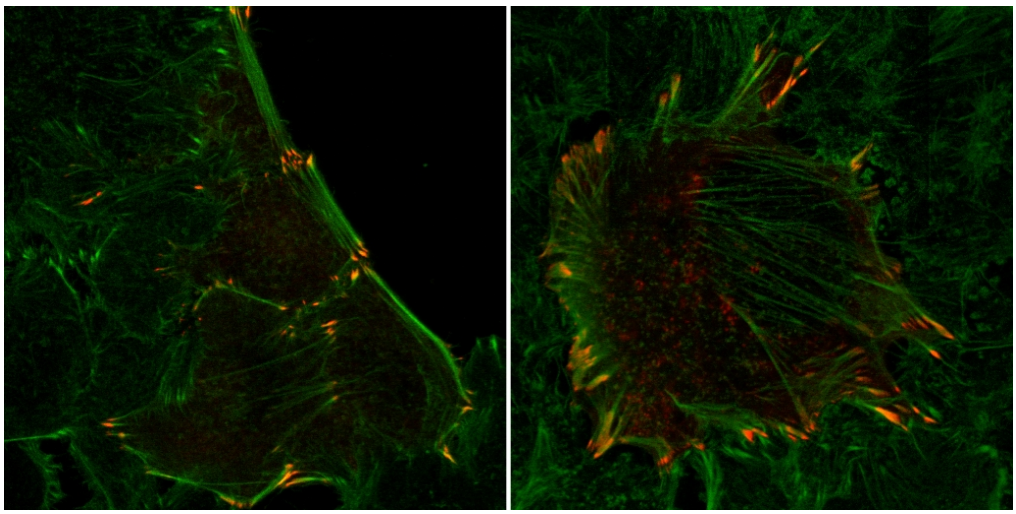

Figure 35: Confocal images of HeLa-cells expressing red profilin II. F-actin is stained in green. Profilin localizes to the tips of actin stress-fibers.

Since those structures resemble focal contacts, counterstaining with antibodies against focal contact proteins was performed. Indeed, tagged profilin shows extensive colocalization with the focal contact proteins VASP and vinculin (see Figure 36).

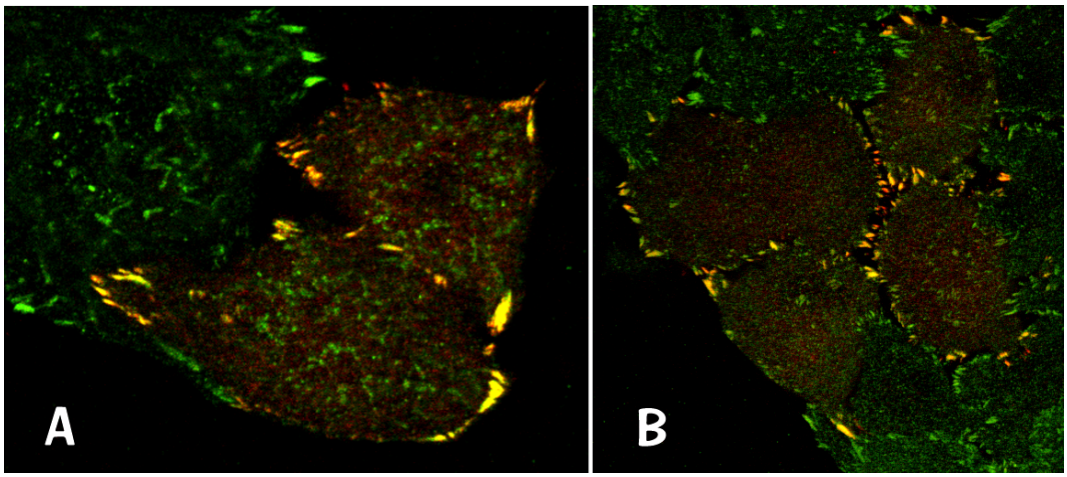

Figure 36: Confocal image of HeLa-cells expressing red profilin II stained with antibodies against focal contact proteins. A: in green: VASP; B: in green vinculin. The overlap appears yellow.

Also in other cell types profilin II shows a similar localization. So can red profilin II be found in actin-rich outgrowths and the "growth cones" of the neuron-like cell line PC12 (Figure 37).

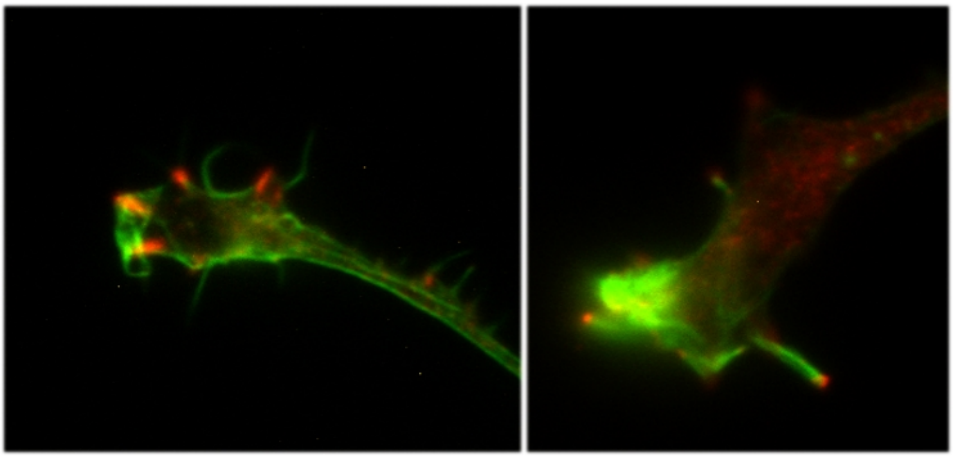

Figure 37: Microscopic images of "growth cones" of PC12-cells expressing red profilin II. F-actin is stained in green. Profilin is located in the tips of actin-rich outgrowths.

2.3.3 Red profilin II localizes to a vesicular perinuclear compartment

When looking at live cells expressing the red fluorescent profilin II-fusion protein, apart from focal contacts, staining in a perinuclear vesicular compartment can be observed in a different focal plane. From this compartment particular motile structures resembling vesicles bud or fuse like shown in Figure 38).

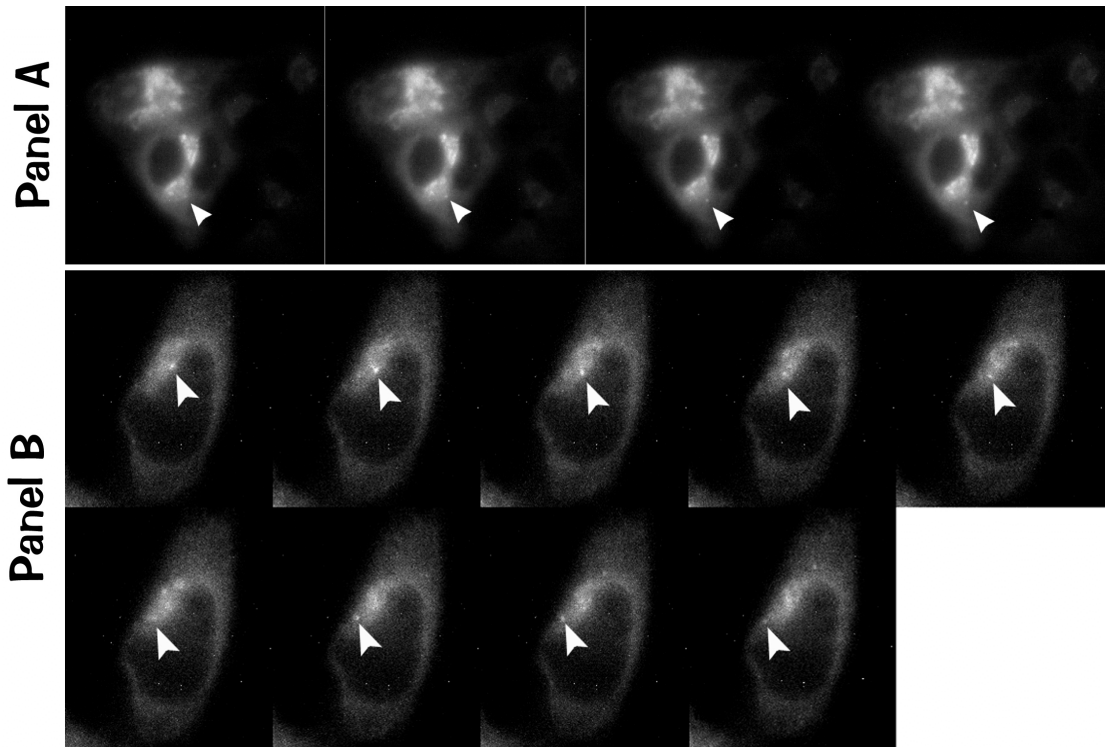

Figure 38: HeLa cells expressing red profilin II obseved with live video microscopy. In this focal plane the fluorescent signal is enriched in the perinuclear region, and vesicle-like structures can be seen budding or being absorbed into it (white arrows).

2.3.4 Red profilin II can inhibit receptor-mediated endocytosis

The previous results show profilin II at actin-rich structures at the plasma membrane, but even in vesicular structures around the nucleus. As mentioned in the Introduction, actin can also influence endocytic vesicle formation, like uptake of the transferrin-receptor, the question if profilin II has an influence on receptor-mediated endocytosis was addressed. HeLa cells were transfected with the red fluorescent profilin II. The population of cells containing profilin II expressers and non-expressers, was

allowed to take up green fluorescent human transferrin. As shown in Figure 39, the majority of cells expressing the red profilin II show a marked decrease in uptake of transferrin when compared to cells not expressing the construct. The decrease was most obvious at early timepoints (5 min. uptake).

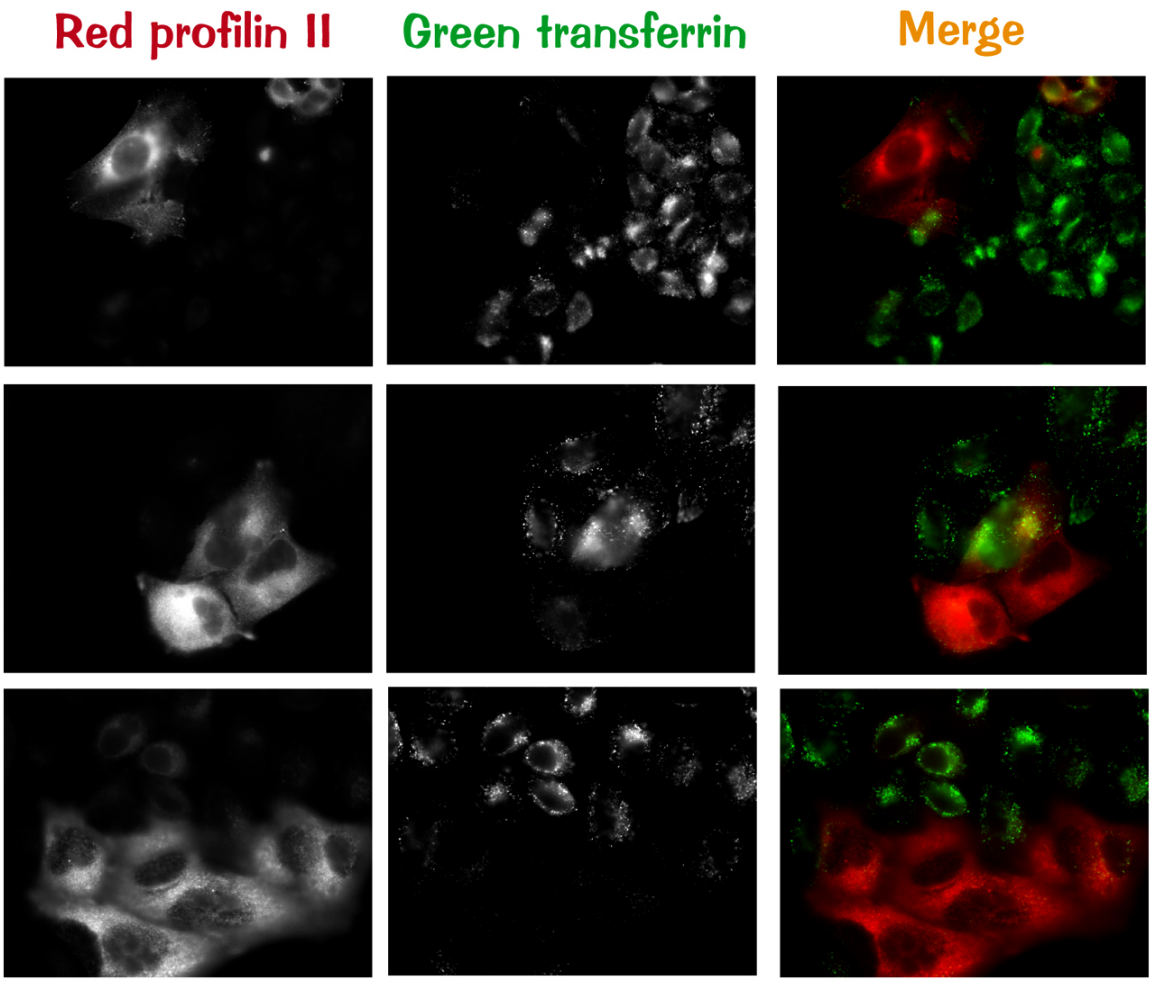

Figure 39: HeLa cells expressing red profilin II and untransfected HeLa cells were allowed to take up flurescently labelled human transferrin. The left panel shows the red fluorescence channel (profilin II), the middle panel shows the green fluorescence channel (transferrin). The merge of the two channels is shown on the right.

2.4 Examination of membrane traffic with FM-dyes

To more specifically address the question whether the presence of profilin II has any influence on membrane uptake or exocytosis, experiments were performed using FM-dyes. Those dyes have been widely used for examining membrane secretion and internalization in a variety of cellular systems (Aguado-Velasco and Bretscher 1999; Cochilla et al. 1999; Hao and Maxfield 2000) and especially neurons (Cousin and Robinson 1999; Diefenbach et al. 1999; Ryan et al. 1996). These dyes are amphiphilic molecules which partition readily between aqueous and lipid phases. Upon insertion into lipid membranes, the FM-dyes become fluorescent, while they are virtually non-fluorescent in the aqueous phase. The dissociation of the dyes from the lipid was shown to be in the range of seconds. In addition, they are non-toxic for cells. This allows one to follow the amount of dye taken up by live cells, which corresponds to the internalized area of membrane.

2.4.1 Uptake and washout of FM 1-43 in HeLa-cells

The first question was to see whether profilin II could affect membrane trafficking in cells which do not normally express it. Therefore, HeLa cells expressing profilin II with the epitope tag from sendai virus were compared to normal HeLa cells grown under the same conditions. Uptake was either followed by fixing the cells at certain time points and measuring the increase of fluorescence over time in a fluorescent plate reader. Cell numbers were accounted for either by staining nuclei with Hoechst and subsequent quantitation in the fluorescent plate reader or by determination of total protein content. Figure 40 shows the uptake of FM 1-43 into normal HeLa-cells and HeLa cells stably expressing sendai-epitope tagged profilin II.

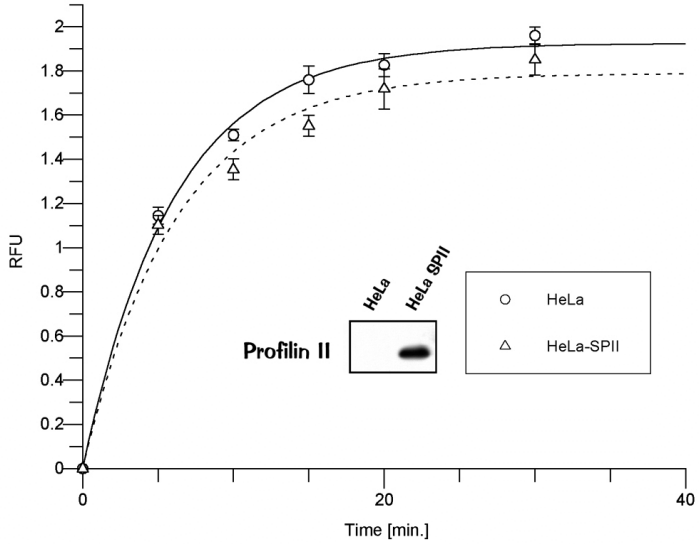

Figure 40: Uptake of FM 1-43 into HeLa-cells. Cells were allowed to take up the dye for various amounts of time, then fixed with ice-cold paraformaldehyde. Fluorescence was measured in a fluorescent plate-reader. The assay was done in quadruplicate, error bars are the standard error of the mean. Curves depict fits against a single exponential growth $y = A\left(1 - e^{-kt}\right)$. Insert shows western blot of the two cell lines probed for profilin II.

The measure-points could be fitted against a single exponential growth curve in the form $y = A\left(1 - e^{-kt}\right)$**.** Rate constants obtained that way were similar and in a range of 0.8-1.2 min^{-1}.

To compare the amount of dye taken up into the cells in equilibrium, cells were incubated with FM 1-43 for 75 min., washed, fixed and fluorescence was measured. The outcome of this experiment is shown in Figure 41. Cells expressing profilin II show a reduction of total uptake of dye in equilibrium compared to HeLa cells of about 10 %.

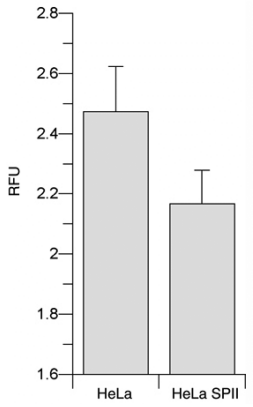

Figure 41: Amount of dye in HeLa-cells in equilibrium. HeLa-cells were incubated with FM 1-43 for 75 min., washed and fluorescence measured in a fluorescent plate-reader.

To see, whether there are differences in membrane secretion, the cells were loaded with FM 1-43 for 30 min. at 37°C. After washing for 2 min. with ice-cold dye-free buffer, cells were allowed to secrete the dye into room-temperature dye-free buffer. Fluorescence was followed in a fluorescent plate-reader. The outcome of this experiment is depicted in Figure 42.

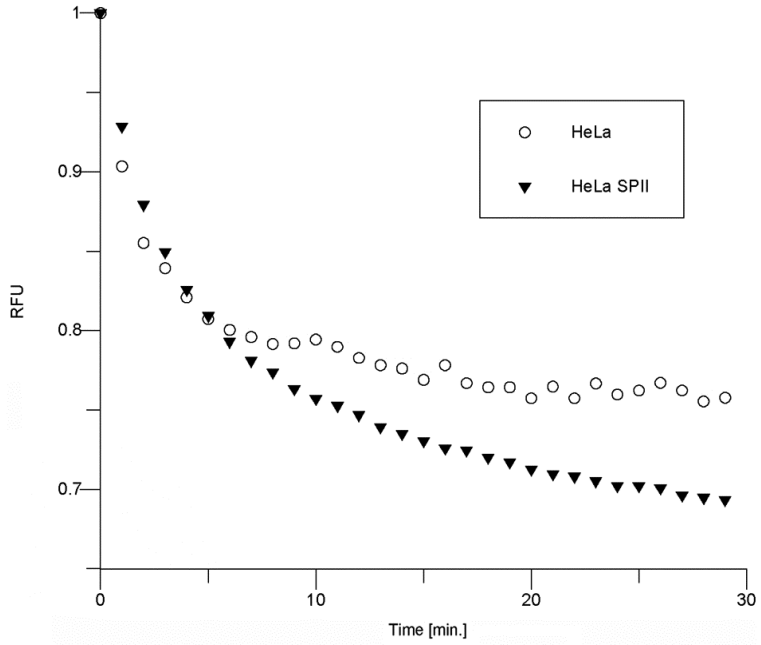

Figure 42: Graph showing the washout of FM 1-43 from HeLa-cells. Cells had been loaded with dye for 30 min., washed and were allowed to secrete the dye into the medium. Fluorescence change was followed at room temperature in a fluorescent plate reader. Measure points are the average of triplicate experiments, error bars have been omitted for sake of clarity.

The washout curves could be fitted against a double exponential decay in the form $y = A_1 e^{-k_1 t} + A_2 e^{-k_2 t}$. F-test proved this fit to be significantly better than a single exponential fit in the form $y = Ae^{-kt}$. This implies that membrane secretion has a two-component kinetic with a fast and a slow process. The existence of the two components has been interpreted as a reflection of the secretion of membrane through at least two different vesicular compartments, the fast component being contributed by immediately recycled vesicles, while the slow component reflects the contribution of the pericentriolar endocytic sorting compartment (Hao and Maxfield 2000). The half-times of the washout

obtained by the fits according to the equation $t_{1/2} = \frac{\ln 2}{k}$ are in the range of 1-1.5 min. for the fast component and 7-10 min. for the slow component and in accordance with published values (Hao and Maxfield 2000). The halftimes for the profilin II-expressing cells are slightly longer than for HeLa cells (9 min. instead of 7). The contributions of the fast component to the secretion lies between 42 and 63%, also this value in accordance with the literature. Washout from cells expressing profilin II is more efficient, with less residual fluorescence. The residual fluorescence is due to fusion of endocytic vesicles with more extensive membrane components and thus diffusion of membrane-inserted dye into lipid bilayers which are not part of the endocytic pathway. One explanation could be that cells expressing profilin keep more dye in compartments which get exported and show less fusion of endocytic with constitutive membrane systems.

2.4.2 Uptake and washout of FM1-43 in primary cortical neurons

If profilin II shows small, yet significant effects on membrane trafficking when ectopically expressed in HeLa cells, which usually do not have this profilin isoform, the opposite effect should be seen if profilin II is taken away from cells which usually express it. To address this question, membrane uptake and exocytosis was investigated in neurons from mice lacking profilin II which had been generated in our lab (Di Nardo 2001), again using FM-dyes as a marker to follow these processes.

The FM-dyes have been used for studying synaptic vesicle endo- and exocytosis (see references under Examination of membrane traffic with FM-dyes). Neurons can be loaded with FM-dyes either under depolarizing conditions (using elevated concentrations of K^+ in the loading medium) or under non-depolarizing conditions. Two separable populations of endosomes form: *evoked* endosomes under stimulating conditions, which can be released by a second round of depolarization, and *constitutive* endosomes, which form in the absence of stimulation and are not released by depolarization (Diefenbach et al. 1999). Figure 43 shows an example of neurons stained with FM-dyes.

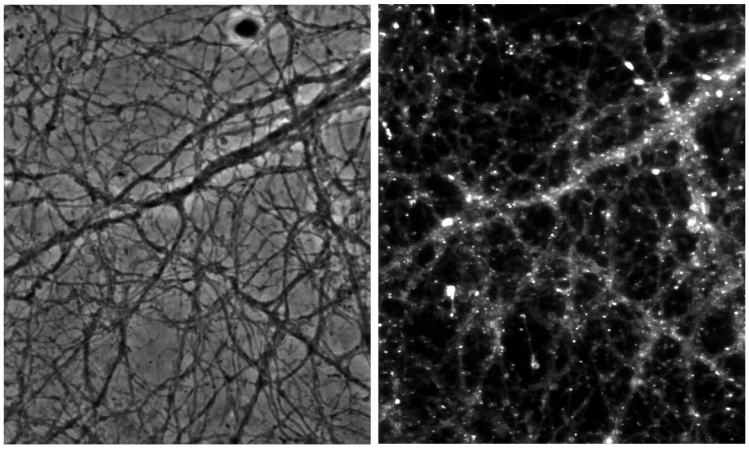

Figure 43: Cultured mouse cortical neurons stained with FM 1-43.

For quantitation of the uptake of FM 1-43, cells were grown in 24-well plates, washed briefly and placed into the fluorescent plate-reader. Uptakes were initiated by injecting dye-containing buffer either with or without 50 mM K^+. The fluorescence change over time was recorded. Figure 44 shows the outcome of these experiments. Neurons prepared from mice lacking profilin II showed more efficient uptake both for stimulated (Figure 44A) and for unstimulated uptake (Figure 44B) when compared to neurons prepared from wildtype mice. The overlay of the graphs for stimulated and unstimulated uptakes (Figure 44C) shows that neurons from wildtype-mice can be stimulated by depolarization to take up more efficiently, while neurons lacking profilin II cannot be further stimulated by addition of K^+.

Washouts were performed by first loading the neurons in the presence of 50 mM potassium for 2 minutes. Then they were washed for 5 minutes in dye-free, low potassium medium, which allowed them to recover from depolarization. For non-depolarizing washouts, the fluorescence-change was followed after addition of low potassium-buffer containing 100 μM sulforhodamine, in order to quench FM 1-43 fluorescence on the outside of the cells. Stimulated washouts were performed by injecting buffer containing sulforhodamine and 100 mM K^+. Figure 45 summarizes the outcome of those experiments.

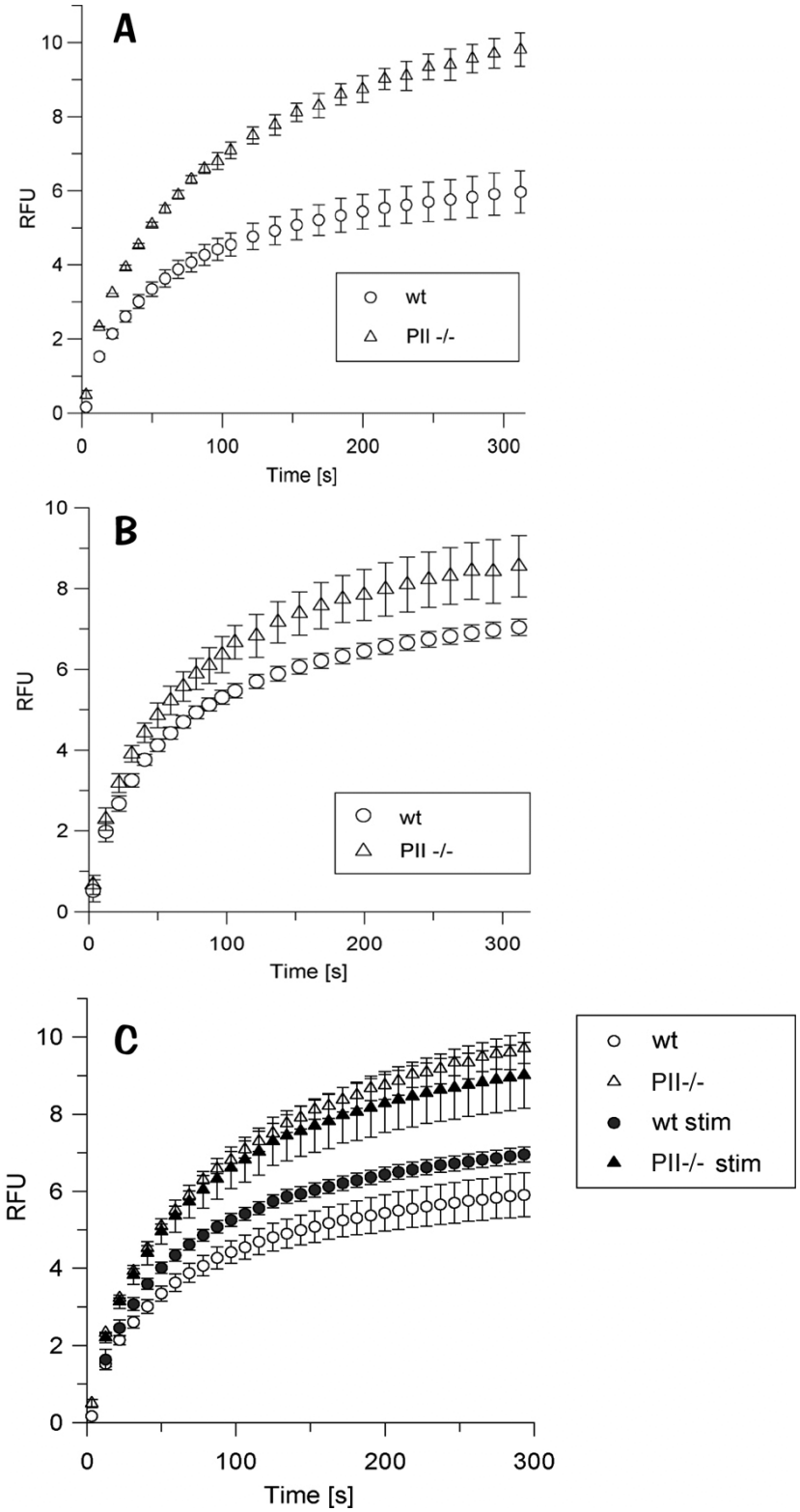

Figure 44: Timecourse of the uptake of FM1-43 into cortical mouse neurons in culture expressed as the change of fluorescence. Measurements were performed in triplicates, error bars depict the standard error of the mena. A: uptake under non-stimulatory conditions; B: uptake under depolarizing conditions using 50 mM K^+; C: overlay of the two graphs shown in A and B.

As in the case with HeLa-cells, the fluorescence change over time could be fitted against a double-exponential decay. Stimulated washouts (Figure 45B) had identical rate constants for wildtype and profilin II-knockout neurons, which were about 0.056 min^{-1} for k_1 and 0.005 min^{-1} for k_2, corresponding to halftimes of 12 and 138 seconds, respectively. In both cases, the fast component accounted for 60% of dye-secretion. Non-stimulated washouts (Figure 45A) showed faster washout for neurons lacking profilin with a halftime of around 4-5 min. for the slow component compared to 8 min. for wildtype neurons. Halftimes for the fast component were comparable and about 1 min.

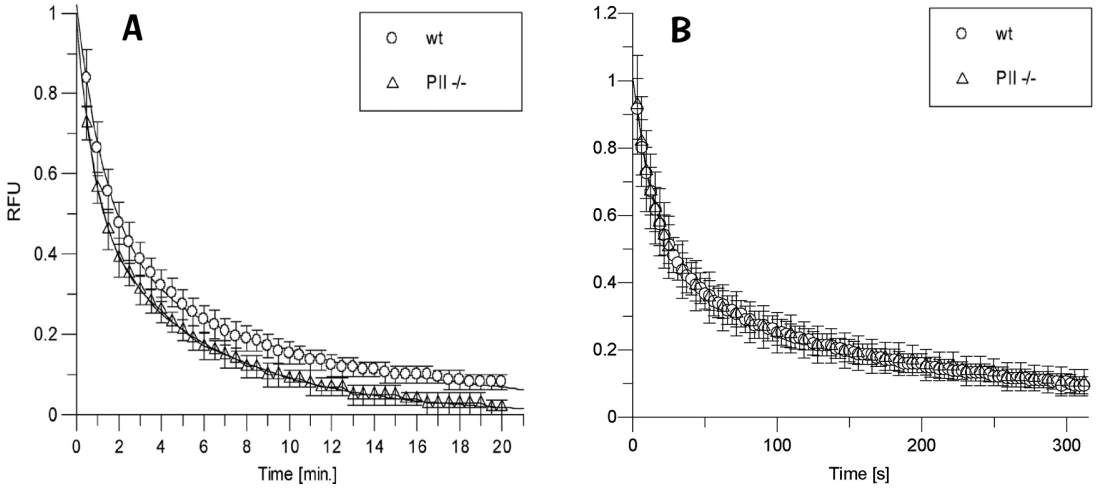

Figure 45: Timecourse of the washout of FM1-43 from mouse cortical neurons in culture. Neurons were loaded for 2 minutes under depolarizing conditions. After washing and recovery for 5 min. washouts were followed by observing the change in fluorescence in the presence of 100 μM sulforhodamine. A: unstimulated washouts in non-depolarizing buffer; B: stimulated washouts in the presence of 100 μM K^+.

These results strongly suggest that profilin II has an effect on membrane-trafficking both in HeLa-cells and in neurons. Seemingly, the lack of profilin increases bulk membrane uptake in both HeLa-cells and neurons, classifying profilin II as a negative regulator of basal membrane-flow.

2.5 The profilin ligands POP-130 and dynamin I

It had become clear from the results shown in the preceding chapters that profilin plays a role in membrane-trafficking events. As shown in the introduction, the actin cytoskeleton is very important for these processes, yet they are unlikely be exclusively explained by profilin's interaction with actin. Since some ligands found in the profilin II complex from brain are key players of cellular membrane traffic, we decided to take a closer look at those binding partners: a novel protein without any known function (POP-130) and a well known key regulator of membrane-traffic, dynamin I.

2.5.1 The profilin-ligand POP-130

One ligand of 130 kD which was found in the profilin II-complex from mouse brain turned out to be a novel protein without any sequence homology to other proteins in the databases.

2.5.1.1 Tissue distribution of POP-130

Nothing is known about tissue-distribution or function of POP-130. Therefore, the polyclonal POP-antibody was used to perform a test for expression of the protein on mouse tissues (see Figure 46).

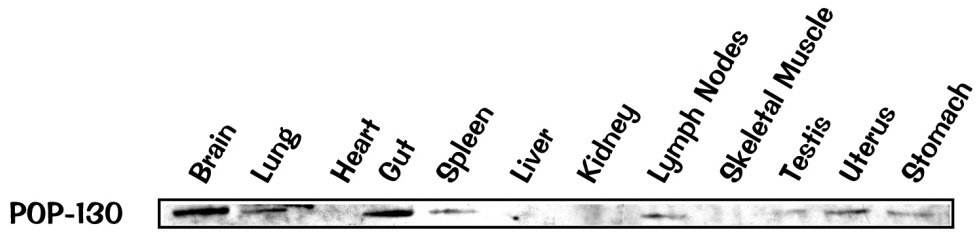

Figure 46: Tissue western blot of various mouse tissues probed with the anti-POP antiserum.

Expression was found to be highest in brain and gut, but the protein is also present in lung, testis, lymph nodes, stomach, and spleen. No expression was found in liver, kidney, heart and skeletal muscle.

In situ hybridization performed on mouse embryos shows staining in brain, tongue, nose, lung, genital tubercle and vertebra (see Figure 47).

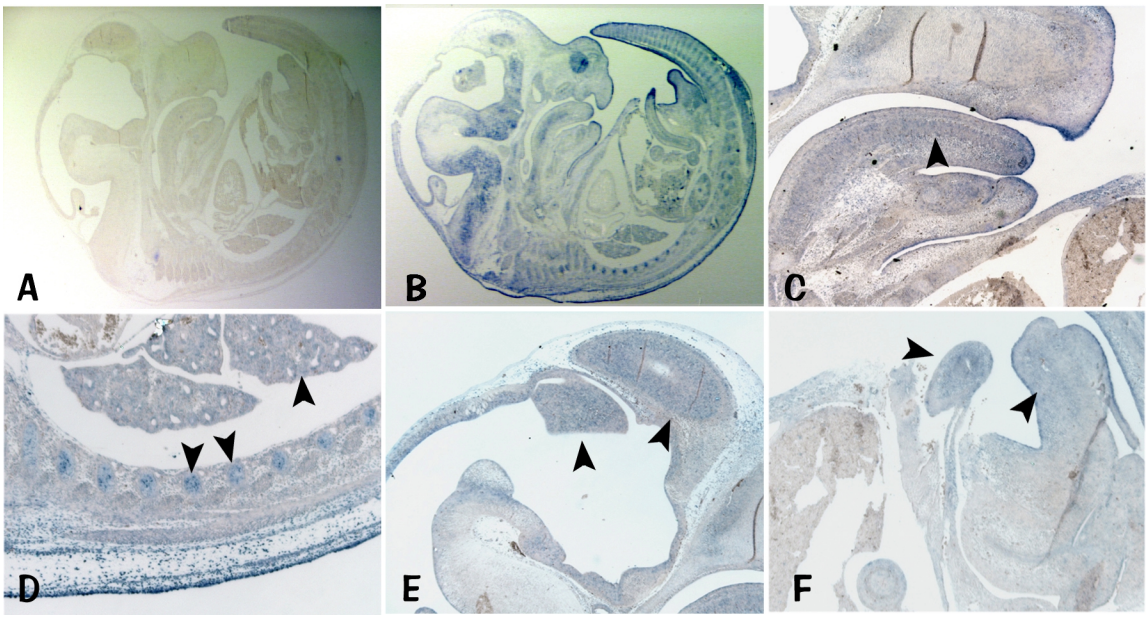

Figure 47: *In situ*-hybridization of mouse-embryoes with POP-sense probe (A) and POP-antisense probes (B-F). C: Expression can be seen in tongue and nose; D: lung and vertebrae; E: developing brain-structures and F: genital tubercles.

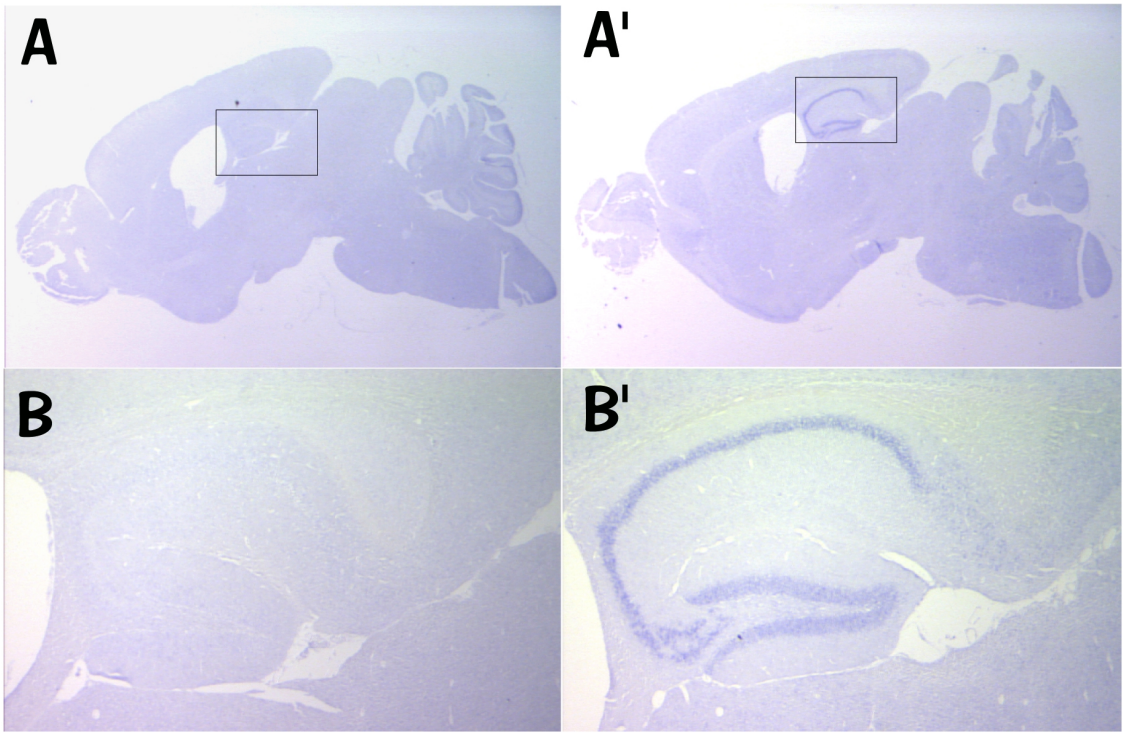

Figure 48: *In situ*-hybridization on adult mouse brain. A and B show hybridization with the sense-probe, while A' and B' show hybridization with the antisense-probe. A strong staining can be seen in the

hippocampus. The lower panel (B and B') shows a higher magnification of the framed regions in the upper panel (A and A').

In adult mouse brain, the POP mRNA is highly expressed in the hippocampus, an area where also profilin II is found to be highly abundant (see Figure 48).

2.5.1.2 Subcellular localization of POP-130

In order to find out where in cells POP-130 can be found, expression vectors for fusion-proteins were made. These fusion-proteins consisted either of the enhanced green fluorescent protein (EGFP) or the DsRed-fluorescent protein (both Clontech) N-terminally fused to the POP-130 cDNA. The expression-vectors were introduced into cells and stable cell lines made.

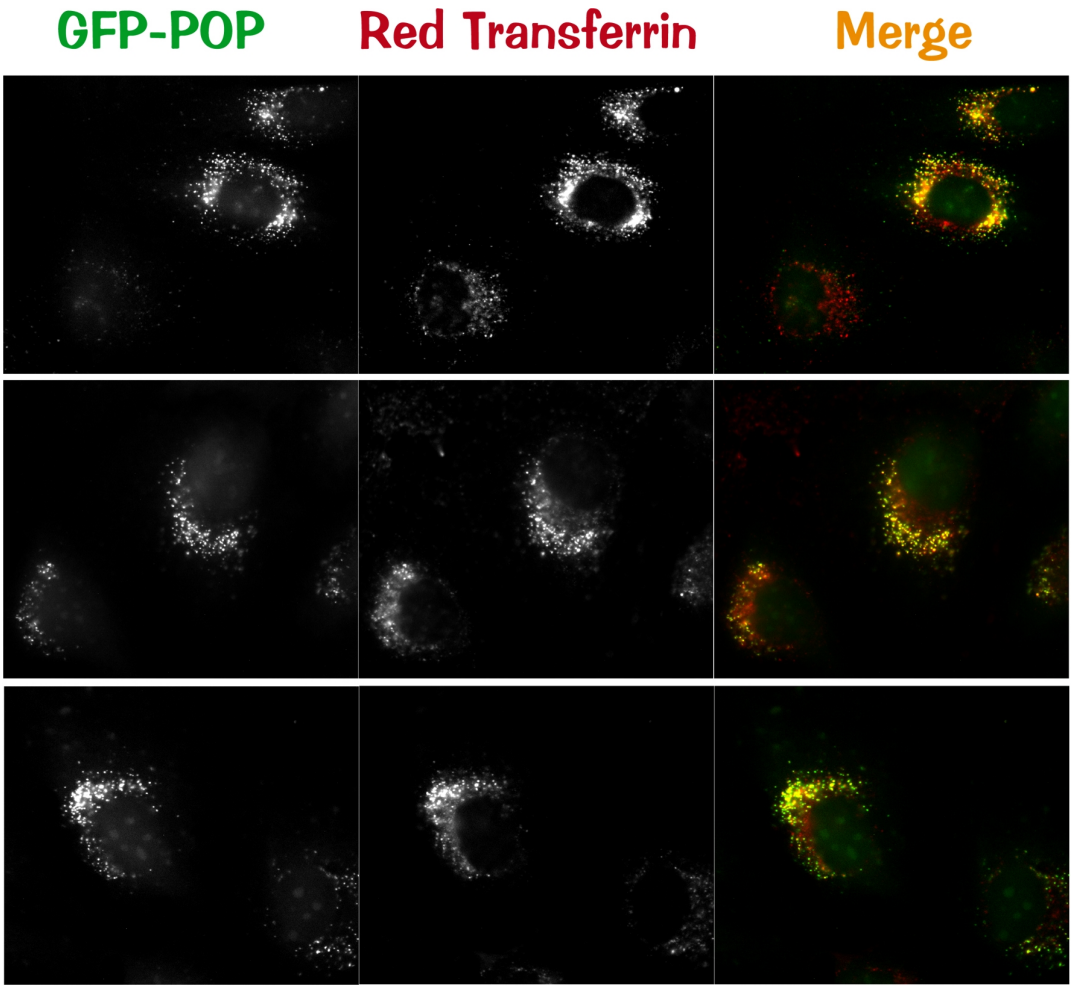

Figure 49: Immunofluorescence micrographs of HeLa-cells expressing GFP-POP which had been allowed to take up transferrin coupled to the red fluorescent dye Texas Red. The left panel shows the green

fluorescence channel with the GFP-POP-signal, the middle panel the red flourescence channel with the transferrin signal. The right panel is a merge of the green and the red image, areas of overlapping signal appear yellow.

The fusion-proteins could be seen to localize to a perinuclear vesicular compartment, as shown in Figure 49. The same structures could be stained with the endocytic marker transferrin after 20 min. of uptake. No colocalization was seen with the early endosomal marker EEA-1 or the trans-Golgi-marker TGN-38 (not shown). These data indicate that POP-130 localizes to a late endocytic compartment.

Interestingly, apart from the perinuclear staining, especially the red fusion protein could be found to localize to cell-cell contacts. Figure 50 shows HeLa cells expressing the red fluorescent POP-fusion protein which brightly decorates contact zones between cells.

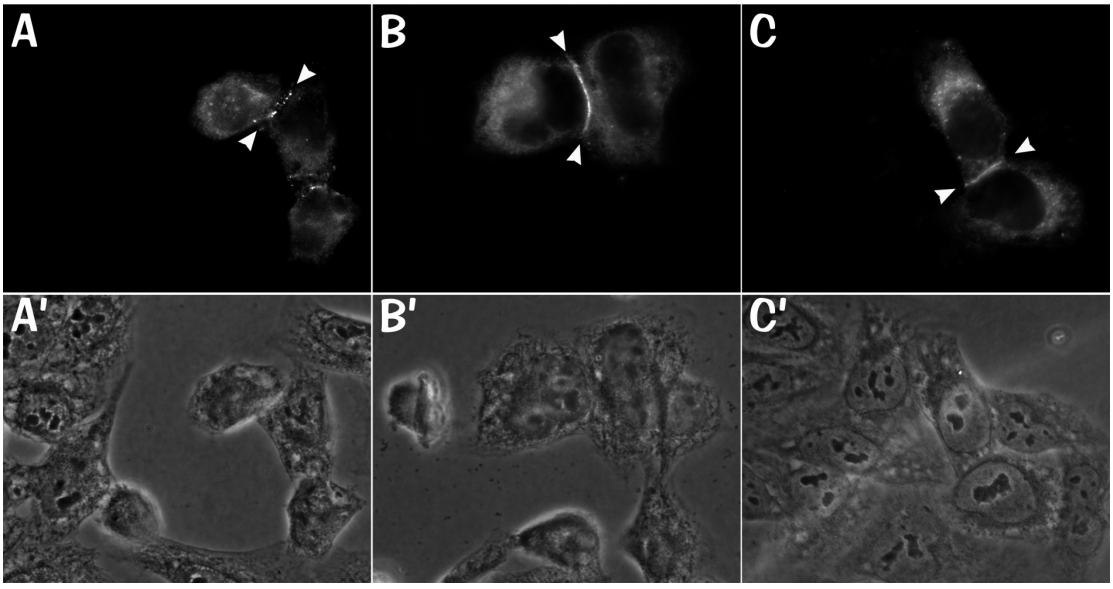

Figure 50: Microscopic images of HeLa-cells expressing a fusion protein of POP-130 and the red fluorescent protein. A, B, C: Red fluorescence channel showing the redPOP-protein in perinuclear vesicles and enriched at cell-cell-contacts. A', B', C': Phase-contrast images of the respective pictures in the upper panel.

Since the localization of the GFP-fusion protein suggested association of POP-130 with vesicles, a subcellular membrane-fractionation on HeLa-cells was performed. Figure 51 shows that much of the POP-protein is associated with membranes. The membranous compartment is of intermediate floating-density, overlapping with the fractions which

stain positive for the lysosome-associated protein CLA-1. The lack of overlap with the ER-marker BiP suggests, that it is not a resident of the endoplasmic reticulum.
The data obtained by microscopic analysis of cells expressing a GFP-fusion-protein and the biochemical data indicate that POP-130 localizes to a vesicular compartment which might be late endosomes.

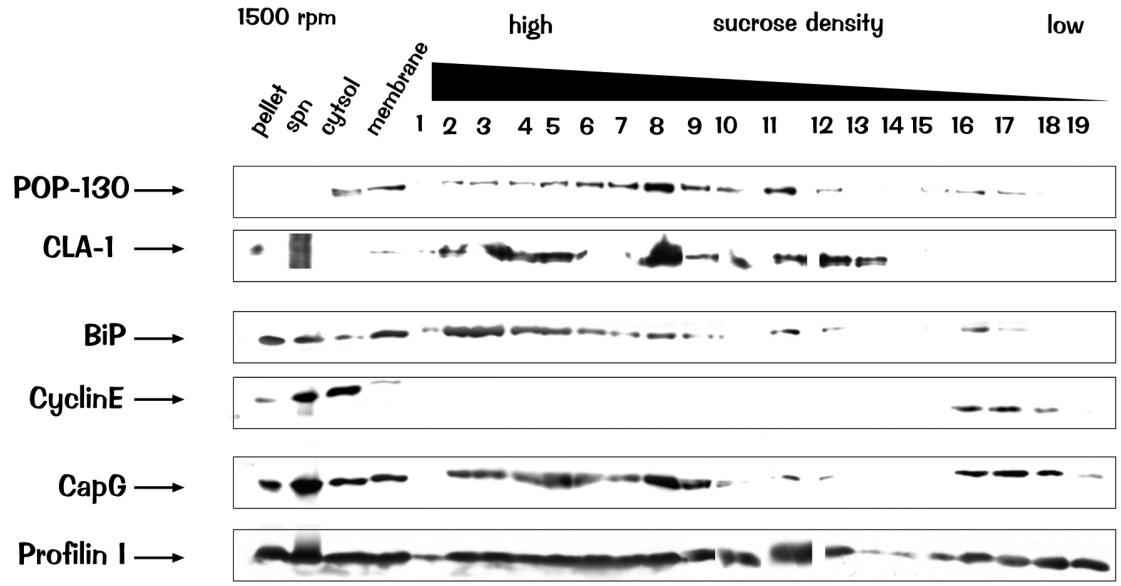

Figure 51: Western blot showing a subcellular membrane-fractionation on sucrose-gradient probed with various antibodies.

2.5.1.3 Co-immunoprecipitation of POP-130 with epitope-tagged profilin II

To answer the question whether POP-130 binds directly to profilin II, a co-immunoprecipitation experiment was performed. HeLa-cells express POP-130, but they normally do no express profilin II. Therefore, a HeLa cell line stably expressing sendai-virus epitope-tagged profilin II was used for immunoprecipitation. POP-130 could be co-immunoprecipitated from HeLa-cells stably expressing this epitope-tagged profilin II (see Figure 52).

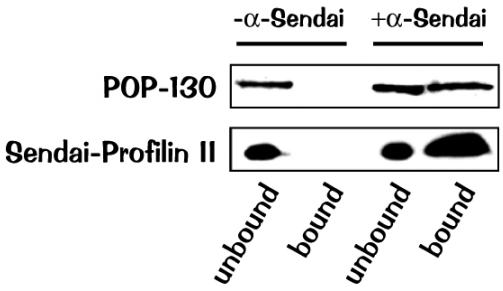

Figure 52: Western blot showing a co-immunoprecipitation experiment. HeLa-cells stably expressing profilin II with an epitope-tag from Sendai-virus can be immunoprecipitated with an anti-Sendai-antibody. The precipitate also contains POP-130.

This experiment suggests that the interaction between profilin II and POP-130 is direct and can occur *in vivo*.

2.5.1.4 Overexpression of POP-130 leads to a decrease in membrane uptake

To address the question what the effect of overxpression of POP-130 in cells would be, stable HeLa cell lines were made expressing the full-length cDNA of POP-130 with an N-terminal epitope-tag from sendai-virus in the IRES-vector. Figure 53 shows a western blot of three clones.

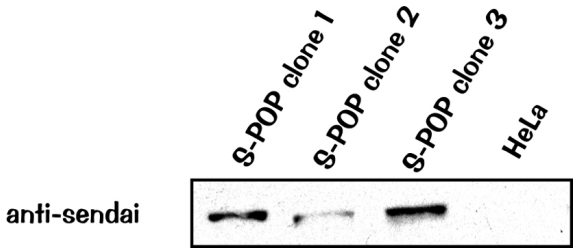

Figure 53: Western blot of cell lysates from three stable cell clones expressing POP-130 tagged with an epitope-tag from sendai virus.

The data obtained from the localization studies suggest that POP-130 is involved in endocytic processes. This hypothesis is further corroborated by the fact that the HeLa cells overexpressing POP show a marked decrease in membrane-uptake as measured by FM-membrane dyes. Figure 54 shows that cells overexpressing POP-130 take up less membrane as compared to wildtype HeLa-cells.

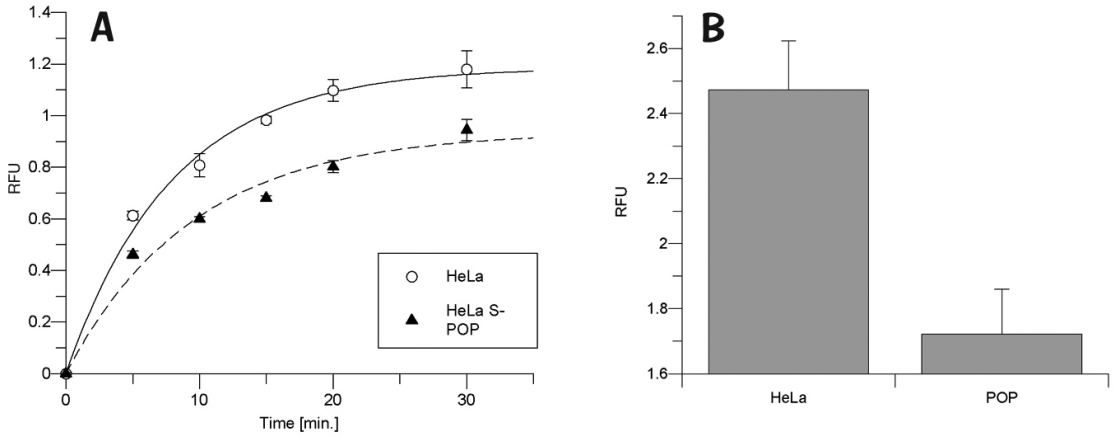

Figure 54: Membrane-uptake of HeLa cells overexpressing POP-130 as measured by fluorescence increase of FM 1-43-dye. A: Kinetics of membrane uptake over time. B: Total FM 1-43 fluorescence in steady-state (after >1 hour of uptake).

Secretion of membrane, however, is unaffected by POP-130. Figure 55 shows the washout of FM 1-43 dye from HeLa cells either overexpressing POP or not. The washout kinetics are essentially identical.

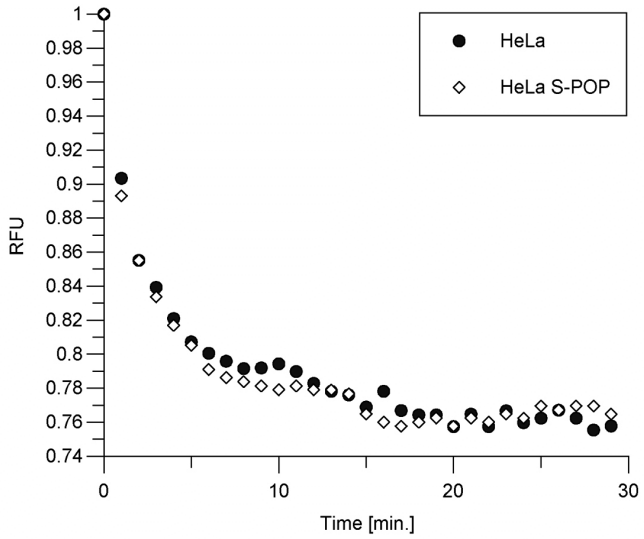

Figure 55: Secretion of membrane visualized by FM 1-43 fluorescence in HeLa-cells and HeLa-cells overexpressing POP-130. Both cell-types show the same washout-kinetics. Measure points are averages of triplicate experiments. Error bars are omitted for sake of clarity.

Part of the decrease in membrane-uptake in the cells overexpressing POP-130 is contributed by less efficient receptor-mediated endocytosis. Figure 56 shows a FACS-analysis of wildtype HeLa and HeLa cells overexpressing POP-130 which had been allowed to take up fluorescently labelled transferrin. The cells overexpressing POP-130 show a significant decrease in fluorescence intensity when compared to normal HeLa cells.

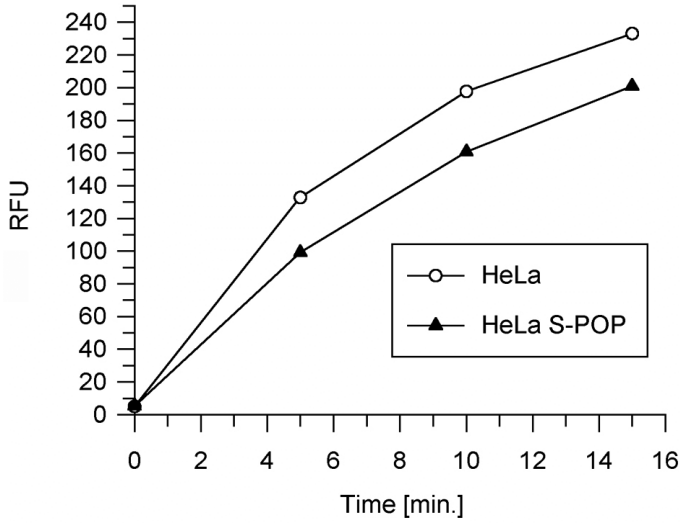

Figure 56: FACS-analysis of cells which were allowed to take up TexasRed-labelled transferrin. Timepoints are average fluorescence intensities of 50.000 cells each. HeLa cells expressing POP-130 show a decrease in transferrin uptake.

These results point towards an influence of POP-130 on membrane-trafficking, which is restricted to the endocytic pathway, but does not affect exocytosis of membrane. Being a direct ligand for profilin II, this protein might mediate part of the profilin II-effects on membrane-trafficking described in the previous chapter (Examination of membrane traffic with FM-dyes).

2.5.2 The interaction of profilin with dynamin

One of the key regulators of membrane-trafficking events and especially synaptic vesicle recycling is the 100 kD GTPase dynamin, which had been shown to be a member

of the profilin II-complex from mouse-brain. Profilin's interaction with dynamin may be one link of profilin II to membrane-trafficking.

2.5.2.1 Expression and purification of full-length dynamin in insect cells

In order to study profilin-dynamin interaction in more detail it was necessary to work with the pure components. To obtain recombinant dynamin, the baculovirus expression system was chosen. A baculovirus strain coding for a fusion-protein of GST and full-length human dynamin Iaa including a cleavage-site for a protease from human rhinovirus ("PreScission"-protease, Amersham Pharmacia) was obtained from Pietro DeCamilli's lab. High Five™-insect cells were infected and harvested after not more than 48 hours. The full-length protein was purified using glutathione-beads. Figure 57 shows an example of a typical purification.

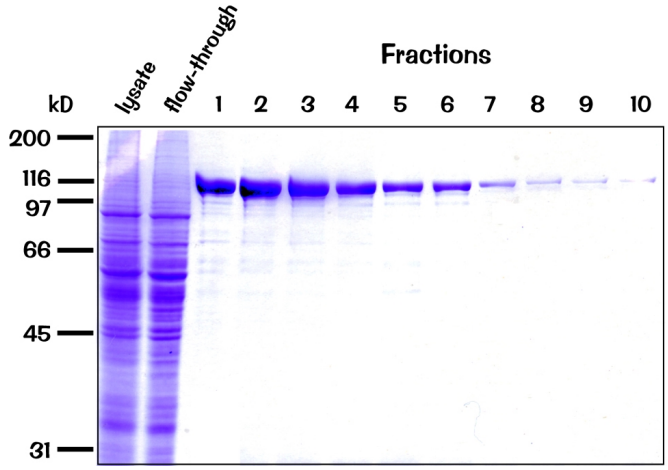

Figure 57: Coomassie gel showing the purification of recombinant dynamin from insect cells.

The GST-portion of the fusion-protein was cleaved off with PreScission protease (Amersham/Pharmacia) in order to avoid any steric hindrance. Figure 58 shows the timecourse and the cleavage-products of this reaction. GST-dynamin was routinely digested for 4 hours.

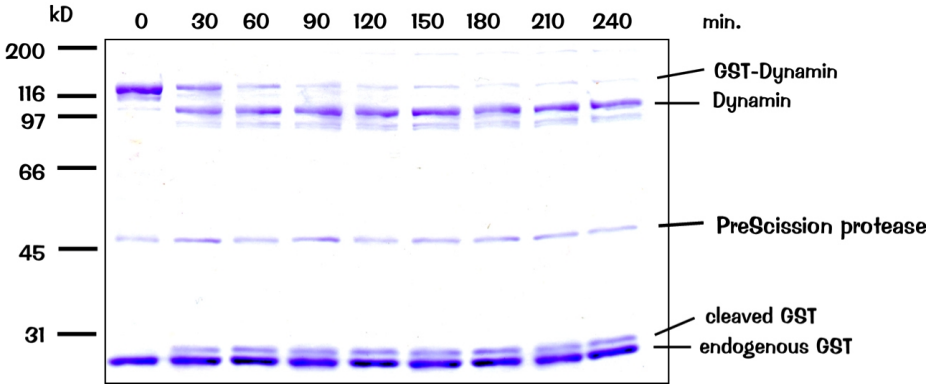

Figure 58: Coomassie-gel showing the timecourse and products of the *in vitro*-cleavage of recombinant GST-dynamin with PreScission protease.

2.5.2.2 Dynamin I binds directly and specifically to profilin II

Incubation of the recombinant dynamin with profilin-beads showed that the dynamin produced in this way is able to bind to profilin II. The binding is therefore direct and, as Figure 59 shows, also specific for the profilin-isoform II, since only very weak binding to profilin I was observed.

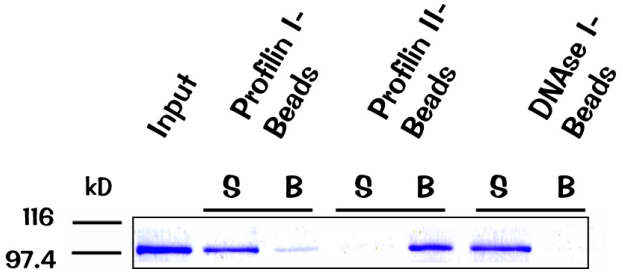

Figure 59: Coomassie gel showing a binding experiment with recombinant dynamin I and immobilized proteins. S stands for unbound fraction, B for bound.

The profilin-dynamin interaction is largely independent on divalent cations (Ca^{2+}, Mg^{2+}, EDTA, EGTA) as shown by Figure 60. Also nucleotides like ATP, GMP, GTP or GTP-γ-S do not have a significant influence on binding. Slightly less binding occurs when GTP-γ-S is present or when divalent cations are missing.

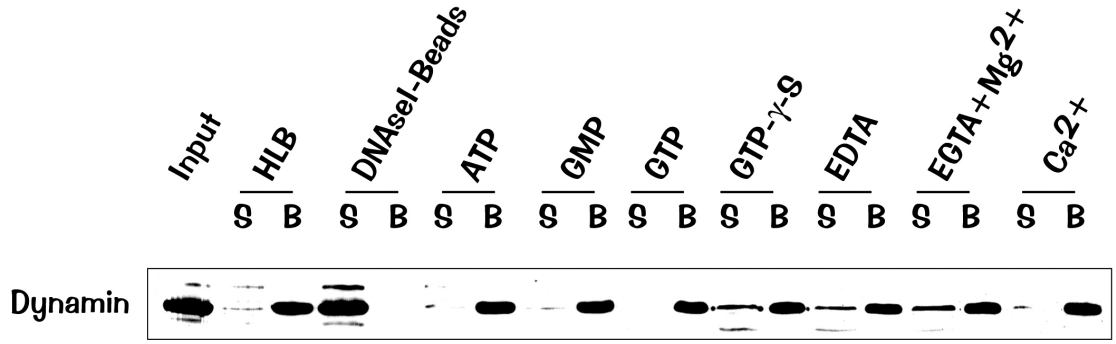

Figure 60: Western blot showing the dependence of dynamin-profilin binding on nucleotides and cations. Profilin II and dynamin were allowed to bind in the presence of 2 mM of various nucleotides or 5 mM EDTA, EGTA or cations. S stands for supernatant or unbound fraction, B for bound.

2.5.2.3 Dynamin I can be co-immunoprecipitated with a profilin II-specific antibody

The profilin II-specific antibody 2T described in the chapter "Polyclonal antibodies" is able to immunoprecipitate the protein from tissue lysates. After mild cell lysis under non-denaturing conditions (see Material and Methods) dynamin I is found to co-precipitate with profilin II (see Figure 61). This result is a further indication of direct binding between dynamin I and profilin II in live cells.

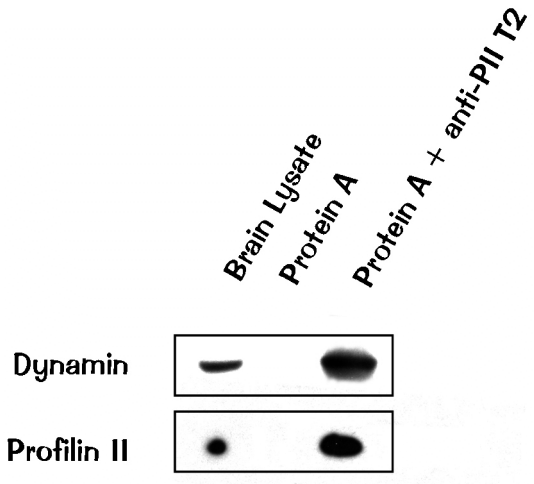

Figure 61: Western blot of a co-immunoprecipitation of dynamin I and profilin II with the profilin II-specific polyclonal antibody T2. Protein A beads alone were used as a control for unspecific binding.

2.5.2.4 Mapping the binding sites

In order to characterize the interaction of profilin II with dynamin I in more detail, it was first necessary to map the binding sites on both molecules.

2.5.2.4.1 Profilin's polyproline-binding site is essential for dynamin-binding

Profilin can be immobilized in such a way that its poly-L-proline-binding site is blocked, simply by binding it to poly-L-proline-beads. Under these conditions actin for example can still bind to profilin. However, dynamin is no longer able to bind when profilin II is immobilized in this way (see Figure 62). From this result it can be concluded that the polyproline-binding site on profilin is essential for binding to dynamin.

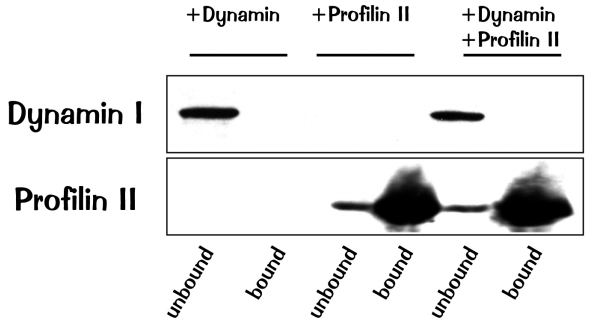

Figure 62: Western blot showing that profilin II immobilized on poly-L-proline beads is not longer able to bind to dynamin. The first lane shows that dynamin alone does not bind to poly-L-proline beads, the second lane shows that profilin II does. The third lane shows that even though a vast excess of profilin is bound to polyproline-beads, dynamin can not longer bind.

2.5.2.4.2 Binding-experiments with profilin II and dynamin-truncates

In order to map the interaction site on dynamin, binding-assays were performed with bacterially expressed truncates of the dynamin-protein. The constructs were obtained from the lab of Dr Pietro De Camilli. As shown in Figure 63, they consist of the first 750 amino acids of human dynamin Iaa fused to a 6xHis-tag (1-750), and various truncated forms of the proline-arginine-rich domain of fused to GST.

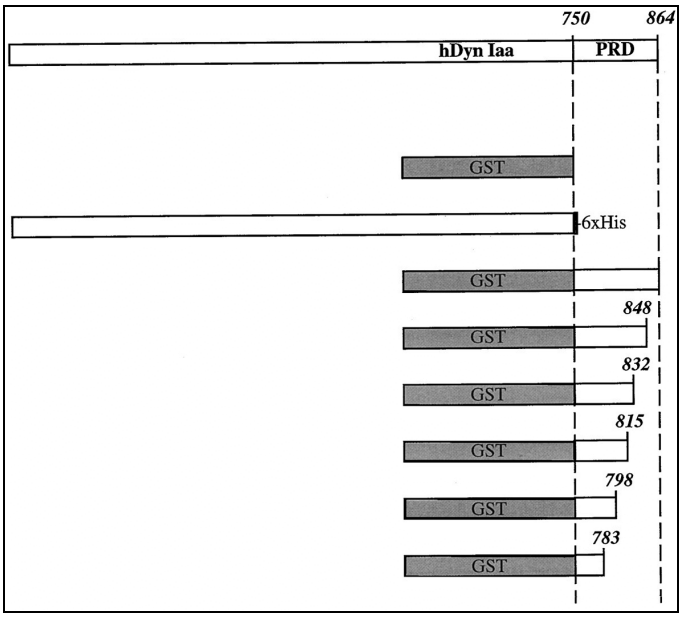

Figure 63: Scheme of some of the truncated forms of dynamin used for binding experiments. The figure was taken from Grabs et al. 1997

As shown in Figure 64, none of those dynamin-truncates bound to profilin II-beads in vitro. Conversely, recombinant profilin II did not bind to any of the immobilized dynamin-truncates (shown in Figure 65).

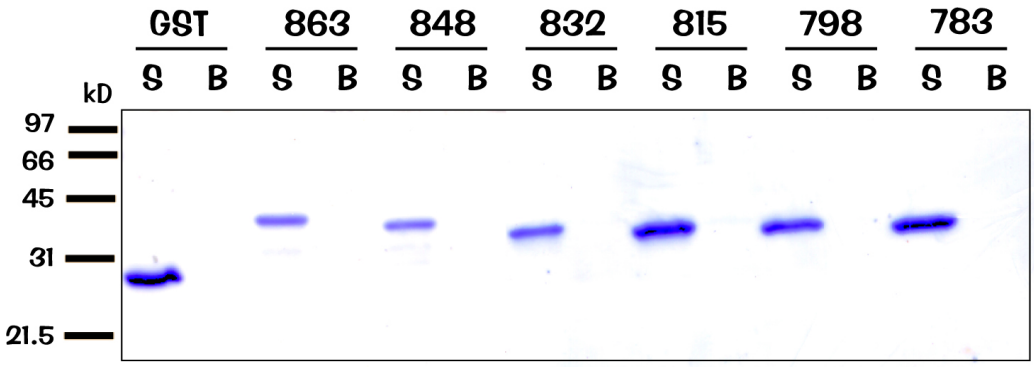

Figure 64: Coomassie-gel showing a binding experiment using profilin II beads and soluble dynamin-truncates. GST was used as a negative control. S stands for supernatant or unbound fraction, B for bound fraction.

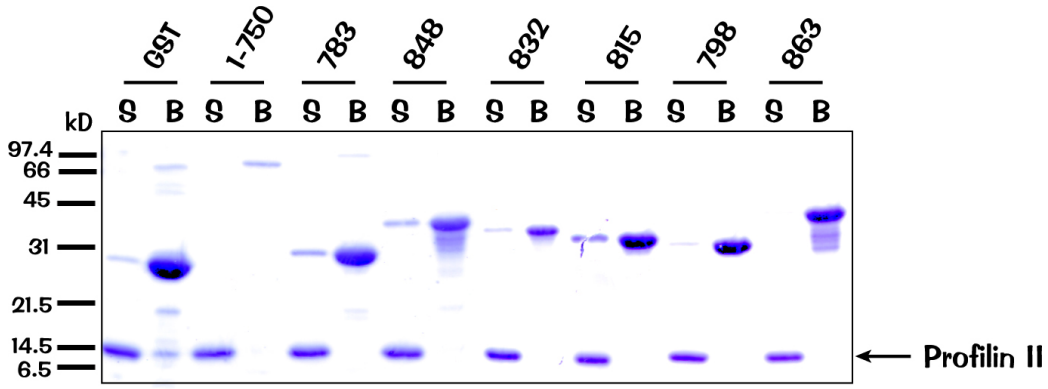

Figure 65: Coomassie-gel showing a binding experiment using immobilized dynamin-truncates and soluble recombinant profilin II. GST was used as a negative control. S stands for supernatant or unbound fraction, B stands for bound fraction.

To address the question whether the lack of binding may be due to non-functional truncates or additional cellular factors, the immobilized dynamin-fragments were incubated with brain-lysate. The bound fractions were analysed for profilin II and a control ligand, Grb2. The results are depicted in Figure 66. The dynamin-fragments are at least functional in terms of Grb2-binding. Profilin, again, does not bind to any of the fragments.

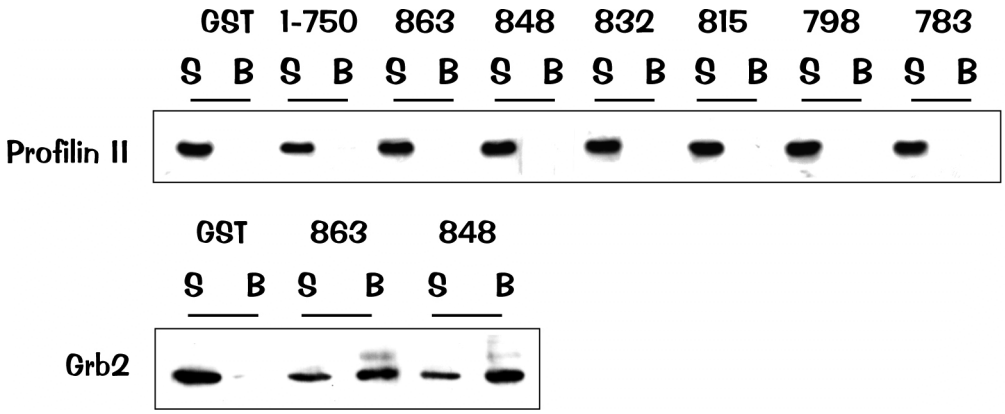

Figure 66: Western blot showing a binding experiment of incubating immobilized dynamin truncates with mouse brain lysate. The upper panel shows probing with anti-profilin II antibody 3003, the lower panel with anti-Grb2 mouse monoclonal antibody. S stands for unbound fraction, B for bound.

Clearly, full-length dynamin binds to profilin II, but bacterially expressed truncates do not, suggesting conformational parameters being essential for profilin binding.

2.5.2.4.3 Dynamin's proline-rich domain binds to profilin

As shown in the preceding chapter, bacterially expressed dynamin-truncates cannot be used for mapping the binding site of profilin on dynamin. Therefore, a strategy was chosen which better preserves individual domains and folds in dynamin. Sweitzer and coworkers had shown that the non-specific protease subtilisin creates a specific digest-pattern of dynamin, in the process of which a 15 kD C-terminal piece containing the proline-rich domain is cleaved off (see Figure 67). The commercially available antibody Hudy-1 binds exactly in this region (Warnock et al. 1995).

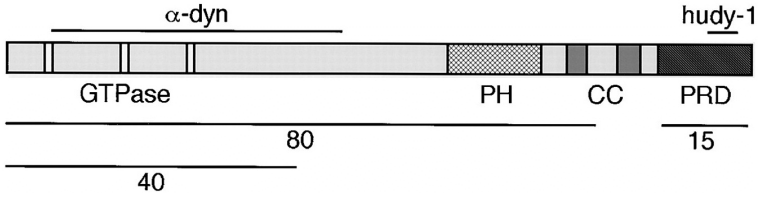

Figure 67: Major fragments generated by digestion of dynamin with subtilisin. Taken from Sweitzer and Hinshaw 1998

Recombinant dynamin was thus digested with varying amounts of subtilisin and subsequently a binding assay on profilin II-beads was performed as shown in Figure 68.

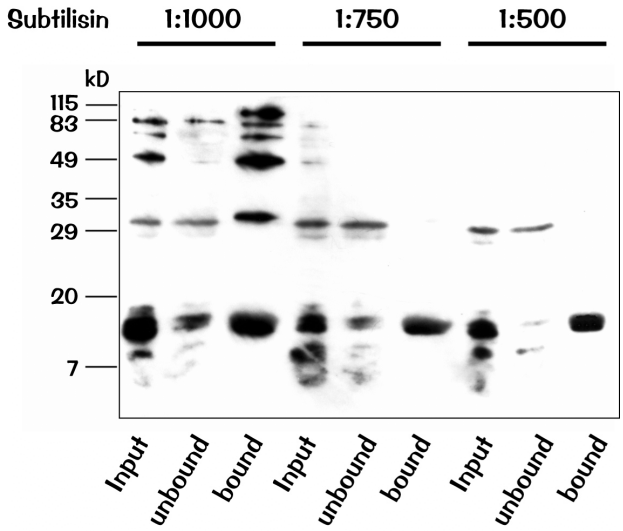

Figure 68: Western blot analysis of a binding experiment with dynamin-fragments created by the non-specific protease subtilisin on profilin II-beads. The blot was probed with the antibody Hudy-1, which recognizes the 15 kD C-terminal fragment that contains dynamin's proline-rich domain.

Bound and unbound fractions were analysed by western blot with the Hudy-1 antibody, which recognizes the C-terminal proline-arginine-rich domain. Figure 68 shows that with increasing protease concentrations a stable 15 kD-fragment is generated which is recognized by Hudy-1 and accumulates specifically on the profilin II-beads. This result shows that the C-terminal 15 kD-fragment containing dynamin's proline-arginine-rich domain binds to profilin II under these conditions.

The antibody Hudy-1 itself can compete for binding of profilin to dynamin as shown by an ELISA binding assay. When profilin II-coated ELISA-plates are incubated with dynamin, the profilin-bound dynamin reacts much less with the monoclonal antibody Hudy-1 as compared with the polyclonal antibody anti-dynamin, although the antibodies react comparably well on wells directly coated with recombinant dynamin I. When mouse-brain lysate is used instead of recombinant dynamin, the native dynamin bound to profilin II does not bind Hudy-1 anymore (see Figure 69).

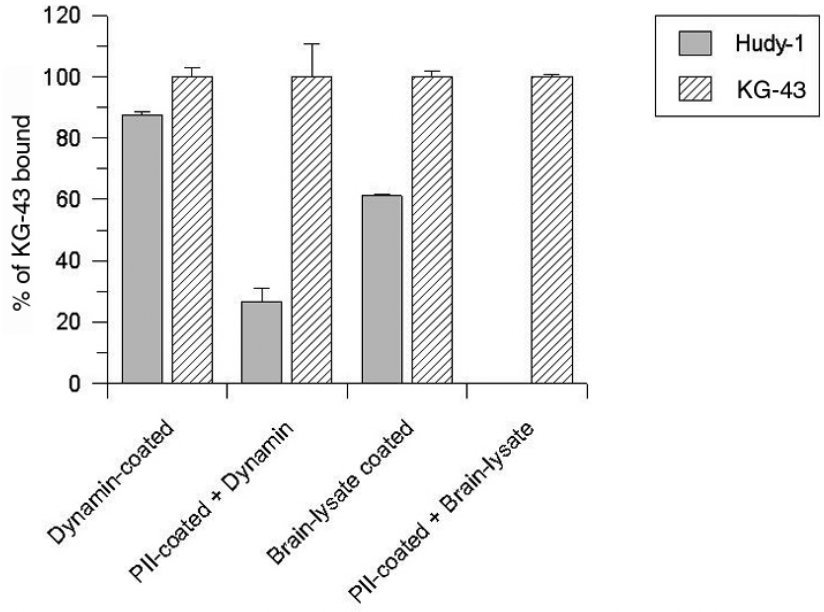

Figure 69: ELISA-experiment showing the binding of the dynamin-antibodies Hudy-1 and KG-43. ELISA-plates were either coated with recombinant dynamin, mouse brain lysate or profilin II. Profilin II-coated wells were then incubated with either recombinant dynamin or mouse brain lysate. The wells were either probed with the monoclonal antibody Hudy-1 or the rabbit antiserum KG-43. The KG-43 rabbit-antiserum reactivity was set as 100% in each individual experiment.

This result suggests that the binding site for Hudy-1 overlaps with a binding-site for profilin II on dynamin I. The exact localization of this site is shown in Figure 70 (Warnock et al. 1995).

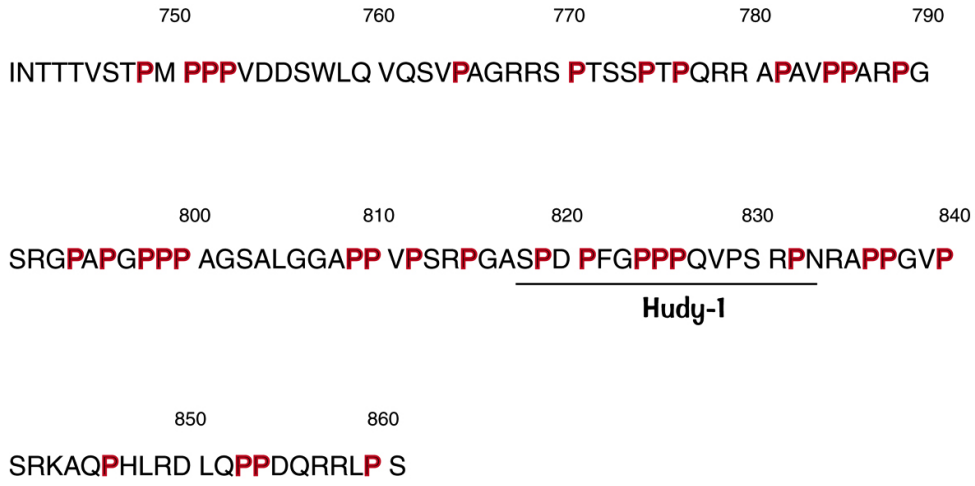

Figure 70: The C-terminal proline-rich domain of human dynamin I. Prolines are shown in red. Amino acid positions are given by numbers, 860 is the C-terminal amino acid. The region which was used as an epitope for Hudy-1 is underlined.

Summarizing the results obtained so far, it has become clear that dynamin I and profilin II interact directly and *in vivo*. The interaction seems to be dependent on conformational parameters on the dynamin side, which cannot be faithfully reproduced by expressing fragments of the protein in bacteria. The data suggest that the binding of the two proteins depends on interaction of profilin's polyproline-binding site with dynamin's proline-rich domain, and that a major binding site for profilin lies in the epitope for the monoclonal antibody Hudy-1 on dynamin's C-terminus.

The next question to be addressed was: what is the functional relevance of the profilin-dynamin interaction?

2.5.2.5 Profilin II, dynamin I and actin

It is tempting to speculate that profilin as an actin-binding protein which at the same time binds one of the key molecules of membrane-traffic might coordinate actin polymerization and endocytosis by promoting formation of a ternary complex of profilin,

actin and dynamin. This complex might either have an influence on nucleating new actin-filaments or profilin might serve as a bridging molecule, thus recruiting actin directly to sites of dynamin-action.

2.5.2.5.1 Dynamin and profilin in actin polymerization assays

To answer the question whether dynamin has an effect on nucleating new actin-filaments, *in vitro* pyrene-actin polymerization assays were performed in the presence of profilin II, dynamin or both at the same time.

As Figure 71 shows, dynamin alone does not have a major effect on actin-polymerization. It slows down polymerization a little bit (right panel of Figure 71), but does not affect polymerization equilibrium. Profilin II instead, as an actin-sequesterer, reduces the speed of actin-polymerization by a factor of 2 under these conditions. If in addition to profilin II dynamin is present, actin-polymerization speeds up again marginally, probably due to the equilibrium-binding of profilin to dynamin, thus sequestering it from actin.

Summarizing these results, dynamin does not have profound effects on the actin-polymerization kinetics and equilibrium in this assay.

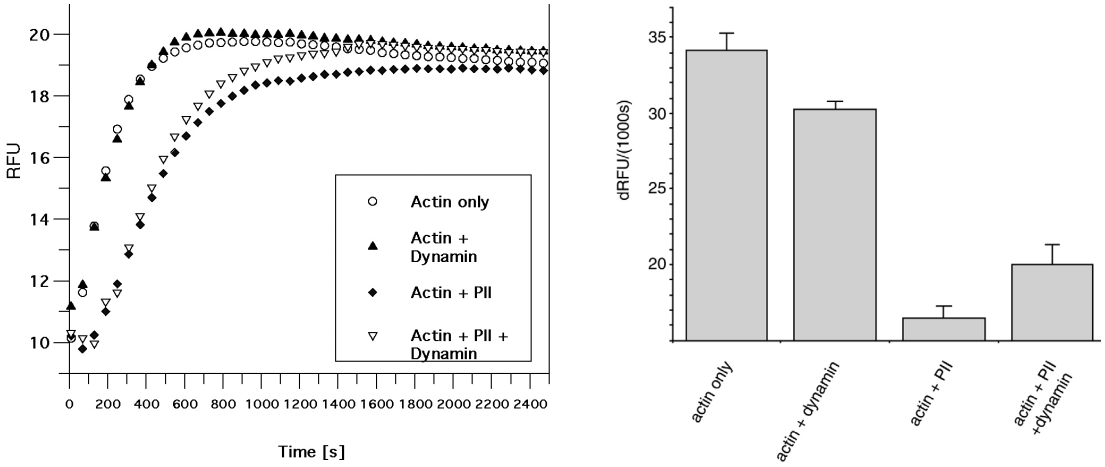

Figure 71: Actin-polymerization assays with 8 μM actin, 5 μM profilin II and 2 μM dynamin. Left panel: Pyrene-actin polymerization assay representing fluorescence (F-actin) over time. Right panel: Graph showing the fluorescence change over time (velocity of polymerization), averaged over three experiments.

2.5.2.5.2 The binding of dynamin and actin to profilin is mutually exclusive

Next, the hypothesis that profilin II might serve as a bridging molecule between actin and dynamin was addressed. To do this, the capability of G-actin to bind to immobilized DNAseI was exploited. DNAseI-beads were saturated with actin in low-salt G-buffer, washed, and then recombinant profilin was bound to the actin on the beads in a buffer which allows good binding of profilin and dynamin. In addition, DNAseI-beads were loaded with the native profilactin-complex isolated from mouse brain, since it has been reported that the profilactin-complex formed *in vitro* may differ from profilactin-complex isolated from tissues (Malm et al. 1983). After washing, the beads were incubated with recombinant dynamin. Figure 72 shows that dynamin does not bind to DNAseI-beads alone, but also cannot bind anymore to profilin which is bound to actin. This result argues against the existence of a ternary complex of dynamin, profilin and actin.

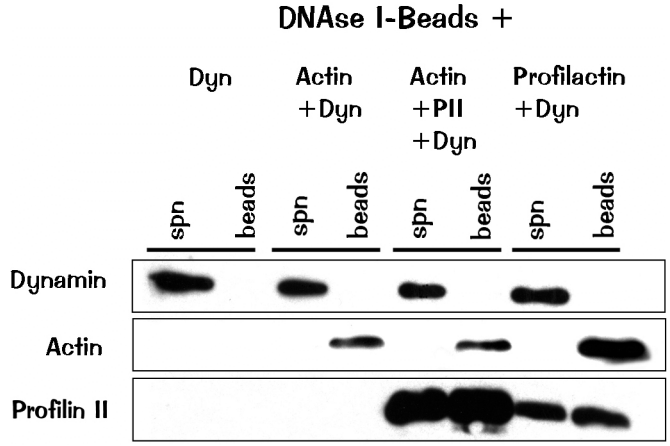

Figure 72: Western blot showing a binding experiment. Actin was immobilized on DNAseI-beads, either as G-actin or as the profilactin-complex from mouse brain. The G-actin bound to the DNAseI-beads was saturated with recombinant profilin II. After washing, the beads were incubated with recombinant dynamin under conditions which normally allow binding of profilin II and dynamin.

This result together with the data obtained from the pyrene-actin polymerization assays (see "Dynamin and profilin in actin polymerization assays") implies that instead of a ternary complex there might in fact be competition of dynamin with actin for binding to profilin II. To test this hypothesis, profilin II-beads were loaded with recombinant dynamin. After washing extensively with G-buffer, the complexes were incubated with

50 μM G-actin in G-buffer or with G-buffer alone. Figure 73 shows that under these conditions dynamin can be eluted from profilin II with actin.

The outcome of those two experiments suggest that the binding of actin and dynamin I to profilin II rather is mutually exclusive.

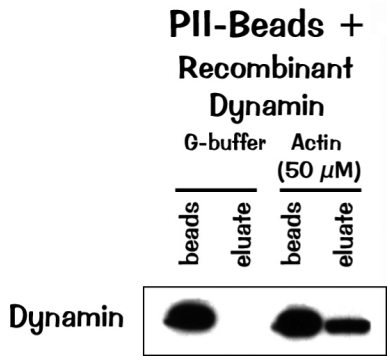

Figure 73: Western blot showing the elution of dynamin from profilin II-beads with actin. Recombinant dynamin was bound to profilin II-beads. After washing the beads in G-buffer, they were incubated either with G-buffer or with 50 μM actin in G-buffer.

2.5.2.6 Profilin II has no effect on the solubility of dynamin

Dynamin is known to form aggregates in low salt buffers, which can be pelleted by high-speed centrifugation. Under increasing salt-concentrations, dynamin becomes more soluble, as shown in Figure 74, panel A. We reasoned that one function of profilin could be to inhibit the oligomerisation of dynamin, which was also shown to stimulate dynamin's GTPase-activity (Warnock et al. 1995).

To test whether profilin has any influence on the aggregation of dynamin, a pelletting-assay was performed, incubating dynamin with increasing amounts of profilin II. As Figure 74, panel B shows, profilin II has apparently no effect on the solubility of dynamin. This is consistent with the finding that profilin II alone also has no influence in dynamin's GTPase activity (data not shown).

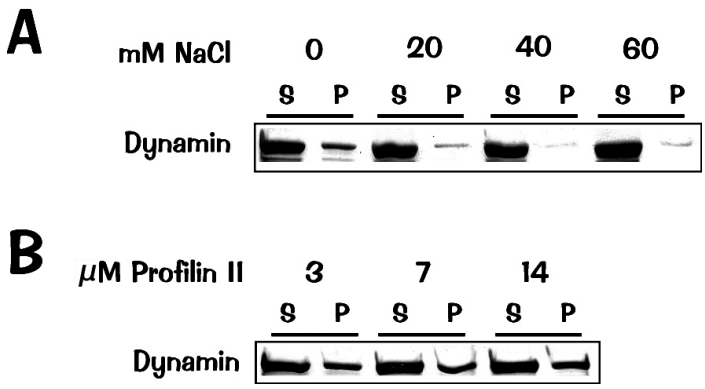

Figure 74: Silver-stained gel of a pelleting assay with dynamin. Panel A: Dynamin was diluted into buffers with various amounts of NaCl before pelletting. Panel B: Dynamin was diluted into the same buffer as in panel without NaCl, but with increasing amounts of profilin II. S stands for soluble fraction, P for pellet.

2.5.2.7 Profilin II competes with other dynamin-ligands in vitro…

The binding site for profilin II on dynamin, namely its proline-arginine-rich domain, has been shown to be a docking-site for other important regulatory molecules for dynamin-function.

It was noticed that although dynamin binds almost quantitatively to profilin II-beads in brain-lysate, certain dynamin-effector molecules like amphiphysin and endophilin were not found in the complex, as shown in Figure 75.

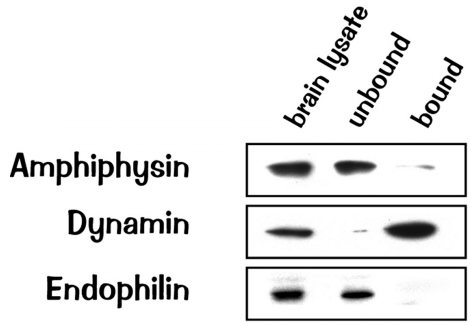

Figure 75: Western blot showing a binding-experiment on profilin II-beads, over which brain lysate had been passed. The wesstern blot was probed with antibodies against amphiphysin, dynamin and endophilin.

This led to the hypothesis that maybe profilin II can compete with SH3-ligands for binding to dynamin. To address this question, an ELISA-based assay was developed. ELISA-plates were coated with the recombinant dynamin-ligands Grb2, endophilin,

amphiphysin and the SH3-domain from src-kinase. After blocking, the wells coated with the dynamin-ligands were incubated with a constant amount of dynamin, mixed with increasing amounts of either profilin II or BSA. After washing off the unbound proteins, the wells were probed with an antibody against dynamin. After another wash, this antibody was detected with an alkaline-phosphatase coupled secondary antibody. The amount of dynamin retained in each of the wells was determined by quantitation of the colour-reaction produced by an alkaline phosphatase substrate in an ELISA-reader. Figure 76 shows the outcome of at least three experiments for each dynamin-ligand. Increasing amounts of BSA had no effect on dynamin's binding to any of the ligands (here only the BSA-effect on Grb2-binding is shown), while dynamin could be competed off its ligands by increasing the amount of profilin II in the assay.

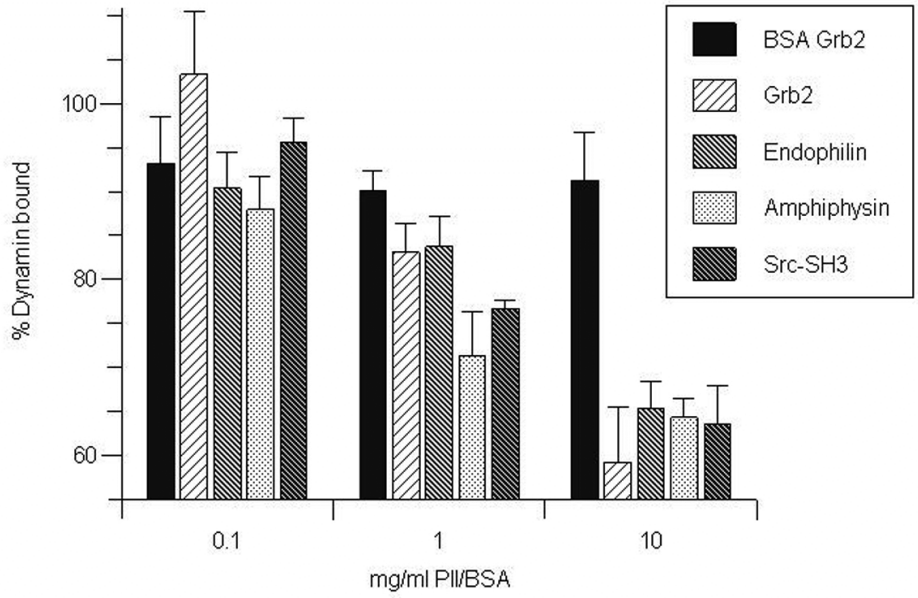

Figure 76: ELISA-based assay for the competition of profilin II with immobilized dynamin-ligands for binding to dynamin.

2.5.2.8 …and in vivo

This finding is supported by experiments with live cells. Plain HeLa-cells and HeLa-cells stably expressing dynamin or profilin II or both from the IRES-expression vectors were

transiently transfected with an expression-vector for GFP-Grb2 (a gift from Michael Way). The IRES-vectors express the protein of interest on a bicistronic mRNA containing an internal ribosomal entry site followed by the antibiotic resistance. This means that only cells expressing the protein of interest can survive antibiotic selection and provides for nearly 100% of expressers. Grb2 binding to activated EGF-receptor when stimulated with EGF leads to a punctate GFP-Grb2 staining of the cells (see Figure 77). It has been shown that dynamin is recruited to stimulated growth factor receptors (Scaife et al. 1994) and in cells expressing myc-tagged dynamin I in addition to GFP-Grb2, the myc-signal can be seen to colocalize with Grb2 in these punctae. However, when these cells overexpress profilin II in addition to dynamin I, the dynamin I-signal is displaced from the puctae and more evenly distributed. This result suggests that profilin II can inhibit the association of Grb2 and dynamin I *in vivo*.

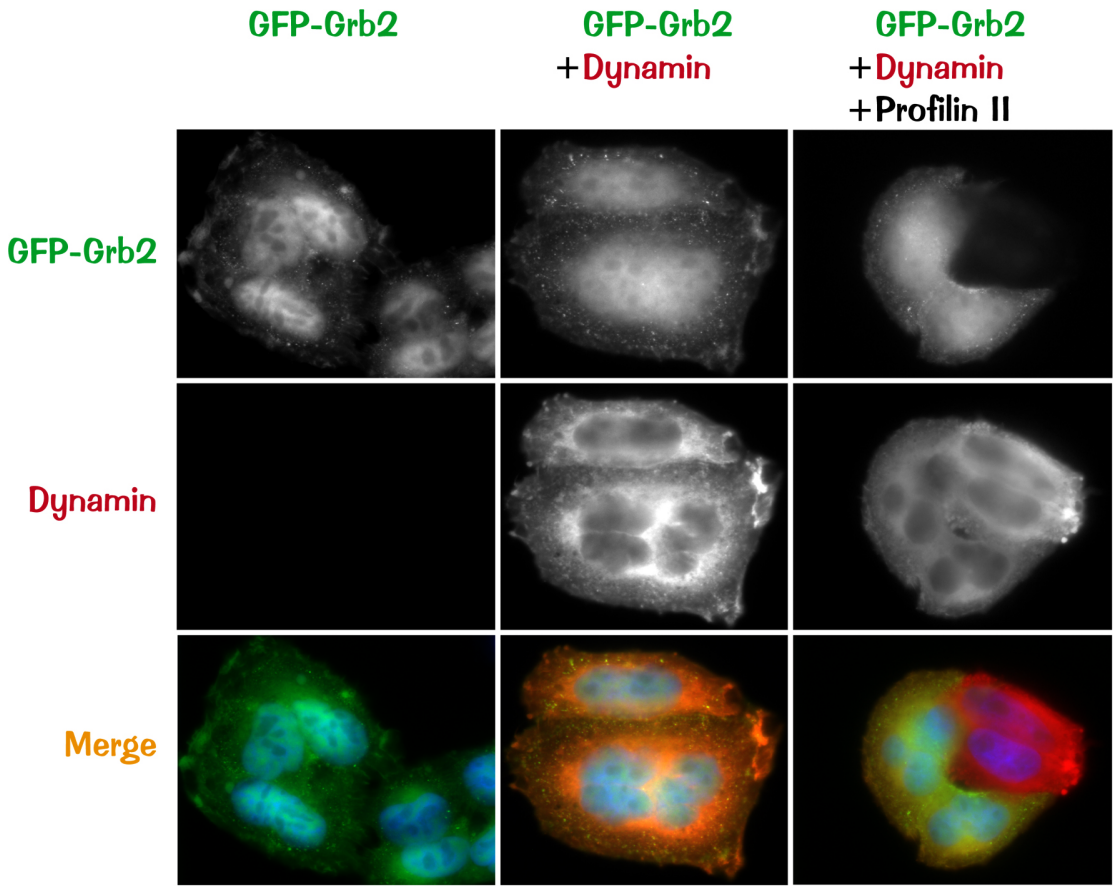

Figure 77: Immunofluorescence micrographs of HeLa-cells transiently transfected with GFP-Grb2.and stimulated with EGF. Left panel: HeLa-cells only expressing GFP-Grb2, middle panel: HeLa-cell line stably expressing myc-dynamin I and transiently GFP-Grb2, right panel: double-stable cell line for profilin

II and myc-dynamin I, transiently expressing GFP-Grb2. After EGF-stimulation, GFP-Grb2 localizes to punctae at the cell membrane, where EGF-receptor is activated. In the cells expressing both Grb2 and myc-dynamin, also the myc-signal can be seen at those punctae, while the myc-dynamin shows a uniform distribution in cells expressing Grb2, myc-dynamin and in addition profilin II.

2.5.2.9 The interaction between profilin II and dynamin I is regulated by phosphoinositides

The binding of profilin II to dynamin and the competition for other dynamin effector molecules might serve as a way of regulating the activity of dynamin. But how can the profilin-dynamin interaction then be regulated?

Profilin and dynamin have been shown to bind to phosphoinositides like phosphatidylinositol-(4,5)-bisphosphate (PIP_2) (Goldschmidt-Clermont et al. 1990; Zheng et al. 1996). These acidic phospholipids are exposed only on the cytosolic side of the plasma membrane and are concentrated at sites of actin polymerization and endocytosis, and they may well serve as spatial regulators of dynamin activation. To investigate the influence of phosphoinositides on the interaction of profilin II and dynamin I, the profilin II-complex from brain was formed on profilin-beads. The complex was then washed with HEPES-buffer and afterwards eluted with micelles made from 300 μM phosphatidylinositol-(4,5)-bisphosphate or mixed phosphatidylinositol phosphates. By analysis of the eluate on an SDS-gel (Figure 78 A) two major bands are visible which come off the beads in the elution: one band of around 45 kD, which is most probably actin, that has been shown to compete with PIP_2 for profilin-binding, and a second band of 100 kD. This 100 kD band has the size of dynamin, and its identity was confirmed by western blot (Figure 78 B, left panel). The susceptibility of the profilin-ligands to elution from the complexes by PIP differs about a wide range: dynamin elutes very well, while VASP or Mena hardly come off the beads. The same is true for the same ligand bound to the two profilin-isoforms: VASP for example is eluted efficiently from profilin I, but not from profilin II. For those ligands there might be a different mechanism of regulating their binding to profilin, most likely phosphorylation. (see Discussion).

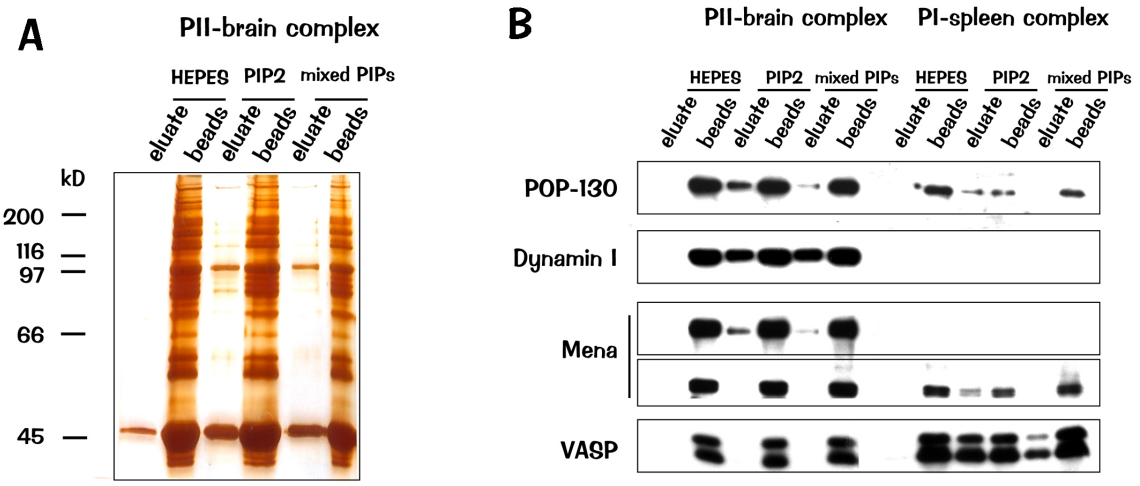

Figure 78: Elution of profilin-complexes with phosphatidylinositolphosphate-micelles. A: Silver-stained gel of the elution of the profilin II-complex from brain. B: Western blot showing the elution of the profilin II-complex from brain in comparison with the profilin I-complex from spleen.

The data presented here suggest that the disruption of the binding between profilin and its ligands by phosphoinositides might thus serve as a control mechanism not only for actin-profilin interaction, but also for profilin binding to polyproline-ligands.

Phosphoinositides do not only regulate dynamin-profilin II interaction, but also stimulate dynamin's GTPase-activity (Zheng et al. 1996). Since profilin also binds to PIPs and has previously been shown to block PLC-g activity, it was examined, whether the presence of profilin II might influence PIP-activated GTP-hydrolysis by dynamin.

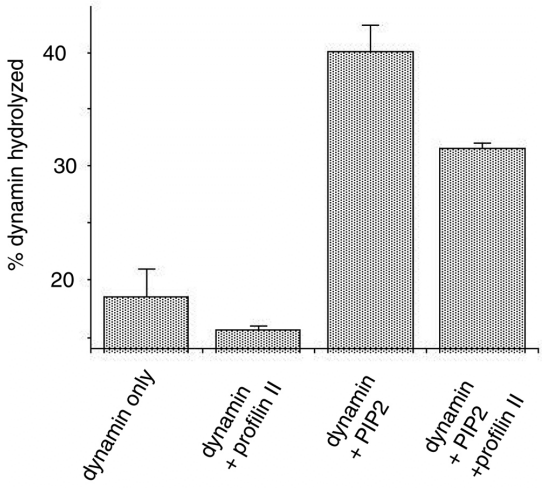

Figure 79: Dynamin GTPase- activity in the presence of PIP2 and profilin II. The assay was carried out in triplicates with 0.5 μM dynamin, 100 μM PIP2 in micellar form and 20 μM profilin II.

As Figure 79 shows, profilin alone has no influence on dynamin's GTPase-activity, while PIP_2 leads to a significant increase in GTP-hydrolysis by dynamin. Interestingly, the PIP_2-induced GTP-hydrolysis by dynamin, however, is reduced in the presence of profilin, suggesting that profilin can compete with dynamin for PIP_2-micelles.

3 DISCUSSION

3.1 Profilin's function is still an enigma

Even about 25 years after its discovery as an actin-binding molecule, profilin's exact molecular function is still not completely clear. Its vital importance, however, has been strikingly demonstrated by the lethal phenotype of the ablation of the ubiquitously expressed profilin I in mice (Witke et al. 2001). The apparent cytokinesis-defects in the developing embryos of the mutant mice resemble the phenotype of yeast cells lacking profilin and can be explained by the failure to form contractile actin-rings during cell division. This is in accordance with profilin's well-established role as a regulator of actin-dynamics.

However, profilin, in addition to actin, also binds to other protein ligands and phospholipids. Above that, mammals and also some lower eukaryotes have more than one profilin gene, which in the case of multicellular organisms are also expressed in a tissue-specific manner. These findings nourish the idea that different profilin isoforms may perform specialized tasks, which are mediated by the isoform-specific binding of distinct protein ligands.

3.2 Profilin is not only an actin-binding protein

The fact that profilin was initially thought to be only an actin-binding protein, makes it come as a surprise to find such a vast variety of ligands bound to affinity-beads made of the recombinant proteins. Clearly, this is mainly due to the fact that profilin can in addition to actin also bind protein ligands which are rich in proline. Polyproline-stretches in proteins have been shown to act both as structural elements, often found to break secondary structures and located in hinge-regions, and as protein-protein interaction sites. Regions of three or more consecutive prolines adopt a so-called polyproline II-helix under physiological conditions - those are left-handed, extended helices with three residues per turn. Their relative rigidity renders proline-rich stretches less motile - a state of low entropy, even before binding of partner molecules - and easily accessible. Due to these two features, binding to polyproline-stretches can occur very fast when compared to other protein-protein interactions (Williamson 1994) and often with low specificity. This makes them versatile binding platforms, which allow rapid and reversible association of several proteins into functional complexes.

3.3 Promiscuous profilin

Indeed, the vast number of ligands we found in the profilin complexes shows that profilin is rather promiscuous in its choice of binding partners, although the biochemically and structurally very similar isoforms profilin I and profilin II bind to a distinct set of molecules. This apparent paradox of promiscuity and specificity is also found in other proline-binding modules, so for example the SH3-domain. Some SH3-domains are very selective, like the Abl-SH3 domain, others promiscuous, like Fyn-SH3. The specificity of binding between SH3-domains and polyproline II-helices has been shown to be due to both non-proline residues in the proline-rich stretches and residues surrounding the generally flat proline-binding pocket. The same might be true for profilin I and profilin II, since dynamin I for example is not found in the profilin I-complex from mouse brain. Figure 80 shows a comparison of the polyproline-binding pockets of human profilin I and profilin II. Despite the overall very similar architecture, there are subtle

differences in the guiding helices and in charged residues surrounding the binding pocket, which might confer specific accessibility for polyproline-ligands.

Six proline-residues in a row have been shown to span the binding pocket of profilin (Petrella et al. 1996), which correspond to two turns of a polyproline II helix. But only 10 or more residues confer best binding. The binding to polyproline does not induce major structural changes in profilin. Profilin binds polyproline mainly via hydrophobic interactions, as shows the fact that the affinity is higher under high-salt conditions (which is true also for dynamin). Hydrophobic residues in the binding-pocket made by the N- and C-terminal helices have been shown to be essential for binding (Bjorkegren et al. 1993). A consequence of this mainly hydrophobic interaction is that binding is not as restricted to one or a few ligands as it is for well defined electrostatic binding surfaces.

Several attemps have been made to assign a profilin-binding consensus-motif; XPPPPP with X being G, L, I, S or A has been suggested (Holt and Koffer 2001). But taking into account a greater number of ligands also a more redundant consensus has been proposed, like ZPPX, where Z is P, G, A or a charged amino acid and X preferentially hydrophobic (Witke et al. 1998).

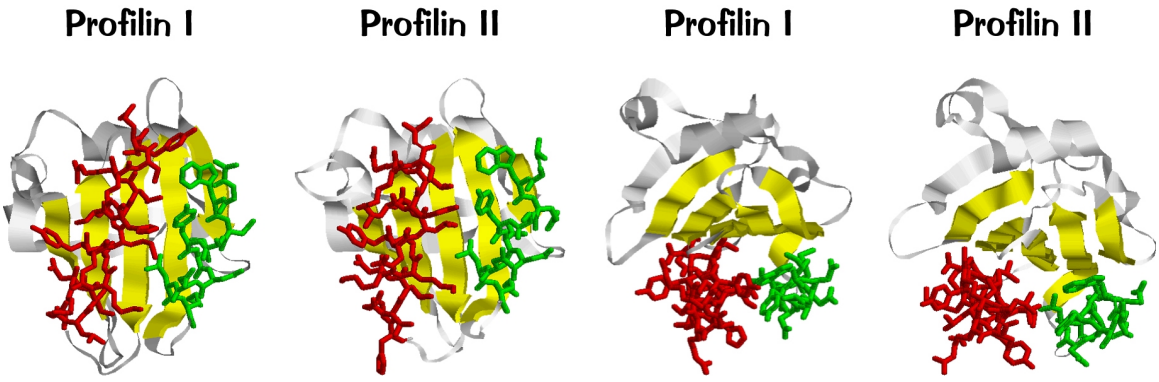

Figure 80: Comparison of the polyproline binding-pockets of human profilin I and profilin II, seen from two different angles. The underlying beta-sheet is shown in yellow, the N-terminal helices in green and the C-terminal helices in red.

Proline-rich stretches like those are often found in proteins regulating the microfilament system.

The Ena/VASP-family is one of the groups of proteins involved in cytoskeletal rearrangements which contain profilin-binding polyproline-motifs. They themselves

contain another proline-binding domains termed EVH1 (Ena/VASP homology 1), which bind to very similar proline-rich sequences. Since those proteins localize to the plasma membrane after activation of cells, they might mediate an increase in actin-concentration at the membrane by recruiting the profilactin complex. As shown here, Mena can be co-immunoprecipitated with profilin II, and profilin II co-localizes with VASP in focal-contacts.

A second class of proline-rich profilin ligands regulates the microfilament system downstream of rho-related small GTPases, either by direct interaction or indirectly with cdc42, rho or rac. The small GTPases usually get activated at membranes, and might thus mediate actin-recruitment to the membrane via profilin. The WASP/N-WASP, SCAR/WAVE and formin-homology (FH) families belong to this group. As shown here, profilin II can be co-immunoprecipitated with the FH-protein diaphanous. Also, another rho-effector, rho-associated coiled-coil kinase (ROCK), can be found in the profilin II-complex. A link to rac-signalling comes from the presence of the adaptor protein Hem2 in the profilin II-brain complex, a protein identical to Nck-adaptor protein 1 which in turn is known to bind to rac (Kitamura et al. 1997).

Apart from these ligands which are involved in eventually conveying signals to the actin-cytoskeleton, we identified a number of molecules in the profilin complexes from mouse brain which are important players of - surprisingly - synaptic vesicle recycling and endocytosis.

3.4 What is an actin-binding protein doing at the synapse?

The presence of so many protein regulators of synaptic vesicle recycling in the profilin-complexes from mouse brain suggests an involvement of profilin in membrane-trafficking events at the synapse. This is further corroborated by the subcellular localization of profilin II at sites of active vesicle secretion and recycling. Brain sections were immunogold-labelled with an antibody against profilin II (in collaboration with M. Sassoe'-Pogneto, University of Torino). Figure 81 shows the localization of profilin II in

synapses. Immunoreactivity is seen throughout the presynaptic terminal and in vicinity of synaptic vesicles (Figure 81B), but especially concentrated at active zones in both pre- and postsynaptic densities (Figure 81C), were vesicle docking and neurotransmitter release and recycling occurs.

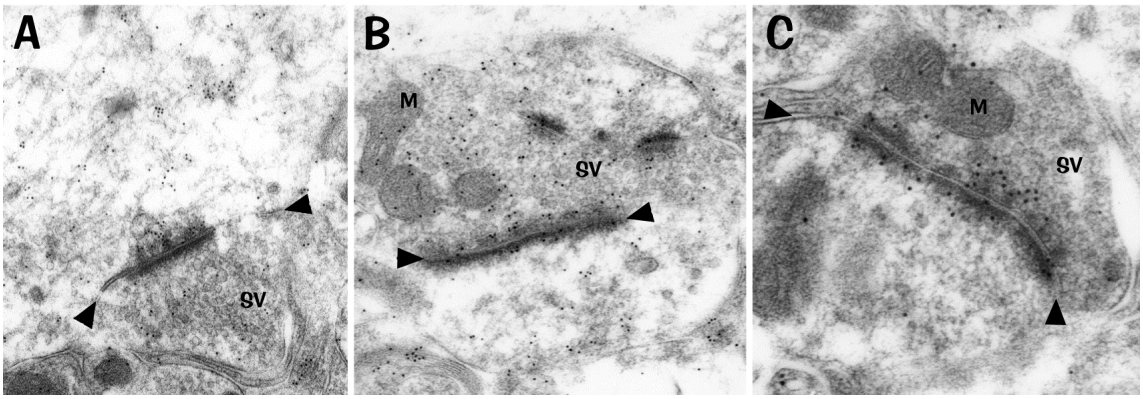

Figure 81: Electron micrographs of synapses in mouse brain with immunogold-labelling for profilin II. SV: synaptic vesicles in the presynaptic compartment; M: mitochondria. Arrows label the synaptic cleft, the electron-dense thickenings of the synaptic clefts are active zones of vesicle docking and release. Photographs provided by M. Sassoe'-Pogneto.

3.5 Profilin II affects membrane traffic

When ectopically expressed in Hela-cells, profilin II leads to a marked decrease in general membrane uptake as measured with FM membrane-dyes. Receptor-mediated endocytosis is one aspect of membrane uptake which is affected, as could be seen by cells expressing red profilin II, where strong expressers take up less transferrin.

If introduction of profilin II into cells which usually do not express it causes a decrease in membrane uptake, taking this profilin isoform away from cells which usually do express it should lead to an increased uptake of membrane. This is in fact the case. Neurons from profilin II mutant mice show a two-faceted phenotype: first, a basal membrane uptake which is twice as high as in neurons from wildtype-mice. And second, this uptake cannot be further stimulated by depolarization, as it is the case in wildtype neurons. These findings suggest that profilin II can control membrane uptake as a negative regulator. This result is corroborated by data from *Dictyostelium*, were profilin null cells exhibit more efficient phagocytosis as compared to wildtype cells (Temesvari et al. 2000).

Furthermore, it seems that in neurons lacking profilin II membrane is constitutively much faster recycled when compared to wildtype neurons. Although exocytosis stimulated by depolarization was identical in wildtype and profilin II mutant cells, unstimulated or constitutive membrane delivery to the plasma membrane was faster by a factor 2 in the cells lacking profilin II. This increase of exocytosis is necessary to counterbalance the increased membrane uptake in these cells and thus keep the plasma membrane area constant.

A recent study established structural similarities of profilin with a molecule involved in exocytosis (Gonzalez et al. 2001), a pathway generally well-conserved between phyla (Bennett and Scheller 1993). Already before, a genetic study showed a link between *S. cerevisiae* profilin and Sec3p, another component of the exocytic pathway in yeast (Finger and Novick 1997). Profilin I has indeed been found associated with exosomes (a secreted subcellular compartment) in dendritic cells (Thery et al. 2001). Furthermore, profilin II was shown to interact with the synapsins (Witke et al. 1998), which are thought to link the reserve pool of synaptic vesicle to the actin cytoskeleton and release it upon stimulation. Taken together, these results argue for a possible involvement of profilin in exocytic events and possibly neurotransmitter release.

What about profilin and internal membrane systems? Using video-microscopy, red profilin II could be seen in a perinuclear vesicular compartment, which might well be part of the Golgi apparatus. Profilin I has been reported to be attached to the Golgi, where it is speculated to be important for formation of transport vesicles (Dong et al. 2000). In HeLa cells, the introduction of profilin II leads to a more efficient washout of FM 1-43 membrane dye as compared to untransfected HeLa, maybe by preventing dilution of dye which had been taken up out of the recycling endocytic into constitutive membrane systems.

For the first time, apart from its regulatory role for the actin cytoskeleton, functional evidence for the involvement of profilin II in membrane trafficking events is presented. But what could be the underlying mechanisms by which profilin II is able to mediate these effects? Both of profilin's non-actin binding features, namely PIP_2- and polyproline binding, may be responsible for the effects seen on membrane trafficking.

3.6 The lipid connection

Profilin is known to bind to acidic phospholipids, and in particular to phosphatidylinositol-(4,5)-bisphosphate (PIP_2). Phosphoinositides are thought to play a critical and general role in adaptor incorporation into plasma membrane clathrin-coated pits by targetting the AP-2 complex and arrestin to these sites (Gaidarov and Keen 1999; Gaidarov et al. 1999a). Phosphatidylinositol phosphates have also been shown to be important for synaptic neurotransmitter release (Khvotchev and Sudhof 1998). Especially $PI(4,5)P_2$, rather than any of its metabolites can serve as binding platform for a range of molecules of the synaptic vesicle docking-, budding- and fusion machinery. So do the synaptotagmins bind PIP_2 - abundant molecules on synaptic vesicles which are thought to coordinate formation of the docking/fusion process in interplay with SNAREs (Schiavo et al. 1996). SNARE-complex formation is further controlled by rab GTPases (Robinson and Martin 1998), which in turn bind the PIP_2-binding molecule rabphilin-3A (Burns et al. 1998). Together, synaptotagmin and rabphilin-3A with rab3 seem to coordinate calcium-mediated docking of synaptic vesicles (Corvera et al. 1999).
Profilin has been shown to protect PIP_2 from hydrolysis by unphosphorylated phospholipase C-γ1 (Goldschmidt-Clermont et al. 1990). If this PIP_2-protecting molecule is removed from cells uncontrolled hydrolysis of phosphoinositol phosphates by PLC-γ1 might occur, which in turn may prevent proper formation of docking/fusion complexes. This again would lead to impairments in neurotransmitter release. The fact that mice lacking profilin II indeed show reduced levels of noradrenaline in the brain (Di Nardo 2001) supports this his hypothesis. Preliminary analysis of lipid content of whole wildtype and mutant brains, however, did not show any gross abnormalities, which does not exclude that subtle defects in phosphatidylinositolphosphate metabolism occur after stimulation, or only in defined subsets of neurons in the brain.

In fact, we found a lipid-modifying enzyme, the phosphatidyl inositol phosphatase synaptojanin (Haffner et al. 1997), specifically associated with profilin II in mouse brain. Synaptojanin has three polyproline-rich domains as potential binding sites for profilin. Unlike PLC-γ1, synaptojanin is able to hydrolyse PIP_2 even when it is bound to profilin to phosphatidylinositol-4-phosphate (Sakisaka et al. 1997). Overexpression of this protein

caused a decrease in actin stress-fibers in COS 7 cells (Sakisaka et al. 1997). It has been speculated that synaptojanin is a molecule involved in linking endocytosis and the actin cytoskeleton in yeast (Singer-Kruger et al. 1998). Mice deficient for synaptojanin die early after birth and have defects in synaptic vesicle recycling (Cremona et al. 1999). Ablation of the *C. elegans* homolog *unc-26* shows the same phenotype as the knockout in mouse, plus defects in tethering the vesicles to the cytoskeleton (Harris et al. 2000). Recently, synaptojanin 2 has been shown to be an effector molecule of the small GTPase rac 1, which regulates clathrin-mediated endocytosis (Malecz et al. 2000). In neurons, synaptojanin and profilin II may act hand in hand in linking synaptic vesicle recycling in interplay with the actin cytoskeleton.

Also the huntingtin-protein was found as a novel member of the profilin II complex from mouse brain. Binding presumably occurs via its very proline-rich first exon, a region which has been shown to bind other huntingtin ligands, like SH3GL3 (Sittler et al. 1998) a Grb2-like SH3-domain containing protein. Some of the symptoms of profilin II mutant mice like increased motor activity (A. Di Nardo, personal communication) are similar to mouse models for Huntington's disease (Bates et al. 1997), a neurodegenerative disorder caused by mutations of the huntingtin-protein. mRNA for both profilin I and II are upregulated in Huntington patients, and mice expressing a mutant form of the huntingtin-protein show cytoskeletal abnormalities (D. Tagle, personal communication). One of its interacting proteins, HIP1R, is thought to connect clathrin-coated vesicles with the actin cytoskeleton (Engqvist-Goldstein et al. 1999).

Apart from the two novel members of the profilin II complex, huntingtin and synaptojanin, which are involved in lipid-metabolism and disease respectively, a variety of other polyproline containing ligands can be found in the profilin II complex which hypothetically could be responsible for the effect of profilin II on membrane trafficking. Since it is beyond the scope of this thesis to analyze all of those ligands, two members were chosen for further investigation: POP-130 and dynamin I.

3.7 POPping vesicles

POP-130 was found as a novel protein in the profilin II complex from mouse brain (Witke et al. 1998) and independently in a screen of a brain-specific cDNA-library with a probe from differentiating P19-cells ("shyc" Koster et al. 1998). It has been stated that POP-130 is only expressed in developing and adult mouse brain, the results presented here, however, prove that the expression is rather widespread. The human orthologue PIR121 has been found in a DNA chip-screen to be upregulated after transfection of tissue-culture cells with the apoptosis-inducing p53-mutant 121F, but by itself proved unable to induce apoptosis (Saller et al. 1999). Homologs have been found also in *C. elegans* (F56A11.1) and in Drosophila (DSra-1). DSra-1 is an effector for Drosophila rac-1 during embryogenesis (Langmann and Harden 2001).

This novel member of the profilin II complex could be shown to directly interact with profilin II by co-immunoprecipitation. Subcellular fractionation proved its localization to a membraneous compartment, and GFP-POP was seen in a perinuclear vesicular localization, which extensively co-stained with transferrin, linking POP to the endocytic pathway. Indeed, overexpression of POP-130 in HeLa cells led to a decrease in membrane uptake as measured by FM-dyes and also by transferrin-uptake. POP therefore seems to be intimately involved in the endocytic route of membrane traffic and may provide a physical link to profilin II.

The overlap of expression with with transferrin-staining in the endocytic recycling-compartment and the fact that DsRa-1 is an effector for rac-1 is reminiscent the small GTPase Arf6, which has the same properties and was speculated to control the shuffling of rac-1 to its sites of action (D'Souza-Schorey et al. 1998).

3.8 The interaction of profilin II with dynamin I

Besides POP, the second profilin II ligand which we looked at in more detail was the 100 kD GTPase dynamin I, a well-known key regulatory molecule of endocytosis and other membrane trafficking events. Dynamin I has been found in the profilin II affinity complex from mouse brain. It interacts directly and *in vivo* with profilin II, as shown by binding experiments with the recombinant proteins and co-immunoprecipitation. In

addition, binding is also specific for the isoform profilin II. The interaction could shown to occur via the proline-arginine rich C-terminal domain of dynamin I and the polyproline binding domain of profilin II.

Bacterially expressed dynamin-fragments to did not bind to profilin II. There are two possible explanation for this fact. First, intramolecular interactions of the dynamin molecule (Muhlberg et al. 1997) may be necessary to create a functional binding site for profilin II, which is lost when expressing isolated fragments. Furthermore, polyproline helices are known to be able to exist in two different conformations; *cis*-peptide bonds form right-handed tight polyproline I helices, while *trans*-bonds form left-handed more extended polyproline I helices. Conversions between the two states are being catalyzed by peptidyl-prolyl isomerases, some of which are restricted to mammals (e.g. PIN1, Lu et al. 1996; Yaffe et al. 1997). This mechanism has been shown to regulate the activity of proteins. The lack of binding of might also be due to the fact that bacteria lack specific isomerases which convert the proline-rich fragments into a conformation which allows efficient binding of profilin II.

The fact that profilin II-bound dynamin shows a marked decrease in binding to the monoclonal antibody Hudy-1, suggests that the epitope for Hudy covers a major profilin binding site (see Figure 82). Nonetheless, dynamin's PRD has more putative consensus profilin binding sites which would fit a degenerate profilin binding motif, like mentioned earlier.

Proline-rich stretches can oftentimes be found in proteins involved in cytoskeletal regulation, but are also also important modules for synaptic vesicle-associated neuronal proteins and proteins involved in membrane trafficking as well as signal transduction (Kay et al. 2000). Polyproline-binding SH3-domain containing proteins have been shown to be important for clathrin-coated vesicle formation. So can the Grb2-, endophilin- and amphiphysin-SH3 domains inhibit coated vesicle formation in vitro (Simpson et al. 1999). It has been shown that clathrin-mediated endocytosis can be perturbed by disruption of interactions with the SH3-domain of endophilin (Gad et al. 2000). All of these molecules (and in addition src-kinase, which also bears an SH3-domain) have been shown to bind to the proline-rich domain of dynamin.

The enrichment of dynamin I in the profilin II complex from brain and the apparent lack of dynamin effector molecules like amphiphysin and endophilin led to the idea that profilin II might be able to compete for these ligands on dynamin. This hypothesis could be confirmed by an ELISA-based competition assay, in which the dynamin ligands Grb2, endophilin, src-SH3 and amphiphysin could be competed off dynamin with increasing amounts of profilin II.

In live cells, the association of dynamin with Grb2 which had been recruited to stimulated growth-factor receptors could be reduced in the presence of profilin II, which further supports the idea of profilin as a competitor for this molecule on dynamin.

The topical basis for the competition of profilin II with Grb2 and amphiphysin on dynamin can be more easily understood by taking a closer look at dynamin's proline-rich domain. Figure 82 shows that it contains various short proline-rich stretches which fit degenerate profilin binding motifs. As suggested by binding assays, one of the putative binding sites for profilin overlaps with the epitope for the monoclonal antibody Hudy-1. The binding-sites for the dynamin-binding molecules Grb2 and amphiphysin have been mapped to the vicinity of this site as well, and, indeed, also the two of them show competition of binding (Grabs et al. 1997). If also profilin binds in this region, steric hindrance might prevent the access of those two dynamin effector-molecules.

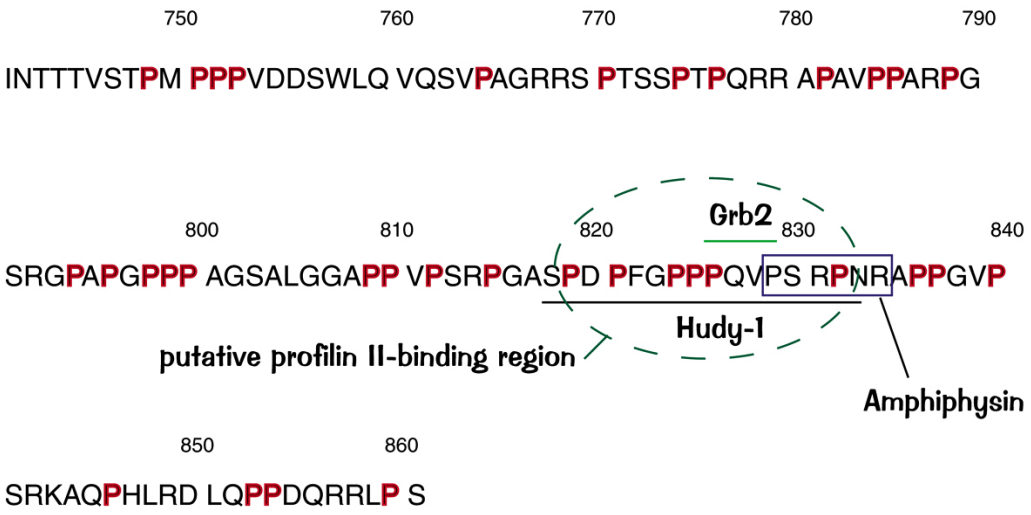

Figure 82: Sequence of the proline-rich domain of human dynamin I. Binding sites for Grb2 (Gout et al. 1993) , amphiphysin (Grabs et al. 1997) and the monoclonal antibody Hudy-1 are indicated.

Profilin II may have a similar buffering function also for synaptojanin. Like dynamin, synaptojanin binds endophilin and amphiphysin in nerve terminals (Micheva et al. 1997). And while endophilin and amphiphysin are excluded, synaptojanin can be found in the profilin II complex from mouse brain. In binding to dynamin, synaptojanin and huntingtin, profilin II resembles very much the members of a protein family called EEN/SH3p/SH3GL, which include for example endophilin. Like profilin II, EEN family members have been shown to be able to compete with amphiphysin for binding to dynamin (So et al. 2000) and have been speculated to play a regulatory role in synaptic function.

3.9 Functional implications for the interaction of profilin II with dynamin I

The endocytotic machinery is a multicomponent complex, whose assembly has to be controlled in a very well-defined manner. Amphiphysin binds to clathrin and the AP2-clathrin adaptor and is thought to recruit dynamin to clathrin-coated pits (Takei et al. 1999). A dynamin mutant which is defective in self-assembly mediated GTPase activity and exhibits a prolonged GTP-bound state when assembled into rings around the necks of budding endocytic vesicles shows a stimulation of endocytosis (Sever et al. 1999). This suggests that rather than using the energy of GTP-hydrolysis like a motor enzyme, dynamin may control a downstream machinery for the pinching process (Yang and Cerione 1999). Endophilin is thought to be part of this downstream machinery and is recruited to sites of endocytosis by dynamin (Huttner and Schmidt 2000). The functional interaction of endophilin and dynamin was shown by the fact that an endophilin mutant no longer able to bind to dynamin cannot promote the formation of synaptic-like microvesicles anymore (Schmidt et al. 1999a). Endophilin itself is an enzyme which can catalyze the formation of phosphatidic acid from lysophosphatidic acid and arachidonoyl-CoA (Schmidt et al. 1999a). By doing this, it transforms a wedge-shaped lipid into a cone-shaped one, thus inducing positive membrane curvature, which is thought to help the pinching process (Barr and Shorter 2000; Scales and Scheller 1999).

By preventing the access of those effector molecules to dynamin, profilin might impede the assembly of the endocytic machinery in a controlled manner. It may inhibit dynamin's recruitment to coated pits by blocking its binding to amphiphysin. Additionally, the access of endophilin may be inhibited by profilin II bound to dynamin. If profilin is missing, this negative regulation may be lost and excessive endocytosis might occur, as it is indeed the case in neurons from profilin II-mutant mice.

We also were able to show that profilin II is able to diminish the stimulatory effect of PIP_2 on dynamin's GTPase activity, which would be an additional way to act as a negative regulator on dynamin, since GTPase activity was shown to be important for dynamin's function in endocytosis (Marks et al. 2001).

The molecular basis of the connection of the endocytic machinery and the actin-cytoskeleton is currently receiving much scientific interest. Profilin II being a molecule which binds both actin and effectors of the endocytic machinery of the synapse may serve as a molecule which coordinates actin polymerization at sites of endocytosis, like the nerve terminal. There are at least two possibilities how profilin might act. Dynamin might for example serve as a molecule which stimulates nucleation of actin filaments from the profilactin complex. Pyrene-actin polymerization assays with profilin II and dynamin, however, argue against this possibility. A second hypothesis is that profilin acts as a bridging molecule between actin and dynamin and thus recruits actin to the sites of dynamin action via a ternary complex. The results presented here, however, speak against trimers of profilin II, dynamin I and actin, since it was shown that a binding of dynamin and actin to profilin II is mutually exclusive. Rather, it seems likely that separate profilactin and profilin-dynamin complexes coexist in the cytosol. Profilin prevents actin from polymerizing but prepares it for the incorporation into filaments. Bound to dynamin, profilin can prevent access of effector-molecules important for dynamin's function. At the membrane, however, acidic phosphoinositides bind profilin and - probably by induced changes in secondary structure (Raghunathan et al. 1992) - disrupt binding of profilin to dynamin. In addition, they also set actin free from the profilactin-complex. This, together with the fact that phosphoinositide-rich membrane regions might serve as places of endocytosis (Martin 2000; Thiele et al. 2000), leads to a model of how dynamin-

activation and actin-polymerization at these sites might be concerted by profilin (see Figure 83).

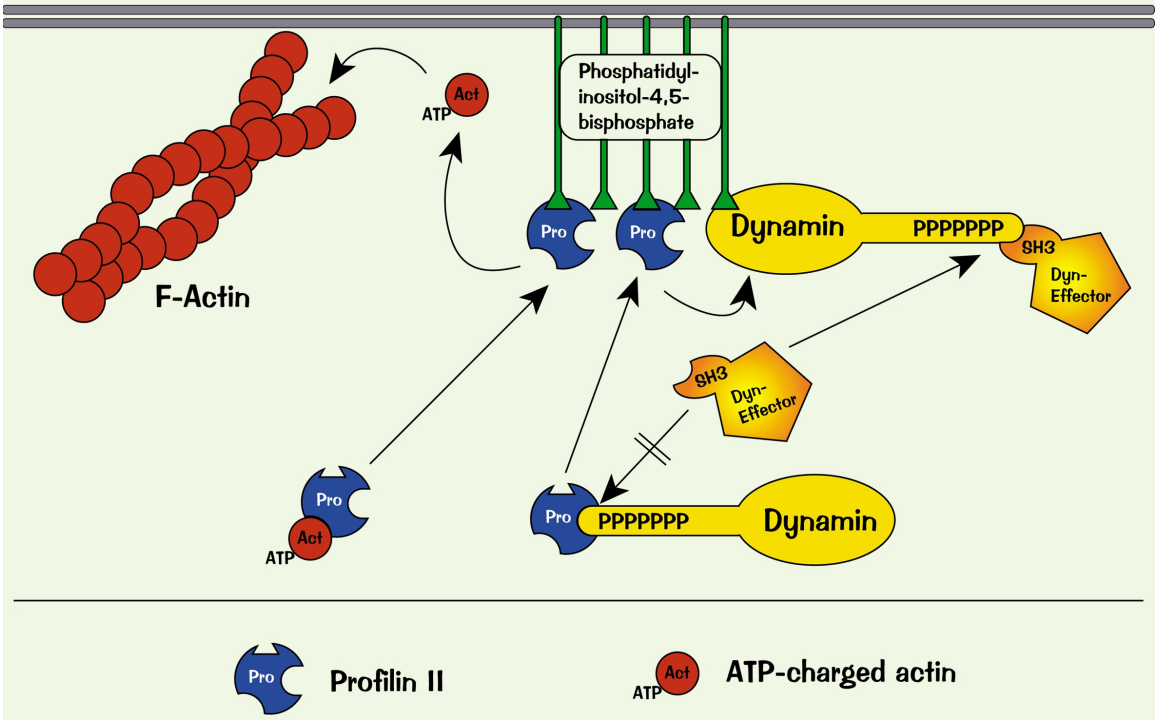

Figure 83: Model of how profilin II might coordinate actin-polymerization and dynamin activation at the plasma-membrane. In the cytoplasm, profilin II keeps actin in monomeric form and prevents the access of effector molecules to dynamin's proline-rich domain. At PIP_2-rich sites of the plasma-membrane, ATP-charged actin is set free for incorporation into filaments, and profilin II lets go of dynamin's dynamin's PRD to allow access of molecules essential for dynamin's activity in endocytosis.

Profilin-bound inactive dynamin reaches phosphoinositide-rich sites at the plasma-membrane. Profilin binds to PIP_2 and releases dynamin, which in turn is now free to bind effector molecules of the endocytic machinery, like endophilin and amphiphysin. The same PIP_2-rich regions serve as sites were ATP-charged actin is set free and is now ready to polymerize into actin-filaments which might facilitate membrane invagination and help the pinching process by forming contractile structures around pinching vesicles (Fujimoto et al. 2000).

3.10 Profilin as a buffering molecule not only for actin, but also for proline-rich domains of proteins

The fact that profilin II is able to compete with SH3-domain proteins for binding to the PRD of dynamin comes is backing up the idea of cross-talk between protein-interaction modules. It has been speculated that there might be degeneracy in binding of proline-rich ligands to polyproline-binding modules with similar affinities, such as WW, EVH1 and SH3 domains and profilin (Chan et al. 1996; Kay et al. 2000; Sudol 1996; Sudol 1998).

No SH3-domain is able to bind pure polyproline as tightly as does profilin. And even the best peptide-ligands just bind their cognate SH3-domains with affinities similar to profilin/polyproline (Petrella et al. 1996). As shown here, profilin is able to bind a huge number of protein ligands containing polyproline-rich stretches. This, together with the fact that profilin is a very abundant protein in cells with concentrations of up to 100 μM, raises the possibility that profilin might act not only as a buffering-molecule for actin (a job it shares with thymosin β-4), but also as a versatile buffer for proteins containing proline-rich stretches in the cell. Apart from dynamin, profilin II has been shown to be able to compete with the nSrc-SH3 domain for binding to the Ena-Vasp-like protein Evl (Lambrechts et al. 2000). By binding to polyproline-stretches of very redundant consensus, profilin may generally keep these ligands in an off-state, just like it keeps actin from polymerizing. Upon signals well defined in space and time, like touching PIP_2-rich regions of the plasma-membrane, profilin lets go not only of actin (in the case of phophoinositides), but also of some polyproline-ligands. The lipid-regulation of polyproline-binding seems to be ligand-specific; as shown here, dynamin is very susceptible to elution by PIP_2, while other ligands like Mena or Vasp still bind profilin II strongly also in the presence of phosphoinositides. For those ligands a different regulatory mechanism must exist. In fact, profilin can be phosphorylated by protein kinase C (Hansson et al. 1988; Singh et al. 1996; Vemuri and Singh 2001) and by src (De Corte et al. 1997). Phospho-profilin is no longer able to bind to poly-L-proline (J. Sutherland, unpublished). Vasp, however, can be eluted from the profilin I-complex with

PIP-micelles, which argues for subtle differences also between the profilin-isoforms. By setting the ligands free of profilin, these signals may eventually allow the access of effector molecules to the polyproline-proteins, leading to events like membrane outgrowth by actin-polymerization (Borisy and Svitkina 2000) or membrane uptake by allowing assembly of the endocytic machinery.

4 MATERIAL AND METHODS

4.1 Molecular biology

All DNA and RNA manipulations, unless otherwise specified, were carried out according to Sambrook (Sambrook et al. 1989).

Epitope tagged PIIA

Sendai/SK vector

An epitope-tag from sendai-virus was cloned as a *Bam*HI/*Xba*I fragment in the Bluescript SK (+/-) vector (sendai/SK vector). The tag is preceded by a Kozak translational start and an ATG:

5'-**GGA TCC** ACC ATG GAC GGC TCC CTG GGC GAC ATC CAG CCC TAC GAC TCC TCC **TCT AGA**-3'

Sendai/PIIA (SK) plasmid

PIIA cDNA was PCR-amplified from a parental plasmid, digested with *Xba*I/*Not*I, and cloned downstream of the sendai epitope in the sendai/SK vector after *Xba*I/*Not*I digestion. Primers for PCR amplification of PIIA cDNA:

1) Forward primer: 5'-CG**TCTAGA**ATGGCCGGTTGGCAGAGC-3'

2) Backward primer: 5'-TA**GCGGCCGC**CTAGAACCCAGAG-3'

Sendai/PIIA plasmid

The sendai/PIIA fragment was recovered from the Sendai/PIIA plasmid upon *Cla*I/*Not*I digestion and cloned in the mammalian expression vector pIRES1neo vector (Clontech).

GFP-constructs

GFP-PIIA vector

Primers for PCR amplification of the PIIA cDNA to clone in the pEGFP-C2 vector (Clontech):

Forward primer:

5'-GC**GGATCC**CCACCATGGCCGGTTGGCAGAGCTACGT-3'

Backward primer:

5'-GC**GAATTC**CTAGAACCCAGAGTCTCTCAAGT-3'

The PCR product was digested with *Bam*HI/*Eco*RI, blunted, gel purified, and ligated to the *Eco*RI digested and blunted pEGFP-C2 vector.

PIIA-GFP vector

Primers for PCR amplification of PIIA cDNA to clone in the pEGFP-N1 vector (Clontech):

Forward primer: 5'-CCG**CTCGAG**ATGGCCGGTTGGCAGAGCT-3'

Backward primer: 5'-CCG**GAATTC**GGAACCCAGAGTCTCTCAAG-3'

The PCR products were XhoI/EcoRI digested, gel-purified and cloned in the XhoI/EcoRI digested pEGFP-N1 vector.

pEGFP-IRESpuro

The AfeI/BamHI-insert of pEGFP-C2 (Clontech) was cloned into the EcoRV/BamHI-sites of pIRESpuro (Clontech).

pEGFP-IRESpuro-sendai

A linker coding for the sendai-virus epitope followed by an EcoRI- and a NotI-site was put into the EcoRI/BamHI-cut pEGFP-IRESpuro. The EcoRI-site gets distroyed in this process, leaving a unique EcoRI-site behind the sendai-epitope.

Linker:

SendaiFW: 5'-**AAT TG**G ACG GCT CCC TGG GCG ACA TCC AGC CCT ACG ACT CCT CCG **GAA TTC GCG GCC GCG**-3'
SendaiBW: 5'-**G ATC CGC GGC CGC GAA TTC** CGG AGG AGT CGT AGG GCT GGA TGT CGC CCA GGG AGC CGT C**C**-3'

GFP-Dynamin
The ATG-suppressed Dynamin Iaa-cDNA in pBluescript (a gift from Dr Pietro DeCamilli) was cut out EcoRI/NotI and cloned in-frame into the respective sites in pEGFP-IRESpuro-sendai.

pEGFP-POP
Sendai-epitope-tagged full-length POP was cut out from S611 with EcoRI/SacII and cloned into pEGFP-C1 EcoRI/SacII

DsRed-constructs

pDsRed-IRESpuro
The primers RedBOT and RedTOP were used to amplify the ORF of the red fluorescent protein from the Clontech-vector DsRed. The PCR-product was digested EcoRV and BamHI and put into the ClaI cut and blunted, BamHI-cut pIRESpuro-vector (Clontech).

RedTOP: 5'-GAT CGA TAT CCG CCA CCA TGG TGC GCT CCT CCA AG-3'
RedBOT: 5'-GAT CGG ATC CCG CGG CCG CCG AAT TCC TGA GTC CGG CCG GAC AGG AAC AGG TGG TGG CGG CC-3'

pDsRedPIIA
The cDNA for profilin IIA was cloned in-frame via EcoRI/BamHI into the same sites in pDsRed-IRESpuro.

pDsRedPOP

Linkers carrying the Kozak translational start and coding for the myc-epitope were set into the EcoRI-site (which gets disrupted in the process) and the BamHI-site of pDsRedIRESpuro:

POPmycTOP: 5'-AA TTG GCC ACC *ATG GAA CAA AAA CTC ATC TCA GAA GAG GAT CTG* AAT TCC TCG AGC GGC CGC CGC G-3'
POPmycBOT: 3'- C CGG *TGG TAC CTT GTT TTT GAG TAG AGT CTT CTC CTA GAC* TTA AGG AGC TCG CCG GCG CCT AG-5'

Partial digest with NotI was necessary to leave a second NotI-site immediately upstream of the disrupted EcoRI-site intact. The EcoRI/NotI-POP-fragment of 611 was cloned into the respective sites of this vector.

<u>DNA-constructs for expression of POP and dynamin</u>

POP-611

Clone 611 from a screen for POP cDNA of a Lambda Zap II brain cDNA-library was subcloned EcoRI/NotI into the same sites into pBluescript SK^-

POP-S611

Vector POP-611 was cut open EcoRI, S1-blunted, NotI-cut out and cloned into the Sendai/SK-vector, which was cut open XbaI, S1-blunted, NotI.

pIRES-POP

The Sendai-epitope-tagged POP was cut out of S611 by ClaI/NotI and put into the same sites of the pIRES1-neo vector (Clontech).

pQE30-S611N

The N-terminal 1.4 kb of POP were cut out of S611 with BamHI/StuI and put into BamHI/SmaI sites of pQE30 (Qiagen).

pmycDynamin

Linkers carrying the Kozak translational start and coding for the myc-epitope were set into the EcoRI-site (which gets disrupted in the process) and the BamHI-site of pIRESpuro (Clontech):

mycTOP: 5'-AA TTG GCC ACC *ATG GAA CAA AAA CTC ATC TCA GAA GAG GAT CTG* GGA ATT CCT CGA GCG GCC GCC GCG-3'
mycBOT: 3'- C CGG *TGG TAC CTT GTT TTT GAG TAG AGT CTT CTC CTA GAC* CCT TAA GGA GCT CGC CGG CGC CTA G-5'

ATG-suppressed dynamin Iaa in pBluescript (a gift from Dr Pietro DeCamilli) was cloned in-frame into the EcoRI and NotI-sites behind the myc-epitope.

4.2 Biochemistry

4.2.1 Lysis of cells and tissues

For further processing of lysates, like immunoprecipitations (see below) or affinity-chromatography (see below), fresh or shock-frozen tissues were routinely lysed in ice-cold HEPES-lysis buffer (HLB, containing 20 mM HEPES pH 7.2, 50 mM NaCl, 5 mM $MgCl_2$, 0.05% Tween-20 and EDTA-free protease-inhibitors (Boehringer, Mannheim)) by 30 strokes at 800 rpm in a teflon-pestle Dounce-homogenizer (Kontes, Vineland, USA) in the cold. After centrifugation at 60.000 rpm at 4˚C in a TLA 120.2 rotor (Beckman), the supernatant was taken off and used further.

Tissue-culture cells were harvested by trypsinization, washed 2 times with PBS, pelleted, and the pellet resuspended in about five times its volume of ice-cold PBS/0.1 % Triton X-100 and protease-inhibitors. Before centrifugation like above, the cells were lysed by 2 optional freeze-thaw cycles in liquid nitrogen or sonication on ice.

4.2.2 Immunoprecipitation

Immunoprecipitation with mouse monoclonal antibodies was done by adding 10 μg of antibody to the cell lysate (see Lysis of cells and tissues, above) and

incubating for 1 h on ice. 30 µl of protein G-sepharose-slurry (Amersham/Pharmacia) was washed with PBS and mixed with the cell lysate with antibody. The immunocomplexes were allowed to bind the beads for 2 hrs by end-over incubation at 4˚C. The beads were washed 5 times with ice-cold lysis-buffer and the proteins eluted by boiling in 1x protein-sample buffer (see Protein gel chromatography and western blotting).

For immunoprecipitations with rabbit polyclonal antisera, 30 µl of protein A-sepharose-slurry (Amersham/Pharmacia) were washed with PBS and incubated with 25 µl of serum in 1 ml PBS for 1-2 hrs at 4˚C end-over. After three washes with lysis-buffer, the beads were incubated with lysate for 2 hrs like before, and treated in the following as above.

4.2.3 ELISA

Maxisorp ELISA-plates (Nunc-Nalgene) were coated with 1-10 µg/ml antigen in 100 µl 50 mM sodium carbonate pH 8.5/0.01 % NaN_3 either ON at 4 ˚C or at RT for 3 hrs. After coating, plates were washed 3 times with 100 µl PBS/0.05 % Tween-20. Then the wells were blocked with 100 µl 2 % BSA in PBS/0.05 % Tween-20 for 3 hrs at RT or ON at 4˚C. After blocking, plates were washed 3 times with 100 µl PBS/0.05 % Tween-20. Then the wells were incubated with hybridoma supernatants or dilutions of primary antibody in 50-100 µl 1 % BSA/PBS/0.05 % Tween-20 for 2 hrs at RT. After incubation with the primary antibody, wells were washed like before and incubated with 100 µl of alkaline phosphatase-coupled secondary antibody (goat anti mouse or goat anti rabbit, 0.6 mg/ml, Pierce) in a 1:5.000 to 1:10.000 dilution in 1 % BSA/PBS/0.05 % Tween-20 for 2 hrs at RT. After the incubation, the wells were washed like before and incubated with the wells were incubated with 100 µl of a 1 mg/ml PNPP (Pierce) solution in 5 mM $MgCl_2$/1 M Na_2CO_3/$NaHCO_3$ pH 9.5 until a discernable yellow signal appeared. The signal was quantitated in an ELISA-plate reader (PBI) at 405 nm.

4.2.4 Protein purification

4.2.4.1 Purification of rabbit muscle actin

4-5 rabbits were supplied and killed by a local butcher. The back muscles were taken out, cleaned from tendons and processed as quickly as possible. Until further processing, the muscles were kept on ice. Muscles were passed twice through a cold fine meat-grinder and extracted twice for 10 min. with 5 l of ice-cold high salt buffer (0.5 M KCl, 0.1 M K_2HPO_4). Inbetween the extractions, the suspension was spun down in 1 l buckets for 10 min. in a J-6M/E Beckman centrifuge at 4˚C. After the extractions, the dry pellet was weighed and resuspended in 3 l of ice-cold water by stirring. The pH was adjusted quickly to about 8.2-8.5 by adding drops of 1 M Na_2CO_3. After stirring for 5-10 min., the suspension was spun like before, the pellet weighed again and resuspended in water. This procedure was repeated until the pellet started swelling (indicated by sudden increase in weight). To the swollen pellet 5 l of -20˚C acetone were stirred in and incubated for 20-30 min. in the cold. The precipitate was washed over a big Büchner-funnel with ice-cold acetone and dried on Whatman-paper ON in a fume-hood. The dried powder was stored as "acetone-powder" in aliquots at -20˚C. For extraction of G-actin, 10 g of acetone-powder were resuspended in ice-cold G-buffer (2 mM Tris pH 8.0, 0.2 mM $CaCl_2$, 0.2 mM ATP, 0.01 % NaN_3) and stirred for 30 min. in the cold. The suspension was filtered over cheese-cloth prewetted with G-buffer, the extract saved and the extraction repeated. The combined extracts were centrifuged for 30 min., 30.000 x g at 4˚C. The actin was polymerized by adjusting the supernatant to 50 mM KCl, 2 mM $MgCl_2$ and 1 mM ATP and incubating for 2 hrs at 4˚C. After increasing the KCl-concentration to 0.8 M by adding solid KCl (to remove tropomyosin from the actin filaments), the actin was pelleted by centrifugation at 150.000 x g for 3 hrs at 4˚C. The pellet was resuspended in 10 ml of cold G-buffer with a tight-fitting Dounce-homogenizer (Kontes) and dialyzed against 2 l of G-buffer for 2 days with buffer changes in the mornings and evenings. After centrifugation at 150.000 x g like before, the upper two thirds of the supernatant were taken as G-actin. Once extracted, G-actin was kept in dialysis against G-buffer, supplied with fresh ATP every second day. Actin-concentration was

calculated by measuring the OD_{290} and applying the formula $conc_{actin} = \frac{OD_{290}}{\varepsilon_{290} \cdot d}$, with $\varepsilon_{290} = 26600\ M^{-1}cm^{-1}$ and d=1 cm.

4.2.4.2 Purification of native profilactin-complex from mouse brain

About 100 mouse brains were lysed in ice-cold 100 ml 30 mM Tris pH 8.0, 0.05 mM benzamidine, 20 % sucrose, 0.5 mM PMSF, 1 mM EGTA in a Dounce-homogenizer (Kontes). The lysate was spun for 1 hr at 4˚C and 40.000 rpm in a Ti65 rotor (Beckman) and the supernatant of this first spin was recentrifuged at 4˚C at 20.000 rpm for 30 min. in a JA25.50 rotor (Beckman).

The supernatant from the second spin was loaded on a DEAE Macroprep (BioRad) XK16-column (Amersham Pharmacia) and washed with TEAN (10 mM Tris pH 8.3, 1 mM EGTA, 0.1 mM ATP, 0.01 % NaN_3). The DEAE-column was eluted with a 0-1 M NaCl gradient in TEAN. Fractions which showed immunoreactivity for profilin and actin in western blot were loaded on a poly-L-proline column, washed with TEAN and eluted with a gradient of 0-50% DMSO in water. Profilin- and actin-positive fractions were concentrated by dialysis against 80 % ammoniumsulfate/TEAN and pelletting the precipitates by a 30 min. spin at 4˚C and 45.000 rpm in a Ti70 rotor (Beckman). Pellets were resuspended in TEAN.

4.2.4.3 Purification of proteins expressed in insect cells

Hi5-cells were grown at 27˚C in TMN-FH media (Invitrogen), supplemented with 10% FCS (GIBCO) and penicillin/streptomycin (GIBCO). Cells were detached by gentle tapping of the flasks against the open hand. Passages were done by splitting the cells 1:5.

4.2.4.3.1 Purification of GST-Dynamin

Hi5-cells were grown to near confluency in 225 cm^2-flasks. At the day of infection, flasks were split 1:2 and cells seeded in 20 ml of TMN-FH together with 1.5 ml of baculovirus-stock to give an m.o.i. of at least 5. Cells were harvested 48 hrs after infection and spun down for 10 min. at 4000 rpm in a Beckman JLA 10.5-rotor. The cell pellets were washed twice with 50 ml PBS in Falcon tubes.

Pellets from 30 225 cm^2-flasks (ca. 5 ml) were resuspended in 15 ml of ice-cold lysis-buffer (30 mM Tris pH 8.0, 5 mM $MgCl_2$, EDTA-free protease-inhibitor-cocktail (Boehringer), 1% Triton X-100, 0.5 mM GTP, 1 mM ATP) supplemented with 10 μg/ml RNAse and DNAse and incubated on ice for 15 min. Then the solution was subjected to 20 strokes in a teflon-pestle Dounce-homogenizer (Kontes), brought to 250 mM NaCl from a 5 M stock solution and treated again with the homogenizer.

After a 30.000 rpm-spin in a Beckman Ti45-rotor at 4°C for 30 min., the supernatant was desalted over Biogel PD6-acrylamide-desalting gel (BioRad) equilibrated in lysis-buffer containing 0.1 M NaCl by spinning for 2 min. at 2000 rpm in Megafuge 1.0R tabletop centrifuge (Heraeus) at 4°C. The flow-through was passed over 0.5 ml Glutathione-Sepharose-slurry (Amersham Pharmacia), equilibrated in lysis-buffer/0.1 M NaCl and recycled twice. Beads were washed with lysis-buffer and then with PBS, until no protein eluted (judged by Bradford protein-assay). GST-Dynamin was eluted by 15 mM glutathione in PBS, pH 8.0 by collecting an initial 1 ml and then 0.5 ml fractions. Collected fractions were analysed by SDS-PAGE and Coomassie-staining, and positive fractions pooled. 100 μl aliquots of the pool were snap-frozen in liquid nitrogen and stored at –80°C. The preparations yielded usually about 2 ml of ca. 5 μM GST-dynamin. The GST-portion of the molecule could be cleaved off by adjusting the buffer-concentration to 1x cleavage-buffer (50 mM Tris pH 7.0, 150 mM NaCl, 1 mM EDTA, 1mM DTT) and incubating with 2-4 U PreScission protease (Amersham/Pharmacia) at 4°C for 4 hrs.

4.2.4.3.2 Purification of His-tagged proteins expressed in insect cells

His-tagged MENA and VASP (gift of F. Gertler) were expressed by infecting Hi5-cells like described above (see Purification of GST-Dynamin) with the respective baculovirus high-titer stocks at an m.o.i. of 5-10. Cells were grown for 1.5 days at

27˚C. Cells were harvested like above and pellets washed twice in PBS. Shock-frozen or fresh pellets were resuspended in 10 ml of ice-cold lysis-buffer (10 mM Tris pH 8.0, 1 % TX-100, 10 mM β-mercapto-ethanol, 5 mM $MgCl_2$, 1x EDTA-free protease-inhibitor cocktail (Boehringer Mannheim)) and allowed to swell on ice for 15 min. The suspension was then sonicated 3 times for 15 s on ice with the K72-probe in an Bandelin Sonopuls GM 200 ultrasonic sonicator (Bandelin). After sonication, the lysate was brought to 0.5 M NaCl and further treated with 20 strokes in a teflon-pestle Dounce-homogenizer (Konton) on ice. The lysate was cleared by centrifugation for 30 min. at 40.000 rpm in a Ti70-rotor (Beckman), 4˚C. The supernatant was loaded on a HR5/5-column (Pharmacia) with Ni-NTA-resin (Qiagen) equilibrated in lysis-buffer/0.5 M NaCl with a flow-rate of 0.1 ml/min. After washing the column with 50 column-volumes of lysis buffer/0.5 M NaCl, the proteins were eluted by a 30 ml-gradient of 0-0.5 M imidazole in lysis buffer/0.5 M NaCl and collected in 0.5 ml fractions.

4.2.4.4 Purification of proteins expressed in E.coli

4.2.4.4.1 Purification of GST-tagged proteins expressed in E.coli

37˚C LB-medium with 50 μg/ml ampicillin was inoculated 1:10-1:20 with fresh ON-cultures of the respective bacteria harbouring the gene of interest in a pGEX-vector (Clontech Inc, USA). Cells were grown to an OD_{600} of 0.8. At this point, protein-expression was induced by adding 1 mM IPTG and growing the bacteria further at 37˚C for 4-6 hrs. The bacteria were harvested by centrifugation at 4000 rpm in a JLA 10.500-rotor (Beckman) for 10 min at 4 ˚C. The pellet was resuspended in PBS/0.1 mM EDTA, 0.1 % Triton X-100 and subjected to 2 rounds of sonication (2x30 s, MS73-probe in a Bandelin Sonopuls GM 200 sonicator) and homogenization in a Dounce-homogenizer (Kontes). After clearing the lysate by a 30 min. spin at 4˚C and 40.000 rpm in a TLA 45-rotor (Beckman), the supernatant was passed over an appropriate amount of glutathione-4B-sepharose beads (Amersham Pharmacia) which had been washed and equilibrated in lysis-buffer. After extensive washing with cold lysis-buffer and briefly with PBS, proteins were eluted with 20 mM glutathione in PBS.

4.2.4.4.2 Purification of profilin expressed in E. coli

1 l of 37˚C LB-medium with 50 μg/ml carbenicillin was inoculated 1:20-1:50 from a fresh ON culture of BL21 DE3 cells harbouring the profilin I or II gene under control of the bacteriophage T7-promoter in the vector pMW-72. At an OD_{600} of 0.7-0.8, protein expression was initiated by adding IPTG to a final concentration of 1 mM, thus inducing expression of T7-polymerase which in turn drives transcription of the profilin gene. After induction, the bacteria were grown ON (about 16 hrs) at 37˚C. Then the cells were pelleted by spinning for 10 min at 4000 rpm in a JLA 10.50-rotor (Beckman). The bacterial pellet was resuspended in 10 ml of 8M lysis-buffer (50 mM Tris pH 7.3, 5 mM EGTA, 0.1 mM EDTA, 50 mM KCl, 8 M urea, 10 mM DTT, 0.1 % Tween-20). The suspension was sonicated on ice 3 times 30 sec. at maximum probe energy with 1 min. intervals. The cleared solution was further homogenized by 20 strokes in a teflon-pestle Dounce-homogenizer (Kontes). The lysate was spun at 12˚C for 30 min. in a Ti45-rotor (Beckman) at 40.000 rpm or in a JA 25.50-rotor (Beckman) for 20.000 rpm. The supernatant was filled into dialysis-tubes with a molecular weight exclusion volume of 6000 (Spectrum) and dialysed ON against dialysis-buffer (50 mM Tris pH 7.3 (at RT), 1 mM EGTA, 0.1 mM EDTA, 50 mM KCl, 1 mM DTT) in the cold. After dialysis, the solution was re-centrifuged like before and the supernatant loaded onto a poly-L-proline column, washed and equilibrated with dialysis-buffer. The column was washed with 5-10 column-volumes of 2 M wash-buffer (8 M lysis-buffer without Tween and dialysis-buffer mixed 1:3). Profilin was eluted with 8 M elution-buffer (8 M lysis-buffer without Tween). Fractions were checked on an SDS-gel (see Protein gel chromatography and western blotting), clean fractions pooled and dialysed against 1x dialysis-buffer for 2-3 days with 5-6 buffer changes. After a clearspin to pellet precipitated protein like above, aliquots were snap-frozen in liquid nitrogen and stored at –80˚C.

4.2.5 Labelling of actin with pyrene

A fresh 50 mM solution of N-(1-pyrene)iodoacetamide (Molecular Probes) was made in dry DMSO freshly before coupling and protected from light throughout the procedure. G-actin (see Purification of rabbit muscle actin) was dialysed for 2 days against 3 changes of P-buffer (see G-actin-beads). Polymerization was started by

bringing the actin to a final concentration of 150 mM KCl/2 mM $MgCl_2$ and while stirring vigorously, a 10-100 fold molar excess of pyrene-iodoacetamide over actin was added from the stock-solution. The solution then was incubated end-over at 4˚C ON. The next day, F-actin was spun down at 150.000 x g and 4˚C for 3 hrs, resuspended in a small 3-4 ml of G-buffer (see Purification of rabbit muscle actin) and dialyzed against 3 changes of G-buffer. After a clearspin at 150.000 x g and 4˚C for 30 min. the concentration of pyrene-actin was calculated by using the formula $conc. = \frac{OD_{290} - 0.127 \cdot OD_{344}}{d \cdot \varepsilon_{290}}$, with ε_{290}=26600 $M^{-1}cm^{-1}$ and d=1 cm. Aliquots of pyrene-actin were snap-frozen in liquid nitrogen and stored at -80˚C.

4.2.6 Actin-polymerization assays

Actin-polymerization was assayed in 100 μl reactions containing 5 μM of actin (containing 5% of pyrene-actin) plus the proteins and effectors of interest in G-buffer. Reactions were started by adding a 90 μl premix into a well of a black 96-well plate (Greiner) containing 10 μl 10x polymerization buffer (0.1 M imidazole, 20 mM $MgCl_2$, 10 mM EGTA). After brief mixing by pipetting up and down, the polymerization-reaction was monitored at 25ºC with a fluorescent plate reader (Fluoroskan Ascent II, Labsystems) in 10 sec intervals by exciting pyrene-fluorescence at 342 nm and measuring fluorescence emission at 388 nm. The results were plotted as relative fluorescence versus time using the program "GraFit" (Erithacus Software Ltd.).

4.2.7 Dynamin pelletting assay

10 μl of a 5 μM solution of dynamin was mixed with 70 μl 5 mM Tris pH 8.0, 0.1 mM DTT, 0.1 mM EDTA containing the effectors to be analysed. The mixture was kept on ice for 15 min and then spun at 50.000 rpm in a TLA 100-rotor (Beckman) at 4˚C for 15 min. The supernatant was carefully taken off and boiled after addition of 20 μl 5x SDS-sample buffer. The pellet was resuspended in 80 μl water plus 20 μl 5x SDS-sample buffer. The supernatant and pellet fractions were analysed by SDS-page and silverstain (see Protein gel chromatography and western blotting).

4.2.8 GTPase assays

GST-dynamin was cleaved with PreScission protease (Amersham Pharmacia) like described in Purification of GST-Dynamin and dialysed for 1 hr against 20 mM HEPES pH 7.2/0.1 mM EDTA in the cold. 50 μl-reactions were pipetted, containing 5-10 μl 5 μM dynamin, 1x GTPase-buffer (20 mM HEPES, 5 mM $MgCl_2$, 0.1 mM DTT) and proteins or other effectors in low salt. The reaction was started by adding 5 μl of 10 x GTP-premix (0.5-1 mM GTP and 5 μl 10 mCi/ml [α-^{32}P] GTP in water). Reactions were carried out at 30°C and stopped by either taking out aliquots at timepoints or incubating the whole reaction at 80°C for 10 min. 2 μl of the reaction were spotted in equidistant spots on a line about 2 cm from the edge of a cellulose-TLC-plate (PEI-cellulose F TLC plastic sheets, 20x20 cm, Merck). The TLC-plate was then placed in a vapour chamber euqilibrated for at least 2 hrs with 0.6 M potassium phosphate pH 3.4 (fill height about 0.5 cm). The run was stopped when the buffer front had reached the upper third of the TLC-plate by taking out the plate, drying it and exposing to a phosphorimager-screen (Molecular Dynamics). Quantitation was done with the ImageQuant software after reading the screen with the phosphorimager (Molecular Dynamics) by calculating the percentage of GDP produced (upper spot) against whole signal (sum of GDP and GTP intensities).

4.2.9 Subcellular membrane fractionation on sucrose-step-gradient

Tissue culture cells/ml were trypsinized and washed twice with PBS. 10^8 cells were resuspended in 1 ml of ice-cold TKM (50 mM Tris pH 7.6, 25 mM KCl, 5 mM $MgCl_2$)/0.25 M sucrose and EDTA-free protease-inhibitor-cocktail (Roche) and homogenized by 30 strokes in a teflon-pestle Dounce-homogenizer (Kontes) on ice. Non-lysed cells were pelleted by a 2 min.-spin of 500 rpm in a Megafuge 1.0R (Heraeus) at 4°C. The supernatant was re-centrifuged at 1500 rpm (700 x g) to pellet nuclei. This 700 x g supernatant was carefully layered on top of 8 ml TKM/0.5 M sucrose over 250 μl TKM/2 M sucrose in an ultracentrifuge tube and spun for 50 min. at 38.000 rpm (180.000 x g) in an SW40Ti-swingout rotor (Beckman) at 4°C. The membranes are separated from the cytosol and accumulate in the 2 M sucrose cushion. The cushion was diluted with 1.8 ml TKM and loaded on a step-gradient

which consisted of (bottom to top): 1.8 M, 1.5 M, 1.3 M, 1.1 M, 0.8 M sucrose in TKM, 1.5 ml each, the uppermost step consisted of 1 ml of 0.5 M sucrose in TKM. After spinning for 3 hrs at 38.000 rpm in the SW40Ti-rotor at 3˚C, distinct bands can be distinguished at the interphases of the steps which are mostly (bottom to top): ER, lysosomes, Golgi-membranes and plasma-membranes. Residual cytosol stays on top of the gradient. By pinching a hole in the base of the centrifuge tube with a syringe-needle, 0.5 ml fractions could be collected.

4.2.10 Affinity chromatography

Tissue lysates (see Lysis of cells and tissues) or recombinant proteins were brought to 1 x HLB (see Lysis of cells and tissues) and incubated with 30 μl of a slurry of affinity-beads (see below) which had been washed and equilibrated in HLB. usually in a volume of 150-250 μl. Binding was carried out for 2 hrs at 4˚C end-over or in BioRad Mini-Columns on ice by recycling the flow-through several times. After binding, beads were pelleted at 4˚C in a swing-out-rotor in an Eppendorf 5417R cooling centrifuge, the supernatant taken off and the beads washed 5 times 5 min. with HLB. Bound proteins were eluted by boiling the beads for 5 min. in 1x SDS-sample buffer (see Protein gel chromatography and western blotting).

4.2.10.1 G-actin-beads

For preparation of G-actin-beads, G-actin (see Purification of rabbit muscle actin) was dialysed against 3 changes of P-buffer (1 mM Na_2CO_3, 0.1 mM $CaCl_2$, 0.2 mM ATP, pH 7.6-7.8) in the cold for 2 days and the dialysate cleared by a 100.000 x g spin for 1 h at 4˚C. CNBr-activated sepharose 4B-beads (Amersham Pharmacia) were deblocked as described in the supplier's manual and washed with P-buffer. The amount of swollen resin and actin was adjusted such that the final loading of the beads would be 2-5 mg G-actin per ml resin. Beads and actin were mixed and incubated end-over at 4˚C ON. Coupling efficiency was checked by comparing protein content before and after coupling by Bradford assay (BioRad). To block reactive sites on the resin, 10 mM ethanolamine pH 8.0 was added and incubated for 2 hrs with the beads. The beads were washed extensively with G-buffer and where

possible used within 2 days, otherwise they were supplied daily with G-buffer containing fresh ATP.

4.2.10.2 Profilin-beads

Profilin-beads were made by dialysing purified recombinant profilin I and II (see Purification of profilin expressed in *E. coli*) against 20 mM Na_2CO_3/$NaHCO_3$ pH 8.0, 1 mM EGTA, 0.1 mM DTT for 2 days in the cold. CNBr-activated sepharose 4B (Amersham Pharmacia) was deblocked with 1 mM HCl according to manufacturer's instructions and after brief neutralization with 10 x PBS given to the supernatant of a 30 min. clearspin of the profilin-dialysate at 100.000 x g, 4˚C. Amounts of resin and proteins were chosen such that a final loading of 2-5 mg protein/ml beads was obtained. The beads were incubated with the protein-solution end-over at 4˚C ON. Coupling efficiency was checked by testing protein content of the solution before and after coupling by Bradford-assay (BioRad). Reactive sites were blocked for 2 hrs and the resin washed with 50 mM Tris pH 7.5, 1 mM EGTA, 0.5 mM NaCl. The beads were stored in 20 mM Tris pH 7.5, 1mM EDTA, 0.01 % NaN_3 at 4˚C.

4.2.10.3 Poly-L-proline-beads

Poly-L-proline beads were made by dissolving 1 g poly-L-proline, MW 40.000 (Sigma) in 50 ml 1 x coupling buffer (0.1 M $NaCO_3$, 0.5 M NaCl, pH 8.5) for several days at 4˚C and deblocking 15 g of dry CNBr-activated sepharose 4B (Amersham Pharmacia) with 1 mM HCl according to supplier's instructions. After deblocking, the beads were washed briefly with cold water and coupling-buffer. The beads were added immediately to the dissolved poly-L-proline and incubated ON end-over at 4˚C. The next day, the beads were washed three times with 200 ml coupling-buffer and blocked with 0.1 M Tris pH 8.0/0.5 M NaCl for 2 hrs at RT. Then the resin was washed 4 times alternatingly with 0.1 M sodium acetate pH 4.0/0.5 M NaCl and 0.1 M Tris pH 8.0/0.5 M NaCl. Afterwards, the beads were washed and stored in 20 mM Tris pH 8.0/5 mM EDTA/0.1 M NaCl/0.1 % NaN_3 at 4˚C.

4.2.11 Lipids

4.2.11.1 Preparation of PIP_2-micelles

Phosphatidylinositol-4,5-bisphosphate (Sigma) was reconstituted in methanol/chloroform 1:1 to a final concentration of 3 mg/ml. For making micelles, an appropriate amount of stock-solution was dried under nitrogen. The lipid film was rehydrated in 20 mM HEPES pH 7.2/0.1 mM EDTA for at least 30 min. at RT with occasional mixing. Finally, the mixture was sonicated in a sonicating-waterbath for 15 min.

4.2.11.2 Lipid-binding assays

A Superdex-200 (Amersham Pharmacia) 10 cm HR10/10 (Amersham Pharmacia) column was equilibrated in 10 mM Hepes pH 7.2 at 0.1 ml/min. Dead volume was accounted for by injection of Blue Dextran. Protein elution was followed by measuring absorbance at 280 nm.

90 μl of profilin II (1.6 μg/μl) were injected to give the retention time of profilin alone (about 90 min.). For lipid-binding, 10 μl of PIP_2-micelles (3 mg/ml) were mixed with 90 μl of profilin II (1.6 μg/μl) for 1 hr at 4˚C. The mixture was injected and two well-separated peaks were visible at 280 nm, the first peak containing micelle-bound profilin II, the second peak free profilin II.

Free lipids are not visible at 280 nm, their presence was confirmed by producing a visible turbid precipitate of phospholipid-Ca-salt when mixing phospholipids and 1 M $CaCl_2$ in a ration of 1:1.

4.2.12 Protein gel chromatography and western blotting

For SDS-PAGE, proteins were diluted in 1x SDS sample buffer (22mM Tris-HCl pH 6.8, 4% Glycerol, 0.8% SDS, 1.6% β-Mercaptoethanol, Bromphenolblue), heated for 5 min at 95 °C and subjected to discontinuous gel electrophoresis. For Coomassie-staining, the gels were stained either with 0.1 % Coomassie Brilliant Blue R 250 (BioRad) in 50 % methanol/10 % acetic acid and destained in 30 % isopropanol/6 % acetic acid or 10 % ethanol/5 % acetic acid. For silver stain, the gels

were fixed in 50 % methanol/12 % acetic acid/0.5ml/l formaldehyde for 1 h, washed 3 times 10 min. with 50 % ethanol, incubated for 1 min. in 0.2 g/l $Na_2S_2O_3$, rinsed 3 times 20 s with water, incubated 20 min. in 2 g/l $AgNO_3$/0.75 ml/l 37% formaldehyde, rinsed twice for 20 s with water and developped in 60 g/l Na_2CO_3/ 0.5 ml/l 37 % formaldehyde/4 mg/l $Na_2S_2O_3$. The developing reaction was stopped by transferring the gel to 10% ethanol/10% acetic acid.

For Western blot, proteins were electrophoretically transferred onto a polyvinylidone difluoride (PVDF) membrane (Immobilon-P, Millipore), using a semi-dry blotting apparatus (Trans-Blot SD, BioRad), by applying 20 V for 1hr. The PVDF-membrane was made hydrophilic by brief incubation in methanol. Gel and membrane were equilibrated in transfer buffer (25mM Tris, 190mM glycine, 20%, methanol pH 8.3) before the transfer. After the transfer, the membrane was incubated in blocking solution (5% non-fat milk powder dissolved in NCP buffer (0.15 M NaCl, 20mM Tris, 0.05% Tween-20, and 0.02% Na-azide) at 4˚C overnight. Primary and secondary antibodies were diluted in blocking solution to the appropriate concentrations. The enhanced chemiluminescence system (Amersham Pharmacia) was used, followed by exposure to x-ray film (X-Omat AR, Eastman Kodak Co.). Between the antibody incubations, the membranes were washed five times in NCP buffer. For detection, horseradish peroxidase (HRP) conjugated secondary goat anti-rabbit or goat anti-mouse antibodies (Pierce, 0.8 mg/ml) dil. 1:1000 were used.

4.2.13 Competition binding assays

Nunc Maxisorp ELISA-plates were coated with 0.5 μg/ml of GST-Grb2, GST-amphiphysin, GST-endophilin and GST-src-SH3-domain in 50 mM $NaHCO_3$ pH 8.5/0.01% NaN_3 ON at 4˚C. The wells were washed 3 times with 100 μl PBS/0.05% Tween-20 at RT. Unspecific binding-sites were blocked with 1% BSA in PBS/0.05% Tween-20 for 2 hrs at RT. The wells were then incubated with an equal amount of GST-cleaved recombinant dynamin with increasing amounts of recombinant profilin (or BSA as nonspecific control) in 1x profilin dialysis-buffer for 2 hrs at 4˚C, Afterwards, the wells were washed like before and incubated with anti-dynamin antibody Hudy-1 1:500 in 1% BSA/PBS/0.05% Tween-20 for 1 h at RT. After washing, 100 μl of alkaline-phosphatase coupled goat-anti-mouse antibody 1:1000 in

1% BSA/PBS/0.05% Tween was put on the wells for 1 h at RT. After five washes like above, the wells were incubated with 100 µl of a 1 mg/ml PNPP (Pierce) solution in in 5 mM $MgCl_2$/1 M Na_2CO_3/$NaHCO_3$ pH 9.5 until a discernable yellow signal appeared. The signal was quantitated in an ELISA-plate reader (PBI) at 405 nm.

4.2.14 Blot overlays

Equal amounts of mouse tissue lysates (see Lysis of cells and tissues) were run on 10% SDS-gels and transferred to Immobilon-membranes (see Protein gel chromatography and western blotting). Membranes were washed in NCP (see Protein gel chromatography and western blotting) and proteins allowed to renature ON at 4˚C in NCP, 5% FCS, 0.5 mM DTT. The membranes were incubated with 30 µg/ml profilin in renaturation buffer for 5 hrs at 4˚C, washed with NCP 3 times 10 min. and incubated with anti-profilin rabbit-antisera 1:1000 in NCP for 45 min. at RT. After washing with NCP for 3 times 10 min., the membranes were incubated with HRP-goat-anti-mouse antibody (Pierce, 0.8 mg/ml) 1:1000 in NCP and developed using ECL (see Protein gel chromatography and western blotting).

4.3 Cell biology

4.3.1 Generation of monoclonal antibodies

4.3.1.1 Generation of hybridoma cells

Mice were immunized with 50-100 µg of recombinant profilins in 250 µl Titermax-adjuvant (Sigma) intraperitoneally. After 2 weeks, mice were boosted with antigen and bled from the tail. The serum was checked by western blot (see Protein gel chromatography and western blotting) and ELISA for immunoreactivity against the recombinant proteins. Boosts were repeated every two weeks until the signal was strong and specific. 3 days after the final boost, the mice were killed with CO_2, the spleen removed sterilly and after removal of connective tissue ground between sterile frosted-end glass slides in RPMI-medium (GIBCO). The single-cell suspension was filled in 50 ml Falcon-tubes and cell clumps allowed to settle down. Meanwhile, 2-3

175cm^2 tissue culture-flasks of the P3-myeloma cell line (ATCC) grown in RPMI/10% FCS were harvested by tapping them loose and washed twice in RPMI. The supernatant of the splenocytes was centrifuged at 1500 rpm for 5 min in a Heraeus Maxifuge and the cells resuspended in RPMI. After counting, P3- and spleen-cells were combined in a ratio of 1:3 in 20 ml RPMI. The cells were pelleted by a 10 min. spin at 1000 rpm. The medium was aspirated and the pellet respun for 5 min. to dry off the last bit of medium. After gently tapping it loose, 1 ml of 37˚C PEG 1500 was given to the cell pellet in a 37˚C waterbath over 1 min. while gently shaking. Then RPMI was added: 1 ml over 1 min., 2 ml over 1 min., 3 ml over 1 min and 15 ml over 3 min. while gently shaking in the waterbath. Afterwards, the Falcon-tube was put on ice for 7-10 min, spun at 700 rpm for 5 min and the supernatant aspirated. The cells were gently resuspended in 40 ml fusion medium (450 ml RPMI, 50 ml FCS, 10 ml 50x HFCS (Roche), 5 ml MEM non-essential amino acids (GIBCO), 2.5 ml penicillin/streptomycin (GIBCO), 5 ml sodium pyruvate (GIBCO), 5 ml 200 mM glutamine (GIBCO), 5 ml MEM-vitamins (GIBCO), 5 ml 1 M HEPES (GIBCO), 4 μl β-mercapto-ethanol (Sigma)). The cell suspension was distributed into 96-well plates in 50 μl aliquots. The next day, 50 μl of fusion medium containing 2x HAT-supplement (from 50x HAT stock, Roche) were added to the wells. After 5 days, the medium was replaced by 100 μl of fusion-medium containing 1x HAT. Medium was changed every five days until cells proliferated well. Then 200 μl 1x HAT medium was put on the cells and after 3 days 100 μl of the supernatant was checked for antibody-production by ELISA. Positive wells were expanded into 12- and 6-wells in fusion-medium with 1x HT-supplement (Roche). From 6-wells, cells were cloned by limiting dilution in HT-medium. The clones were checked for antibody-production by ELISA, positive clones expanded, early passages frozen away and cells grown in fusion medium.

4.3.1.2 Purification of monoclonal antibodies from hybridoma cell supernatant

For purification of the monoclonal antibodies, hybridoma supernatants were brought slowly to 55 % saturation with ammoniumsulfate by adding the solid salt while stirring in the cold. Antibodies were allowed to precipitate ON in the cold. The precipitate was pelleted by centrifugation for 20 min. at 8000 x g and the pellet

dissolved in 20-30 ml of PBS. After dialysis against 2 changes of PBS and a clearspin for 10 min. at 10.000 x g. the supernatant was recycled over a protein A (Amersham Pharmacia) -column which had been equilibrated in PBS. The column was washed with 10 column volumes of PBS, then with 2 volumes of water and the antibody was eluted with 0.1 M acetic acid/150 mM NaCl in 900 μl fractions into 100 μl 1 M Tris pH 8.0. Protein concentration was determined by measuring the OD_{280} and calculating the concentration as c_{ab} [mg/ml] = OD_{280}/1.5. Protein-containing fractions were pooled and dialysed against PBS/0.02% NaN_3 and snap-frozen in liquid nitrogen.
The antibody subtypes were assessed with the mouse hybridoma subtyping kit from Roche.

4.3.2 Generation of polyclonal antibodies

0.3-0.5 mg antigen was diluted in 0.5 ml of normal saline, mixed with 0.5 ml of Titermax adjuvant (Sigma), chilled on ice, sonicated 3 times for 10 s with the MS72 probe in a Bandelin Sonopuls GM200-sonicator and injected into rabbits subcutaneously. The rabbits were boosted after 3 weeks with another injection of antigen, bleeds were checked by western-blotting of tissue-lysates and recombinant antigens. Boosts were repeated every 3-4 weeks until a satisfactory immune reaction was seen.The final bleed was allowed to clot at RT ON, centrifuged at 4300 rpm for 30 min. in a Megafuge 1.0R (Heraeus) tabletop centrifuge, the supernatant snap-frozen in aliquots in liquid nitrogen and stored at -20°C.

4.3.3 Transfection of cells and generation of stable cell lines

Unless otherwise stated, tissue culture cell lines were grown in DMEM supplemented with 10 % FCS, 10 mM Hepes-buffer, MEM non-essential amino acids, 1 mM sodium pyruvate, 2 mM glutamine, 100 U/ml penicillin and 100 μg/ml streptomycin (all GIBCO).
Transfections were done either by lipofection (Lipofectamine 2000, GIBCO) according to the manufacturer's instructions or by electroporation. For electroporation, adherent cells were trypsinized and washed 2 times in DMEM (GIBCO)/20 mM Hepes. Then they were diluted to a density of $2 \cdot 10^7$/ml in

DMEM/20 mM Hepes. 0.8 ml of the cell suspension was mixed with the DNA to be transfected, the mixture filled in an electroporation cuvette (Gene Pulser Cuvette 0.4 cm, BioRad) and pulsed with an electrical field of 500 μF/250 V in a Gene Pulser II electroporation device (BioRad). After the pulse, cells were immediately diluted into 10 ml of 37°C full medium and distributed into 10 cm-dishes.

To generate stable cell lines, selection was started 24 hours after transfection. Generally, neomycin-resistance conferring plasmids were selected for in HeLa-cells with 750 μg/ml G418 in full medium, puromycin-conferring plasmids with 1 μg/ml puromycin.

Double-stable cell lines were generated by first selecting for one resistance, and only after obtaining a stable cell line the second plasmid was transfected.

4.3.4 Immunostaining

Cultured cells were plated on cover slips. The cells were fixed in 4% paraformaldehyde (PFA)/PBS for 30 min and permeabilized for 10 min in 0.1% TX-100/4% PFA. Cells were washed in 50 mM glycine in PBT (PBS/0.05% Tween-20), and incubated in blocking buffer (PBT, 2% BSA, 0.05% gelatin, 50 mM glycine) for 1hr. Primary antibodies were diluted in blocking-buffer and incubated on the cells for 45 min. After washing in PBT, fluorescence-conjugated secondary antibodies were allowed to bind for 30 min at room temperature diluted in blocking-buffer. Nuclei were stained by including a dilution of Hoechst 33342 (10 mg/ml, Molecular Probes) 1:30.000 in PBT in one of the final washes. After briefly dipping in water, the coverslips were mounted on glass slides in gelvatol.

4.3.5 Preparation of primary cortical neuronal cultures

Mouse embryos (day 14-16) were decapitated and the brains removed sterilly in HBSS containing penicillin/streptomycin. The two cerebral hemispheres were prepared and stripped of the meninges. The cortices were collected in 15 ml Falcon-tubes in HBSS. For trypsinization, the HBSS was aspirated and replaced by 3 ml 37°C trypsin/EDTA (GIBCO) and incubated for 15 min. in a 37°C waterbath. Then the trypsin was removed and replaced by 5 ml MEM-HS (0.6 % glucose, 2 mM

glutamine, 0.22% $NaHCO_3$, 10% horse serum in 1 x MEM). After 2 min., the MEM-HS was aspirated and replaced by new MEM-HS. The cortices were dissociated by careful pipetting with a normal plugged pasteur-pipet first, and then with one which had been fire-polished to about half its diameter. After letting undissolved clumps settle for 5 min., the cells were seeded either on poly-lysine-coated plastic-dishes or on coverslips, which had been treated ON with 1-2 N HCl, washed extensively with deionized water, boiled in deionized water, dried separately on Whatman-paper and heat-sterilized. The sterile coverslips were incubated at least overnight with freshly prepared 1 mg/ml poly-l-lysine in 50 mM borate-buffer pH 8.5. After 3 hrs, the medium was aspirated and replaced by N2-maintenance medium (0.6 % glucose, 2 mM glutamine (GIBCO), 0.22% $NaHCO_3$ (Merck), pyruvate (GIBCO), 1x N2-supplement (GIBCO), 0.1% ovalbumin (Sigma) in 1x MEM (GIBCO)).

4.3.6 Uptake of fluorescently labelled transferrin into cells

HeLa cells in exponential growth phase were harvested by trypsinization, and starved for at least three hours in minimal medium. Cells were counted and cell numbers adjusted to an equal number of cells (up to 10^7) in 1 ml of DMEM (GIBCO). Uptakes were started by adding 200 μl FCS containing 5-10 μg/ml TexasRed- or Alexa488-labelled human transferrin (Molecular Probes) and rotating the cells end-over at 37˚C. At timepoints ranging from 0-40 min 150 μl-aliquots were taken from the reactions and pipetted into ice-cold 4 % paraformaldehyde/PBS. After fixing for 30 min. on ice, the cells were washed with PBS, taken up in FACS-buffer (PBS/1% BSA/0.01% NaN_3) and analysed with a fluorescence activated cell scanner (FACSCalibur, Beckton Dickinson).

For microscopic analyses, cells were seeded on coverslips in non-selective medium, and after 2 days were starved in serum-free growth medium for 3 hrs to overnight. The uptakes were started by replacing the starving-medium by serum-containing-medium with either 20 μg/ml fluorescent transferrin or 5 mg/ml fluorescent dextran. The uptake was stopped at timepoints by taking out the coverslips, dipping them into ice-cold PBS and transferring them to ice-cold 4 % paraformaldehyde/PBS.

4.3.7 Uptake of FM-dyes into cells

FM 1-43 and FM 4-64 (Molecular Probes) were reconstituted to a final concentration of 10 mM in DMSO. Before use, they were diluted appropiately in assay-buffer, sonicated briefly (2 x 10 s, lowest energy) and spun for 10 min. at 7000 x g. The supernatant was used for the experiments.

4.3.7.1 Uptake of FM 1-43 into cells and quantitation by fluorescence scanning

HeLa cells were seeded at a density of $1.5x10^5$ in 24-well plates and grown for 2 days to about 90 % confluency in non-selective medium. FM 1-43 was diluted in HBSS/0.04 g/l glucose to a concentration of 10 μM and prewarmed to 37˚C. Wells were rinsed twice with HBSS/glucose and uptakes started by adding 400 μl of the warm FM-dilution at staggered timepoints. Uptake was performed at 37˚C. To stop the uptake, cells were rinsed quickly with ice-cold PBS and fixed in ice-cold 4 % paraformaldehyde/PBS. Quantitation was carried out in a fluorescent plate reader (Fluoroskan Ascent II, Labsystems), exciting FM 1-43 fluorescence at 485 nm and reading emission at 590 nm. Cell numbers were accounted for by incubating the cells with Hoechst 33342 (10 mg/ml, Molecular Probes) 1:30.000 in PBS/0.1% Tween-20 for 20 min. at RT and reading the fluorescence signal at 460 nm after washing 3 times with PBS and exciting at 355 nm.

The washout of FM 1-43 could be followed in live cells. After loading the cells with 10 μM FM 1-43 in HBSS/glucose for 30 min at 37˚C, they were briefly rinsed with warm HBSS/glucose without FM 1-43 and the fluorescence change at 590 nm followed over 30 min. at 37˚C or RT after excitation at 485 nm in the fluorescent plate reader in 1 min. intervals.

Steady-state analysis was done by fixing the cells after uptake at 37˚C for 1 h and quantitating like before.

Kinetic data was analysed with the GraFit program (Erithacus Software Ltd.). Data points were fitted against a single exponential growth curve for the uptake and a double exponential decay for the washout.

4.3.7.2 Uptake of FM 1-43 and FM 4-64 into neurons

Primary cortical neurons were cultured on coverslips (see Preparation of primary cortical neuronal cultures) for 5-6 days. Cells were loaded with 8-10 μM FM-dyes in Tyrode-solution (150 mM NaCl, 4 mM KCl, 2 mM $MgCl_2$, 2 mM $CaCl_2$, 10 mM glucose, 10 mM HEPES pH 7.4) either unstimulated or depolarization-stimulated (by adding 45-60 mM KCl) by dipping coverslips first into RT-Tyrode-solution, then into dye-containing Tyrode-soulution for 60-90 s, then into an excess of dye-free Tyrode-solution to wash off non-internalized dye. Cells were fixed by placing the coverslips into ice-cold 4% paraformaldehyde/Tyrode. Fluorescence of non-internalized FM 1-43 could be significantly reduced by mounting the cells in gelvatol containing 100 μM sulforhodamine. Coverslips were kept at 4°C ON and could be viewed the next day without any loss of signal.

For comparative kinetic studies, mouse cortical neurons of wildtype and profilin II-mutant mice were prepared the same day under the same conditions. Cells were seeded at $5 \cdot 10^5$ per well into 24 wells and allowed to grow and spread for 5-6 days (about 90-95% confluency). Before the experiment, cells were washed 2 times with Tyrode-solution, and the solution was aspirated. Uptakes were initiated by injecting 400 μl of 10 μM FM 1-43 either in Tyorode-solution (unstimulated uptake) or in Tyrode-solution containing 60 mM KCl (stimulated uptake) into the wells in a fluorescent plate reader (Fluoroskan Ascent II, Labsystems), exciting FM 1-43 fluorescence at 485 nm and reading emission at 590 nm in 3 second-intervals.

Washouts were done after loading the neurons under stimulating conditions for 2 min. with FM 1-43. Cells were then washed for 5 min. with ice-cold normal Tyrode-solution. Washouts were started by injecting either normal room-temperature Tyrode-solution containing 100 μM sulforhodamine (unstimulated washouts) or Tyrode-solution with 100 μM KCl/100 μM sulforhodamine (stimulated washouts) and the fluorescence was followed as described above.

Cell numbers were accounted for by counterstaining with Hoechst-dye (see Uptake of FM 1-43 into cells and quantitation by fluorescence scanning) or by quantitation of whole protein content by Bradford assay (BioRad).

4.3.8 In situ hybridisation

POP fragments containing the 3'-most 1.4 kb and 250 bp 2.3 kb downstream of the ATG of the cDNA were cloned in to pBluescript SK-. *In vitro* transcription was performed according to Jostarndt et al. Jostarndt et al. 1994, using digoxigenin labeled nucleotides (Boehringer Mannheim), from the T3 or from the T7 promoter, for transcription of sense and antisense-probes, respectively. The probes were used for *in situ* hybridization on paraffin sections of adult brains or E13 embryo. Hybridization solution contained the digoxygenin-11-UTP-labeled riboprobe (1ng/ml) in 40% formamide, 5x SSC, 1x Denardt's solution, 100 µg/ml each of the denatured salmon testis DNA and tRNA. Hybridazation was performed for overnight at 65 °C. Slides with sections were floated off in 5x SSC, followed by a 40 min wash in 0.5x SSC, 20% formamide at 60 °C and a 15 min wash in NTE (0.5 M NaCl, 10 mM Tris/HCl, pH 7.0, 5 mM EDTA). The sections were treated with 20 µg/ml RNase A in NTE for 30 min at 37 °C and washed in NTE for 15 min, in 0.5x SSC, 20% formamide for 20 min at 60 °C, and then in 2x SSC for 25 min. Antibody incubation and detection were performed according to the manufacturer's description (Boehringer Mannheim) and signal was developed using BCIP/NBT (Vector Labs).

5 Bibliography

Aguado-Velasco, C., and Bretscher, M. S. (1999). “Circulation of the plasma membrane in Dictyostelium.” *Mol Biol Cell*, 10(12), 4419-27.

Ayscough, K. R. (1998). “In vivo functions of actin-binding proteins.” *Curr Opin Cell Biol*, 10(1), 102-11.

Balasubramanian, M. K., Hirani, B. R., Burke, J. D., and Gould, K. L. (1994). “The Schizosaccharomyces pombe cdc3+ gene encodes a profilin essential for cytokinesis.” *J Cell Biol*, 125(6), 1289-301.

Barr, F. A., and Shorter, J. (2000). “Membrane traffic: do cones mark sites of fission?” *Curr Biol*, 10(4), R141-4.

Bates, G. P., Mangiarini, L., Mahal, A., and Davies, S. W. (1997). “Transgenic models of Huntington's disease.” *Hum Mol Genet*, 6(10), 1633-7.

Bennett, M. K., and Scheller, R. H. (1993). “The molecular machinery for secretion is conserved from yeast to neurons.” *Proc Natl Acad Sci U S A*, 90(7), 2559-63.

Bhargavi, V., Chari, V. B., and Singh, S. S. (1998). “Phosphatidylinositol 3-kinase binds to profilin through the p85 alpha subunit and regulates cytoskeletal assembly.” *Biochem Mol Biol Int*, 46(2), 241-8.

Binette, F., Benard, M., Laroche, A., Pierron, G., Lemieux, G., and Pallotta, D. (1990). “Cell-specific expression of a profilin gene family.” *DNA Cell Biol*, 9(5), 323-34.

Bjorkegren, C., Rozycki, M., Schutt, C. E., Lindberg, U., and Karlsson, R. (1993). "Mutagenesis of human profilin locates its poly(L-proline)-binding site to a hydrophobic patch of aromatic amino acids." *FEBS Lett*, 333(1-2), 123-6.

Blasco, R., Cole, N. B., and Moss, B. (1991). "Sequence analysis, expression, and deletion of a vaccinia virus gene encoding a homolog of profilin, a eukaryotic actin-binding protein." *J Virol*, 65(9), 4598-608.

Boquet, I., Boujemaa, R., Carlier, M. F., and Preat, T. (2000). "Ciboulot regulates actin assembly during Drosophila brain metamorphosis [In Process Citation]." *Cell*, 102(6), 797-808.

Borgstahl, G. E., Williams, D. R., and Getzoff, E. D. (1995). "1.4 A structure of photoactive yellow protein, a cytosolic photoreceptor: unusual fold, active site, and chromophore." *Biochemistry*, 34(19), 6278-87.

Borisy, G. G., and Svitkina, T. M. (2000). "Actin machinery: pushing the envelope." *Curr Opin Cell Biol*, 12(1), 104-12.

Bubb, M. R., Baines, I. C., and Korn, E. D. (1998). "Localization of actobindin, profilin I, profilin II, and phosphatidylinositol-4,5-bisphosphate (PIP2) in Acanthamoeba castellanii." *Cell Motil Cytoskeleton*, 39(2), 134-46.

Burns, M. E., Sasaki, T., Takai, Y., and Augustine, G. J. (1998). "Rabphilin-3A: a multifunctional regulator of synaptic vesicle traffic." *J Gen Physiol*, 111(2), 243-55.

Cao, H., Garcia, F., and McNiven, M. A. (1998). "Differential distribution of dynamin isoforms in mammalian cells." *Mol Biol Cell*, 9(9), 2595-609.

Cao, H., Thompson, H. M., Krueger, E. W., and McNiven, M. A. (2000). "Disruption of Golgi structure and function in mammalian cells expressing a mutant dynamin." *J Cell Sci*, 113(Pt 11)(1), 1993-2002.

Carlsson, L., Nystrom, L. E., Sundkvist, I., Markey, F., and Lindberg, U. (1977). "Actin polymerizability is influenced by profilin, a low molecular weight protein in non-muscle cells." *J Mol Biol*, 115(3), 465-83.

Cedergren-Zeppezauer, E. S., Goonesekere, N. C., Rozycki, M. D., Myslik, J. C., Dauter, Z., Lindberg, U., and Schutt, C. E. (1994). "Crystallization and structure determination of bovine profilin at 2.0 A resolution." *J Mol Biol*, 240(5), 459-75.

Chan, D. C., Bedford, M. T., and Leder, P. (1996). "Formin binding proteins bear WWP/WW domains that bind proline-rich peptides and functionally resemble SH3 domains." *Embo J*, 15(5), 1045-54.

Chang, F., Drubin, D., and Nurse, P. (1997). "cdc12p, a protein required for cytokinesis in fission yeast, is a component of the cell division ring and interacts with profilin." *J Cell Biol*, 137(1), 169-82.

Chaudhary, A., Chen, J., Gu, Q. M., Witke, W., Kwiatkowski, D. J., and Prestwich, G. D. (1998). "Probing the phosphoinositide 4,5-bisphosphate binding site of human profilin I." *Chem Biol*, 5(5), 273-81.

Cochilla, A. J., Angleson, J. K., and Betz, W. J. (1999). "Monitoring secretory membrane with FM1-43 fluorescence." *Annu Rev Neurosci*, 22, 1-10.

Cooley, L., Verheyen, E., and Ayers, K. (1992). "chickadee encodes a profilin required for intercellular cytoplasm transport during Drosophila oogenesis." *Cell*, 69(1), 173-84.

Corvera, S., D'Arrigo, A., and Stenmark, H. (1999). "Phosphoinositides in membrane traffic." *Curr Opin Cell Biol*, 11(4), 460-5.

Cousin, M. A., and Robinson, P. J. (1999). "Mechanisms of synaptic vesicle recycling illuminated by fluorescent dyes." *J Neurochem*, 73(6), 2227-39.

Cremona, O., Di Paolo, G., Wenk, M. R., Luthi, A., Kim, W. T., Takei, K., Daniell, L., Nemoto, Y., Shears, S. B., Flavell, R. A., McCormick, D. A., and De Camilli, P. (1999). "Essential role of phosphoinositide metabolism in synaptic vesicle recycling." *Cell*, 99(2), 179-88.

D'Souza-Schorey, C., van Donselaar, E., Hsu, V. W., Yang, C., Stahl, P. D., and Peters, P. J. (1998). "ARF6 targets recycling vesicles to the plasma membrane: insights from an ultrastructural investigation." *J Cell Biol*, 140(3), 603-16.

David, C., McPherson, P. S., Mundigl, O., and de Camilli, P. (1996). "A role of amphiphysin in synaptic vesicle endocytosis suggested by its binding to dynamin in nerve terminals." *Proc Natl Acad Sci U S A*, 93(1), 331-5.

De Corte, V., Gettemans, J., and Vandekerckhove, J. (1997). "Phosphatidylinositol 4,5-bisphosphate specifically stimulates PP60(c- src) catalyzed phosphorylation of gelsolin and related actin-binding proteins." *FEBS Lett*, 401(2-3), 191-6.

de Curtis, I. (2001). "Cell migration: GAPs between membrane traffic and the cytoskeleton." *EMBO Rep*, 2(4), 277-81.

Deaton, J. D., Guerrero, T., and Howard, T. H. (1992). “Role of gelsolin interaction with actin in regulation and creation of actin nuclei in chemotactic peptide activated polymorphonuclear neutrophils.” *Mol Biol Cell*, 3(12), 1427-35.

Di Nardo, A. (2001). “Function of the actin binding protein profilin II in mice.

Inaugural-Dissertation zur Erlangung der Doktorwürde der naturwissenschaftlich-mathematischen Gesamtfakultät der Ruprecht-Karls-Universität Heidelberg.,” .

Di Nardo, A., Gareus, R., Kwiatkowski, D., and Witke, W. (2000). “Alternative splicing of the mouse profilin II gene generates functionally different profilin isoforms.” *J Cell Sci*, 113 Pt 21(7), 3795-803.

Diefenbach, T. J., Guthrie, P. B., Stier, H., Billups, B., and Kater, S. B. (1999). “Membrane recycling in the neuronal growth cone revealed by FM1-43 labeling.” *J Neurosci*, 19(21), 9436-44.

Dong, J., Radau, B., Otto, A., Muller, E., Lindschau, C., and Westermann, P. (2000). “Profilin I attached to the Golgi is required for the formation of constitutive transport vesicles at the trans-Golgi network.” *Biochim Biophys Acta*, 1497(2), 253-60.

Doussau, F., and Augustine, G. J. (2000). “The actin cytoskeleton and neurotransmitter release: an overview.” *Biochimie*, 82(4), 353-63.

Durrbach, A., Louvard, D., and Coudrier, E. (1996). “Actin filaments facilitate two steps of endocytosis.” *J Cell Sci*, 109(Pt 2), 457-65.

Eads, J. C., Mahoney, N. M., Vorobiev, S., Bresnick, A. R., Wen, K. K., Rubenstein, P. A., Haarer, B. K., and Almo, S. C. (1998). “Structure determination and characterization of Saccharomyces cerevisiae profilin.” *Biochemistry*, 37(32), 11171-81.

Engqvist-Goldstein, A. E., Kessels, M. M., Chopra, V. S., Hayden, M. R., and Drubin, D. G. (1999). “An actin-binding protein of the Sla2/Huntingtin interacting protein 1 family is a novel component of clathrin-coated pits and vesicles.” *J Cell Biol*, 147(7), 1503-18.

Evans, L. L., and Bridgman, P. C. (1995). “Particles move along actin filament bundles in nerve growth cones.” *Proc Natl Acad Sci U S A*, 92(24), 10954-8.

Fedorov, A. A., Ball, T., Valenta, R., and Almo, S. C. (1997). “X-ray crystal structures of birch pollen profilin and Phl p 2.” *Int Arch Allergy Immunol*, 113(1-3), 109-13.

Finger, F. P., and Novick, P. (1997). "Sec3p is involved in secretion and morphogenesis in Saccharomyces cerevisiae." *Mol Biol Cell*, 8(4), 647-62.

Foster-Barber, A., and Bishop, J. M. (1998). "Src interacts with dynamin and synapsin in neuronal cells." *Proc Natl Acad Sci U S A*, 95(8), 4673-7.

Frey, D., Laux, T., Xu, L., Schneider, C., and Caroni, P. (2000). "Shared and unique roles of CAP23 and GAP43 in actin regulation, neurite outgrowth, and anatomical plasticity." *J Cell Biol*, 149(7), 1443-54.

Frohlich, K. U., Fries, H. W., Rudiger, M., Erdmann, R., Botstein, D., and Mecke, D. (1991). "Yeast cell cycle protein CDC48p shows full-length homology to the mammalian protein VCP and is a member of a protein family involved in secretion, peroxisome formation, and gene expression." *J Cell Biol*, 114(3), 443-53.

Fujimoto, L. M., Roth, R., Heuser, J. E., and Schmid, S. L. (2000). "Actin assembly plays a variable, but not obligatory role in receptor-mediated endocytosis in mammalian cells." *Traffic*, 1(2), 161-71.

Gad, H., Ringstad, N., Low, P., Kjaerulff, O., Gustafsson, J., Wenk, M., Di Paolo, G., Nemoto, Y., Crun, J., Ellisman, M. H., De Camilli, P., Shupliakov, O., and Brodin, L. (2000). "Fission and uncoating of synaptic clathrin-coated vesicles are perturbed by disruption of interactions with the SH3 domain of endophilin." *Neuron*, 27(2), 301-12.

Gaidarov, I., and Keen, J. H. (1999). "Phosphoinositide-AP-2 interactions required for targeting to plasma membrane clathrin-coated pits." *J Cell Biol*, 146(4), 755-64.

Gaidarov, I., Krupnick, J. G., Falck, J. R., Benovic, J. L., and Keen, J. H. (1999a). "Arrestin function in G protein-coupled receptor endocytosis requires phosphoinositide binding." *Embo J*, 18(4), 871-81.

Gaidarov, I., Santini, F., Warren, R. A., and Keen, J. H. (1999b). "Spatial control of coated-pit dynamics in living cells." *Nat Cell Biol*, 1(1), 1-7.

Gertler, F. B., Niebuhr, K., Reinhard, M., Wehland, J., and Soriano, P. (1996). "Mena, a relative of VASP and Drosophila Enabled, is implicated in the control of microfilament dynamics." *Cell*, 87(2), 227-39.

Giansanti, M. G., Bonaccorsi, S., Williams, B., Williams, E. V., Santolamazza, C., Goldberg, M. L., and Gatti, M. (1998). "Cooperative interactions between the

central spindle and the contractile ring during Drosophila cytokinesis." *Genes Dev*, 12(3), 396-410.

Gieselmann, R., Kwiatkowski, D. J., Janmey, P. A., and Witke, W. (1995). "Distinct biochemical characteristics of the two human profilin isoforms." *Eur J Biochem*, 229(3), 621-8.

Gold, E. S., Underhill, D. M., Morrissette, N. S., Guo, J., McNiven, M. A., and Aderem, A. (1999). "Dynamin 2 is required for phagocytosis in macrophages." *J Exp Med*, 190(12), 1849-56.

Goldschmidt-Clermont, P. J., Kim, J. W., Machesky, L. M., Rhee, S. G., and Pollard, T. D. (1991a). "Regulation of phospholipase C-gamma 1 by profilin and tyrosine phosphorylation." *Science*, 251(4998), 1231-3.

Goldschmidt-Clermont, P. J., Machesky, L. M., Baldassare, J. J., and Pollard, T. D. (1990). "The actin-binding protein profilin binds to PIP2 and inhibits its hydrolysis by phospholipase C." *Science*, 247(4950), 1575-8.

Goldschmidt-Clermont, P. J., Machesky, L. M., Doberstein, S. K., and Pollard, T. D. (1991b). "Mechanism of the interaction of human platelet profilin with actin." *J Cell Biol*, 113(5), 1081-9.

Gonzalez, L. C., Weis, W. I., and Scheller, R. H. (2001). "A novel SNARE N-terminal domain revealed by the crystal structure of Sec22b." *J Biol Chem*, 17, 17.

Gottlieb, T. A., Ivanov, I. E., Adesnik, M., and Sabatini, D. D. (1993). "Actin microfilaments play a critical role in endocytosis at the apical but not the basolateral surface of polarized epithelial cells." *J Cell Biol*, 120(3), 695-710.

Gout, I., Dhand, R., Hiles, I. D., Fry, M. J., Panayotou, G., Das, P., Truong, O., Totty, N. F., Hsuan, J., Booker, G. W., and et al. (1993). "The GTPase dynamin binds to and is activated by a subset of SH3 domains." *Cell*, 75(1), 25-36.

Grabs, D., Slepnev, V. I., Songyang, Z., David, C., Lynch, M., Cantley, L. C., and De Camilli, P. (1997). "The SH3 domain of amphiphysin binds the proline-rich domain of dynamin at a single site that defines a new SH3 binding consensus sequence." *J Biol Chem*, 272(20), 13419-25.

Guruprasad, L., Dhanaraj, V., Timm, D., Blundell, T. L., Gout, I., and Waterfield, M. D. (1995). "The crystal structure of the N-terminal SH3 domain of Grb2." *Journal of Molecular Biology*, 248, 856-866.

Gustafsson, J., Shupliakov, O., Takei, K., Low, P., De Camilli, P., and Brodin, L. (1998). "GTPgS induces an actin matrix associated with coated endocytic intermediates in presynaptic regions." *Neurosci. Soc. Abstr.*, 327, 19.

Gutsche-Perelroizen, I., Lepault, J., Ott, A., and Carlier, M. F. (1999). "Filament assembly from profilin-actin." *J Biol Chem*, 274(10), 6234-43.

Haarer, B. K., Lillie, S. H., Adams, A. E., Magdolen, V., Bandlow, W., and Brown, S. S. (1990). "Purification of profilin from Saccharomyces cerevisiae and analysis of profilin-deficient cells." *J Cell Biol*, 110(1), 105-14.

Haffner, C., Takei, K., Chen, H., Ringstad, N., Hudson, A., Butler, M. H., Salcini, A. E., Di Fiore, P. P., and De Camilli, P. (1997). "Synaptojanin 1: localization on coated endocytic intermediates in nerve terminals and interaction of its 170 kDa isoform with Eps15." *FEBS Lett*, 419(2-3), 175-80.

Hansson, A., Skoglund, G., Lassing, I., Lindberg, U., and Ingelman-Sundberg, M. (1988). "Protein kinase C-dependent phosphorylation of profilin is specifically stimulated by phosphatidylinositol bisphosphate (PIP2)." *Biochem Biophys Res Commun*, 150(2), 526-31.

Hao, M., and Maxfield, F. R. (2000). "Characterization of rapid membrane internalization and recycling." *J Biol Chem*, 275(20), 15279-86.

Harder, T., and Simons, K. (1999). "Clusters of glycolipid and glycosylphosphatidylinositol-anchored proteins in lymphoid cells: accumulation of actin regulated by local tyrosine phosphorylation." *Eur J Immunol*, 29(2), 556-62.

Harris, T. W., Hartwieg, E., Horvitz, H. R., and Jorgensen, E. M. (2000). "Mutations in synaptojanin disrupt synaptic vesicle recycling." *J Cell Biol*, 150(3), 589-600.

Hartwig, J. H., Chambers, K. A., Hopcia, K. L., and Kwiatkowski, D. J. (1989). "Association of profilin with filament-free regions of human leukocyte and platelet membranes and reversible membrane binding during platelet activation." *J Cell Biol*, 109(4 Pt 1), 1571-9.

Haugwitz, M., Noegel, A. A., Karakesisoglou, J., and Schleicher, M. (1994). "Dictyostelium amoebae that lack G-actin-sequestering profilins show defects in F-actin content, cytokinesis, and development." *Cell*, 79(2), 303-14.

Haugwitz, M., Noegel, A. A., Rieger, D., Lottspeich, F., and Schleicher, M. (1991). "Dictyostelium discoideum contains two profilin isoforms that differ in structure and function." *J Cell Sci*, 100(Pt 3), 481-9.

Henley, J. R., Cao, H., and McNiven, M. A. (1999). "Participation of dynamin in the biogenesis of cytoplasmic vesicles." *Faseb J*, 13 Suppl 2(1), S243-7.

Herman, I. M. (1993). "Actin isoforms." *Curr Opin Cell Biol*, 5(1), 48-55.

Herskovits, J. S., Burgess, C. C., Obar, R. A., and Vallee, R. B. (1993a). "Effects of mutant rat dynamin on endocytosis." *J Cell Biol*, 122(3), 565-78.

Herskovits, J. S., Shpetner, H. S., Burgess, C. C., and Vallee, R. B. (1993b). "Microtubules and Src homology 3 domains stimulate the dynamin GTPase via its C-terminal domain." *Proc Natl Acad Sci U S A*, 90(24), 11468-72.

Ho, Y. S., Burden, L. M., and Hurley, J. H. (2000). "Structure of the GAF domain, a ubiquitous signaling motif and a new class of cyclic GMP receptor." *Embo J*, 19(20), 5288-99.

Holt, M. R., and Koffer, A. (2001). "Cell motility: proline-rich proteins promote protrusions." *Trends Cell Biol*, 11(1), 38-46.

Honore, B., Madsen, P., Andersen, A. H., and Leffers, H. (1993). "Cloning and expression of a novel human profilin variant, profilin II." *FEBS Lett*, 330(2), 151-5.

Hu, E., Chen, Z., Fredrickson, T., and Zhu, Y. (2001). "Molecular cloning and characterization of profilin-3: a novel cytoskeleton-associated gene expressed in rat kidney and testes." *Exp Nephrol*, 9(4), 265-74.

Huang, J. D., Brady, S. T., Richards, B. W., Stenolen, D., Resau, J. H., Copeland, N. G., and Jenkins, N. A. (1999). "Direct interaction of microtubule- and actin-based transport motors." *Nature*, 397(6716), 267-70.

Hummel, T., Leifker, K., and Klambt, C. (2000). "The Drosophila HEM-2/NAP1 homolog KETTE controls axonal pathfinding and cytoskeletal organization." *Genes Dev*, 14(7), 863-73.

Huttner, W. B., and Schmidt, A. (2000). "Lipids, lipid modification and lipid-protein interaction in membrane budding and fission--insights from the roles of endophilin A1 and synaptophysin in synaptic vesicle endocytosis." *Curr Opin Neurobiol*, 10(5), 543-51.

Imamura, H., Tanaka, K., Hihara, T., Umikawa, M., Kamei, T., Takahashi, K., Sasaki, T., and Takai, Y. (1997). "Bni1p and Bnr1p: downstream targets of the Rho family small G-proteins which interact with profilin and regulate actin cytoskeleton in Saccharomyces cerevisiae." *Embo J*, 16(10), 2745-55.

Jostarndt, K., Puntschart, A., Hoppeler, H., and Billeter, R. (1994). "The use of 33P-labelled riboprobes for in situ hybridizations: localization of myosin alkali light-chain mRNAs in adult human skeletal muscle." *Histochem J*, 26(1), 32-40.

Kaiser, D. A., Goldschmidt-Clermont, P. J., Levine, B. A., and Pollard, T. D. (1989). "Characterization of renatured profilin purified by urea elution from poly-L-proline agarose columns." *Cell Motil Cytoskeleton*, 14(2), 251-62.

Kaiser, D. A., Sato, M., Ebert, R. F., and Pollard, T. D. (1986). "Purification and characterization of two isoforms of Acanthamoeba profilin." *J Cell Biol*, 102(1), 221-6.

Kang, F., Purich, D. L., and Southwick, F. S. (1999). "Profilin promotes barbed-end actin filament assembly without lowering the critical concentration." *J Biol Chem*, 274(52), 36963-72.

Karakesisoglou, I., Janssen, K. P., Eichinger, L., Noegel, A. A., and Schleicher, M. (1999). "Identification of a suppressor of the Dictyostelium profilin-minus phenotype as a CD36/LIMP-II homologue." *J Cell Biol*, 145(1), 167-81.

Kay, B. K., Williamson, M. P., and Sudol, M. (2000). "The importance of being proline: the interaction of proline-rich motifs in signaling proteins with their cognate domains." *Faseb J*, 14(2), 231-41.

Kessels, M. M., Engqvist-Goldstein, A. E., Drubin, D. G., and Qualmann, B. (2001). "Mammalian Abp1, a signal-responsive F-actin-binding protein, links the actin cytoskeleton to endocytosis via the GTPase dynamin." *J Cell Biol*, 153(2), 351-66.

Khvotchev, M., and Sudhof, T. C. (1998). "Newly synthesized phosphatidylinositol phosphates are required for synaptic norepinephrine but not glutamate or gamma-aminobutyric acid (GABA) release." *J Biol Chem*, 273(34), 21451-4.

Kitamura, T., Kitamura, Y., Yonezawa, K., Totty, N. F., Gout, I., Hara, K., Waterfield, M. D., Sakaue, M., Ogawa, W., and Kasuga, M. (1996). "Molecular cloning of p125Nap1, a protein that associates with an SH3 domain of Nck." *Biochem Biophys Res Commun*, 219(2), 509-14.

Kitamura, Y., Kitamura, T., Sakaue, H., Maeda, T., Ueno, H., Nishio, S., Ohno, S., Osada, S., Sakaue, M., Ogawa, W., and Kasuga, M. (1997). "Interaction of Nck-associated protein 1 with activated GTP-binding protein Rac." *Biochem J*, 322(Pt 3), 873-8.

Korey, C. A., and Van Vactor, D. (2000). "From the growth cone surface to the cytoskeleton: one journey, many paths." *J Neurobiol*, 44(2), 184-93.

Koster, F., Schinke, B., Niemann, S., and Hermans-Borgmeyer, I. (1998). "Identification of shyc, a novel gene expressed in the murine developing and adult nervous system." *Neurosci Lett*, 252(1), 69-71.

Kreitzer, G., Marmorstein, A., Okamoto, P., Vallee, R., and Rodriguez-Boulan, E. (2000). "Kinesin and dynamin are required for post-Golgi transport of a plasma-membrane protein." *Nat Cell Biol*, 2(2), 125-7.

Kwiatkowski, D. J., Aklog, L., Ledbetter, D. H., and Morton, C. C. (1990). "Identification of the functional profilin gene, its localization to chromosome subband 17p13.3, and demonstration of its deletion in some patients with Miller-Dieker syndrome." *Am J Hum Genet*, 46(3), 559-67.

Kwiatkowski, D. J., and Bruns, G. A. (1988). "Human profilin. Molecular cloning, sequence comparison, and chromosomal analysis." *J Biol Chem*, 263(12), 5910-5.

Lamaze, C., Chuang, T. H., Terlecky, L. J., Bokoch, G. M., and Schmid, S. L. (1996). "Regulation of receptor-mediated endocytosis by Rho and Rac." *Nature*, 382(6587), 177-9.

Lamaze, C., Fujimoto, L. M., Yin, H. L., and Schmid, S. L. (1997). "The actin cytoskeleton is required for receptor-mediated endocytosis in mammalian cells." *J Biol Chem*, 272(33), 20332-5.

Lambrechts, A., Kwiatkowski, A. V., Lanier, L. M., Bear, J. E., Vandekerckhove, J., Ampe, C., and Gertler, F. B. (2000). "cAMP-dependent protein kinase phosphorylation of EVL, a Mena/VASP relative, regulates its interaction with actin and SH3 domains." *J Biol Chem*, 275(46), 36143-51.

Langford, G. M. (1995). "Actin- and microtubule-dependent organelle motors: interrelationships between the two motility systems." *Curr Opin Cell Biol*, 7(1), 82-8.

Langmann, C., and Harden, N. (2001). "DSra-1 is an effector for DRac1 during Drosophila embryogenesis." *Molecular Biology and Biochemistry, submitted 03.04.2001*.

Lanier, L. M., Gates, M. A., Witke, W., Menzies, A. S., Wehman, A. M., Macklis, J. D., Kwiatkowski, D., Soriano, P., and Gertler, F. B. (1999). "Mena is required for neurulation and commissure formation." *Neuron*, 22(2), 313-25.

Lassing, I., and Lindberg, U. (1985). "Specific interaction between phosphatidylinositol 4,5-bisphosphate and profilactin." *Nature*, 314(6010), 472-4.

Laux, T., Fukami, K., Thelen, M., Golub, T., Frey, D., and Caroni, P. (2000). "GAP43, MARCKS, and CAP23 modulate PI(4,5)P(2) at plasmalemmal rafts, and regulate cell cortex actin dynamics through a common mechanism." *J Cell Biol*, 149(7), 1455-72.

Lindberg, U., Schutt, C. E., Hellsten, E., Tjader, A. C., and Hult, T. (1988). "The use of poly(L-proline)-Sepharose in the isolation of profilin and profilactin complexes." *Biochim Biophys Acta*, 967(3), 391-400.

Liu, Y., Casey, L., and Pike, L. J. (1998). "Compartmentalization of phosphatidylinositol 4,5-bisphosphate in low-density membrane domains in the absence of caveolin." *Biochem Biophys Res Commun*, 245(3), 684-90.

Lu, J., and Pollard, T. D. (2001). "Profilin Binding to Poly-L-Proline and Actin Monomers along with Ability to Catalyze Actin Nucleotide Exchange Is Required for Viability of Fission Yeast." *Mol Biol Cell*, 12(4), 1161-75.

Lu, K. P., Hanes, S. D., and Hunter, T. (1996). "A human peptidyl-prolyl isomerase essential for regulation of mitosis." *Nature*, 380(6574), 544-7.

Machesky, L. M., Atkinson, S. J., Ampe, C., Vandekerckhove, J., and Pollard, T. D. (1994a). "Purification of a cortical complex containing two unconventional actins from Acanthamoeba by affinity chromatography on profilin-agarose." *J Cell Biol*, 127(1), 107-15.

Machesky, L. M., Cole, N. B., Moss, B., and Pollard, T. D. (1994b). "Vaccinia virus expresses a novel profilin with a higher affinity for polyphosphoinositides than actin." *Biochemistry*, 33(35), 10815-24.

Machesky, L. M., Goldschmidt-Clermont, P. J., and Pollard, T. D. (1990). "The affinities of human platelet and Acanthamoeba profilin isoforms for polyphosphoinositides account for their relative abilities to inhibit phospholipase C." *Cell Regul*, 1(12), 937-50.

Mahoney, N. M., and Almo, S. C. (1998). "Crystallization and preliminary X-ray analysis of human platelet profilin complexed with an oligo proline peptide." *Acta Crystallogr D Biol Crystallogr*, 54(Pt 1), 108-10.

Mahoney, N. M., Janmey, P. A., and Almo, S. C. (1997). "Structure of the profilin-poly-L-proline complex involved in morphogenesis and cytoskeletal regulation

[published erratum appears in Nat Struct Biol 1997 Dec;4(12):1047].” *Nat Struct Biol*, 4(11), 953-60.

Mahoney, N. M., Rozwarski, D. A., Fedorov, E., Fedorov, A. A., and Almo, S. C. (1999). “Profilin binds proline-rich ligands in two distinct amide backbone orientations.” *Nat Struct Biol*, 6(7), 666-71.

Malecz, N., McCabe, P. C., Spaargaren, C., Qiu, R., Chuang, Y., and Symons, M. (2000). “Synaptojanin 2, a novel Rac1 effector that regulates clathrin-mediated endocytosis.” *Curr Biol*, 10(21), 1383-6.

Malm, B., Larsson, H., and Lindberg, U. (1983). “The profilin--actin complex: further characterization of profilin and studies on the stability of the complex.” *J Muscle Res Cell Motil*, 4(5), 569-88.

Mammoto, A., Sasaki, T., Asakura, T., Hotta, I., Imamura, H., Takahashi, K., Matsuura, Y., Shirao, T., and Takai, Y. (1998). “Interactions of drebrin and gephyrin with profilin.” *Biochem Biophys Res Commun*, 243(1), 86-9.

Manseau, L., Calley, J., and Phan, H. (1996). “Profilin is required for posterior patterning of the Drosophila oocyte.” *Development*, 122(7), 2109-16.

Marks, B., Stowell, M. H., Vallis, Y., Mills, I. G., Gibson, A., Hopkins, C. R., and McMahon, H. T. (2001). “GTPase activity of dynamin and resulting conformation change are essential for endocytosis.” *Nature*, 410(6825), 231-5.

Martin, T. F. (2000). “Racing lipid rafts for synaptic-vesicle formation.” *Nat Cell Biol*, 2(1), E9-11.

Mayer, H., Salzer, U., Breuss, J., Ziegler, S., Marchler-Bauer, A., and Prohaska, R. (1998). “Isolation, molecular characterization, and tissue-specific expression of a novel putative G protein-coupled receptor.” *Biochim Biophys Acta*, 1395(3), 301-8.

McNiven, M. A. (1998). “Dynamin: a molecular motor with pinchase action.” *Cell*, 94(2), 151-4.

McNiven, M. A., Cao, H., Pitts, K. R., and Yoon, Y. (2000a). “The dynamin family of mechanoenzymes: pinching in new places.” *Trends Biochem Sci*, 25(3), 115-20.

McNiven, M. A., Kim, L., Krueger, E. W., Orth, J. D., Cao, H., and Wong, T. W. (2000b). “Regulated interactions between dynamin and the actin-binding protein cortactin modulate cell shape.” *J Cell Biol*, 151(1), 187-98.

Merrifield, C. J., Moss, S. E., Ballestrem, C., Imhof, B. A., Giese, G., Wunderlich, I., and Almers, W. (1999). "Endocytic vesicles move at the tips of actin tails in cultured mast cells." *Nat Cell Biol*, 1(1), 72-4.

Metzler, W. J., Constantine, K. L., Friedrichs, M. S., Bell, A. J., Ernst, E. G., Lavoie, T. B., and Mueller, L. (1993). "Characterization of the three-dimensional solution structure of human profilin: 1H, 13C, and 15N NMR assignments and global folding pattern." *Biochemistry*, 32(50), 13818-29.

Metzler, W. J., Farmer, B. T., 2nd, Constantine, K. L., Friedrichs, M. S., Lavoie, T., and Mueller, L. (1995). "Refined solution structure of human profilin I." *Protein Sci*, 4(3), 450-9.

Micheva, K. D., Kay, B. K., and McPherson, P. S. (1997). "Synaptojanin forms two separate complexes in the nerve terminal. Interactions with endophilin and amphiphysin." *J Biol Chem*, 272(43), 27239-45.

Miki, H., Miura, K., and Takenawa, T. (1996). "N-WASP, a novel actin-depolymerizing protein, regulates the cortical cytoskeletal rearrangement in a PIP2-dependent manner downstream of tyrosine kinases." *Embo J*, 15(19), 5326-35.

Muhlberg, A. B., Warnock, D. E., and Schmid, S. L. (1997). "Domain structure and intramolecular regulation of dynamin GTPase." *Embo J*, 16(22), 6676-83.

Mundigl, O., Ochoa, G. C., David, C., Slepnev, V. I., Kabanov, A., and De Camilli, P. (1998). "Amphiphysin I antisense oligonucleotides inhibit neurite outgrowth in cultured hippocampal neurons." *J Neurosci*, 18(1), 93-103.

Murphy, C., Saffrich, R., Grummt, M., Gournier, H., Rybin, V., Rubino, M., Auvinen, P., Lutcke, A., Parton, R. G., and Zerial, M. (1996). "Endosome dynamics regulated by a Rho protein." *Nature*, 384(6608), 427-32.

Nakagawa, H., Miki, H., Ito, M., Ohashi, K., Takenawa, T., and Miyamoto, S. (2001). "N-WASP, WAVE and Mena play different roles in the organization of actin cytoskeleton in lamellipodia." *J Cell Sci*, 114(Pt 8), 1555-65.

Nicoziani, P., Vilhardt, F., Llorente, A., Hilout, L., Courtoy, P. J., Sandvig, K., and van Deurs, B. (2000). "Role for dynamin in late endosome dynamics and trafficking of the cation-independent mannose 6-phosphate receptor." *Mol Biol Cell*, 11(2), 481-95.

Novick, P., and Zerial, M. (1997). "The diversity of Rab proteins in vesicle transport." *Curr Opin Cell Biol*, 9(4), 496-504.

Ochoa, G. C., Slepnev, V. I., Neff, L., Ringstad, N., Takei, K., Daniell, L., Kim, W., Cao, H., McNiven, M., Baron, R., and De Camilli, P. (2000). "A functional link between dynamin and the actin cytoskeleton at podosomes." *J Cell Biol*, 150(2), 377-89.

Ostrander, D. B., Ernst, E. G., Lavoie, T. B., and Gorman, J. A. (1999). "Polyproline binding is an essential function of human profilin in yeast." *Eur J Biochem*, 262(1), 26-35.

Pantaloni, D., and Carlier, M. F. (1993). "How profilin promotes actin filament assembly in the presence of thymosin beta 4." *Cell*, 75(5), 1007-14.

Petrella, E. C., Machesky, L. M., Kaiser, D. A., and Pollard, T. D. (1996). "Structural requirements and thermodynamics of the interaction of proline peptides with profilin." *Biochemistry*, 35(51), 16535-43.

Pike, L. J., and Casey, L. (1996). "Localization and turnover of phosphatidylinositol 4,5-bisphosphate in caveolin-enriched membrane domains." *J Biol Chem*, 271(43), 26453-6.

Pike, L. J., and Miller, J. M. (1998). "Cholesterol depletion delocalizes phosphatidylinositol bisphosphate and inhibits hormone-stimulated phosphatidylinositol turnover." *J Biol Chem*, 273(35), 22298-304.

Pleasure, I. T., Black, M. M., and Keen, J. H. (1993). "Valosin-containing protein, VCP, is a ubiquitous clathrin-binding protein." *Nature*, 365(6445), 459-62.

Pollard, T. D. (1986). "Rate constants for the reactions of ATP- and ADP-actin with the ends of actin filaments." *J Cell Biol*, 103(6 Pt 2), 2747-54.

Pollard, T. D., Blanchoin, L., and Mullins, R. D. (2000). "Molecular mechanisms controlling actin filament dynamics in nonmuscle cells [In Process Citation]." *Annu Rev Biophys Biomol Struct*, 29, 545-76.

Pollard, T. D., and Cooper, J. A. (1986). "Actin and actin-binding proteins. A critical evaluation of mechanisms and functions." *Annu Rev Biochem*, 55, 987-1035.

Ponting, C. P., and Aravind, L. (1997). "PAS: a multifunctional domain family comes to light." *Curr Biol*, 7(11), R674-7.

Pring, M., Weber, A., and Bubb, M. R. (1992). "Profilin-actin complexes directly elongate actin filaments at the barbed end." *Biochemistry*, 31(6), 1827-36.

Qualmann, B., and Kelly, R. B. (2000). "Syndapin isoforms participate in receptor-mediated endocytosis and actin organization." *J Cell Biol*, 148(5), 1047-62.

Qualmann, B., Kessels, M. M., and Kelly, R. B. (2000). "Molecular links between endocytosis and the actin cytoskeleton." *J Cell Biol*, 150(5), F111-6.

Qualmann, B., Roos, J., DiGregorio, P. J., and Kelly, R. B. (1999). "Syndapin I, a synaptic dynamin-binding protein that associates with the neural Wiskott-Aldrich syndrome protein." *Mol Biol Cell*, 10(2), 501-13.

Radhakrishna, H., Al-Awar, O., Khachikian, Z., and Donaldson, J. G. (1999). "ARF6 requirement for Rac ruffling suggests a role for membrane trafficking in cortical actin rearrangements." *J Cell Sci*, 112(Pt 6), 855-66.

Raghunathan, V., Mowery, P., Rozycki, M., Lindberg, U., and Schutt, C. (1992). "Structural changes in profilin accompany its binding to phosphatidylinositol, 4,5-bisphosphate." *FEBS Lett*, 297(1-2), 46-50.

Randazzo, P. A., Andrade, J., Miura, K., Brown, M. T., Long, Y. Q., Stauffer, S., Roller, P., and Cooper, J. A. (2000). "The Arf GTPase-activating protein ASAP1 regulates the actin cytoskeleton." *Proc Natl Acad Sci U S A*, 97(8), 4011-6.

Reinhard, M., Giehl, K., Abel, K., Haffner, C., Jarchau, T., Hoppe, V., Jockusch, B. M., and Walter, U. (1995). "The proline-rich focal adhesion and microfilament protein VASP is a ligand for profilins." *Embo J*, 14(8), 1583-9.

Reinhard, M., Halbrugge, M., Scheer, U., Wiegand, C., Jockusch, B. M., and Walter, U. (1992). "The 46/50 kDa phosphoprotein VASP purified from human platelets is a novel protein associated with actin filaments and focal contacts." *Embo J*, 11(6), 2063-70.

Reiss, J., Gross-Hardt, S., Christensen, E., Schmidt, P., Mendel, R. R., and Schwarz, G. (2001). "A mutation in the gene for the neurotransmitter receptor-clustering protein gephyrin causes a novel form of molybdenum cofactor deficiency." *Am J Hum Genet*, 68(1), 208-13.

Ringstad, N., Nemoto, Y., and De Camilli, P. (1997). "The SH3p4/Sh3p8/SH3p13 protein family: binding partners for synaptojanin and dynamin via a Grb2-like Src homology 3 domain." *Proc Natl Acad Sci U S A*, 94(16), 8569-74.

Robinson, L. J., and Martin, T. F. (1998). "Docking and fusion in neurosecretion." *Curr Opin Cell Biol*, 10(4), 483-92.

Roos, J., and Kelly, R. B. (1999). "The endocytic machinery in nerve terminals surrounds sites of exocytosis." *Curr Biol*, 9(23), 1411-4.

Rozelle, A. L., Machesky, L. M., Yamamoto, M., Driessens, M. H., Insall, R. H., Roth, M. G., Luby-Phelps, K., Marriott, G., Hall, A., and Yin, H. L. (2000). "Phosphatidylinositol 4,5-bisphosphate induces actin-based movement of raft-enriched vesicles through WASP-Arp2/3." *Curr Biol*, 10(6), 311-20.

Ryan, T. A., Smith, S. J., and Reuter, H. (1996). "The timing of synaptic vesicle endocytosis." *Proc Natl Acad Sci U S A*, 93(11), 5567-71.

Safer, D., Elzinga, M., and Nachmias, V. T. (1991). "Thymosin beta 4 and Fx, an actin-sequestering peptide, are indistinguishable." *J Biol Chem*, 266(7), 4029-32.

Sakisaka, T., Itoh, T., Miura, K., and Takenawa, T. (1997). "Phosphatidylinositol 4,5-bisphosphate phosphatase regulates the rearrangement of actin filaments." *Mol Cell Biol*, 17(7), 3841-9.

Saller, E., Tom, E., Brunori, M., Otter, M., Estreicher, A., Mack, D. H., and Iggo, R. (1999). "Increased apoptosis induction by 121F mutant p53." *Embo J*, 18(16), 4424-37.

Sambrook, J., Fritsch, E. F., and Maniatis, T. (1989). *Molecular cloning*, Cold Spring Harbor Laboratory Press.

Scaife, R., Gout, I., Waterfield, M. D., and Margolis, R. L. (1994). "Growth factor-induced binding of dynamin to signal transduction proteins involves sorting to distinct and separate proline-rich dynamin sequences." *Embo J*, 13(11), 2574-82.

Scales, S. J., and Scheller, R. H. (1999). "Lipid membranes shape up." *Nature*, 401(6749), 123-4.

Schiavo, G., Gu, Q. M., Prestwich, G. D., Sollner, T. H., and Rothman, J. E. (1996). "Calcium-dependent switching of the specificity of phosphoinositide binding to synaptotagmin." *Proc Natl Acad Sci U S A*, 93(23), 13327-32.

Schmidt, A., Wolde, M., Thiele, C., Fest, W., Kratzin, H., Podtelejnikov, A. V., Witke, W., Huttner, W. B., and Soling, H. D. (1999a). "Endophilin I mediates synaptic vesicle formation by transfer of arachidonate to lysophosphatidic acid." *Nature*, 401(6749), 133-41.

Schmidt, A., Wolde, M., Thiele, C., Fest, W., Kratzin, H., Podtelejnikov, A. V., Witke, W., Huttner, W. B., and Soling, H. D. (1999b). "Endophilin I mediates

synaptic vesicle formation by transfer of arachidonate to lysophosphatidic acid [see comments].” *Nature*, 401(6749), 133-41.

Schutt, C. E., Myslik, J. C., Rozycki, M. D., Goonesekere, N. C., and Lindberg, U. (1993). “The structure of crystalline profilin-beta-actin.” *Nature*, 365(6449), 810-6.

Seedorf, K., Kostka, G., Lammers, R., Bashkin, P., Daly, R., Burgess, W. H., van der Bliek, A. M., Schlessinger, J., and Ullrich, A. (1994). “Dynamin binds to SH3 domains of phospholipase C gamma and GRB-2.” *J Biol Chem*, 269(23), 16009-14.

Sever, S., Muhlberg, A. B., and Schmid, S. L. (1999). “Impairment of dynamin's GAP domain stimulates receptor-mediated endocytosis.” *Nature*, 398(6727), 481-6.

Simpson, F., Hussain, N. K., Qualmann, B., Kelly, R. B., Kay, B. K., McPherson, P. S., and Schmid, S. L. (1999). “SH3-domain-containing proteins function at distinct steps in clathrin-coated vesicle formation.” *Nat Cell Biol*, 1(2), 119-24.

Singer-Kruger, B., Nemoto, Y., Daniell, L., Ferro-Novick, S., and De Camilli, P. (1998). “Synaptojanin family members are implicated in endocytic membrane traffic in yeast.” *J Cell Sci*, 111(Pt 22), 3347-56.

Singh, S. S., Chauhan, A., Murakami, N., Styles, J., Elzinga, M., and Chauhan, V. P. (1996). “Phosphoinositide-dependent in vitro phosphorylation of profilin by protein kinase C. Phospholipid specificity and localization of the phosphorylation site.” *Recept Signal Transduct*, 6(2), 77-86.

Sittler, A., Walter, S., Wedemeyer, N., Hasenbank, R., Scherzinger, E., Eickhoff, H., Bates, G. P., Lehrach, H., and Wanker, E. E. (1998). “SH3GL3 associates with the Huntingtin exon 1 protein and promotes the formation of polygln-containing protein aggregates.” *Mol Cell*, 2(4), 427-36.

So, C. W., Sham, M. H., Chew, S. L., Cheung, N., So, C. K., Chung, S. K., Caldas, C., Wiedemann, L. M., and Chan, L. C. (2000). “Expression and protein-binding studies of the EEN gene family, new interacting partners for dynamin, synaptojanin and huntingtin proteins.” *Biochem J*, 348 Pt 2, 447-58.

Sohn, R. H., Chen, J., Koblan, K. S., Bray, P. F., and Goldschmidt-Clermont, P. J. (1995). “Localization of a binding site for phosphatidylinositol 4,5-bisphosphate on human profilin.” *J Biol Chem*, 270(36), 21114-20.

Southwick, F. S., and Young, C. L. (1990). “The actin released from profilin--actin complexes is insufficient to account for the increase in F-actin in chemoattractant-stimulated polymorphonuclear leukocytes.” *J Cell Biol*, 110(6), 1965-73.

Stowell, M. H., Marks, B., Wigge, P., and McMahon, H. T. (1999). “Nucleotide-dependent conformational changes in dynamin: evidence for a mechanochemical molecular spring.” *Nat Cell Biol*, 1(1), 27-32.

Sudol, M. (1996). “The WW module competes with the SH3 domain?” *Trends Biochem Sci*, 21(5), 161-3.

Sudol, M. (1998). “From Src Homology domains to other signaling modules: proposal of the 'protein recognition code'.” *Oncogene*, 17(11 Reviews), 1469-74.

Suetsugu, S., Miki, H., and Takenawa, T. (1998). “The essential role of profilin in the assembly of actin for microspike formation.” *Embo J*, 17(22), 6516-26.

Sugiura, Y. (1981). “Structure of molecular aggregates of 1-(3-sn-phosphatidyl)-L-myo-inositol 3,4-bis(phosphate) in water.” *Biochim Biophys Acta*, 641(1), 148-59.

Svitkina, T. M., and Borisy, G. G. (1999). “Arp2/3 complex and actin depolymerizing factor/cofilin in dendritic organization and treadmilling of actin filament array in lamellipodia.” *J Cell Biol*, 145(5), 1009-26.

Sweitzer, S. M., and Hinshaw, J. E. (1998). “Dynamin undergoes a GTP-dependent conformational change causing vesiculation.” *Cell*, 93(6), 1021-9.

Takei, K., Slepnev, V. I., Haucke, V., and De Camilli, P. (1999). “Functional partnership between amphiphysin and dynamin in clathrin-mediated endocytosis.” *Nat Cell Biol*, 1(1), 33-9.

Tanaka, M., and Shibata, H. (1985). “Poly(L-proline)-binding proteins from chick embryos are a profilin and a profilactin.” *Eur J Biochem*, 151(2), 291-7.

Taunton, J., Rowning, B. A., Coughlin, M. L., Wu, M., Moon, R. T., Mitchison, T. J., and Larabell, C. A. (2000). “Actin-dependent propulsion of endosomes and lysosomes by recruitment of N-WASP.” *J Cell Biol*, 148(3), 519-30.

Temesvari, L., Zhang, L., Fodera, B., Janssen, K. P., Schleicher, M., and Cardelli, J. A. (2000). “Inactivation of lmpA, encoding a LIMPII-related endosomal protein, suppresses the internalization and endosomal trafficking defects in profilin-null mutants.” *Mol Biol Cell*, 11(6), 2019-31.

Thery, C., Boussac, M., Veron, P., Ricciardi-Castagnoli, P., Raposo, G., Garin, J., and Amigorena, S. (2001). “Proteomic analysis of dendritic cell-derived exosomes: a

secreted subcellular compartment distinct from apoptotic vesicles." *J Immunol*, 166(12), 7309-18.

Thiele, C., Hannah, M. J., Fahrenholz, F., and Huttner, W. B. (2000). "Cholesterol binds to synaptophysin and is required for biogenesis of synaptic vesicles." *Nat Cell Biol*, 2(1), 42-9.

Thorn, K. S., Christensen, H. E., Shigeta, R., Huddler, D., Shalaby, L., Lindberg, U., Chua, N. H., and Schutt, C. E. (1997). "The crystal structure of a major allergen from plants." *Structure*, 5(1), 19-32.

Trifaro, J., Rose, S. D., Lejen, T., and Elzagallaai, A. (2000). "Two pathways control chromaffin cell cortical F-actin dynamics during exocytosis." *Biochimie*, 82(4), 339-52.

Tuxworth, R. I., and Titus, M. A. (2000). "Unconventional myosins: anchors in the membrane traffic relay." *Traffic*, 1(1), 11-8.

Vemuri, B., and Singh, S. S. (2001). "Protein kinase C isozyme-specific phosphorylation of profilin." *Cell Signal*, 13(6), 433-9.

Vinson, V. K., Archer, S. J., Lattman, E. E., Pollard, T. D., and Torchia, D. A. (1993). "Three-dimensional solution structure of Acanthamoeba profilin-I." *J Cell Biol*, 122(6), 1277-83.

Vojtek, A., Haarer, B., Field, J., Gerst, J., Pollard, T. D., Brown, S., Wigler, M. (1991). "Evidence for a functional link between profilin and CAP in the yeast S. cerevisiae."Cell 66 (3), 497-505.

Wang, X., Kibschull, M., Laue, M. M., Lichte, B., Petrasch-Parwez, E., and Kilimann, M. W. (1999). "Aczonin, a 550-kD putative scaffolding protein of presynaptic active zones, shares homology regions with Rim and Bassoon and binds profilin." *J Cell Biol*, 147(1), 151-62.

Wang, Y., Thiele, C., and Huttner, W. B. (2000). "Cholesterol is required for the formation of regulated and constitutive secretory vesicles from the trans-Golgi network." *Traffic*, 1(12), 952-62.

Warnock, D. E., Terlecky, L. J., and Schmid, S. L. (1995). "Dynamin GTPase is stimulated by crosslinking through the C-terminal proline-rich domain." *Embo J*, 14(7), 1322-8.

Watanabe, N., Kato, T., Fujita, A., Ishizaki, T., and Narumiya, S. (1999). "Cooperation between mDia1 and ROCK in Rho-induced actin reorganization." *Nat Cell Biol*, 1(3), 136-43.

Watanabe, N., Madaule, P., Reid, T., Ishizaki, T., Watanabe, G., Kakizuka, A., Saito, Y., Nakao, K., Jockusch, B. M., and Narumiya, S. (1997). "p140mDia, a mammalian homolog of Drosophila diaphanous, is a target protein for Rho small GTPase and is a ligand for profilin." *Embo J*, 16(11), 3044-56.

Williamson, M. P. (1994). "The structure and function of proline-rich regions in proteins." *Biochem J*, 297(Pt 2), 249-60.

Wills, Z., Marr, L., Zinn, K., Goodman, C. S., and Van Vactor, D. (1999). "Profilin and the Abl tyrosine kinase are required for motor axon outgrowth in the Drosophila embryo." *Neuron*, 22(2), 291-9.

Witke, W., Podtelejnikov, A. V., Di Nardo, A., Sutherland, J. D., Gurniak, C. B., Dotti, C., and Mann, M. (1998). "In mouse brain profilin I and profilin II associate with regulators of the endocytic pathway and actin assembly." *Embo J*, 17(4), 967-76.

Witke, W., Sutherland, J. D., Sharpe, A., Arai, M., and Kwiatkowski, D. J. (2001). "Profilin I is essential for cell survival and cell division in early mouse development." *Proc Natl Acad Sci U S A*, 98(7), 3832-6.

Wittenmayer, N., Rothkegel, M., Jockusch, B. M., and Schluter, K. (2000). "Functional characterization of green fluorescent protein-profilin fusion proteins." *Eur J Biochem*, 267(16), 5247-5256.

Yaffe, M. B., Schutkowski, M., Shen, M., Zhou, X. Z., Stukenberg, P. T., Rahfeld, J. U., Xu, J., Kuang, J., Kirschner, M. W., Fischer, G., Cantley, L. C., and Lu, K. P. (1997). "Sequence-specific and phosphorylation-dependent proline isomerization: a potential mitotic regulatory mechanism." *Science*, 278(5345), 1957-60.

Yang, C., Huang, M., DeBiasio, J., Pring, M., Joyce, M., Miki, H., Takenawa, T., and Zigmond, S. H. (2000). "Profilin enhances Cdc42-induced nucleation of actin polymerization." *J Cell Biol*, 150(5), 1001-12.

Yang, W., and Cerione, R. A. (1999). "Endocytosis: Is dynamin a 'blue collar' or 'white collar' worker?" *Curr Biol*, 9(14), R511-4.

Zheng, J., Cahill, S. M., Lemmon, M. A., Fushman, D., Schlessinger, J., and Cowburn, D. (1996). "Identification of the binding site for acidic phospholipids on

the pH domain of dynamin: implications for stimulation of GTPase activity." *J Mol Biol*, 255(1), 14-21.